UTILITY OF HEPATIC PHOSPHORUS-31 MAGNETIC RESONANCE SPECTROSCOPY IN THE HEALTHY AND DISEASED LIVER

By

IAN CORBIN

A Thesis
Submitted to the Faculty of Graduate Studies
In Partial Fulfilment of the Requirements
For the degree of

DOCTOR OF PHILOSOPHY

Department of Pharmacology and Therapeutics
Faculty of Medicine
University of Manitoba
Winnipeg, Manitoba

THE UNIVERSITY OF MANITOBA

FACULTY OF GRADUATE STUDIES

*****

COPYRIGHT PERMISSION PAGE

UTILITY OF HEPATIC PHOSPHORUS-31 MAGNETIC RESONANCE SPECTROSCOPY IN THE HEALTHY AND DISEASED LIVER

BY

IAN CORBIN

A Thesis/Practicum submitted to the Faculty of Graduate Studies of The University of Manitoba in partial fulfillment of the requirements of the degree of

Doctor of Philosophy

ACKNOWLEDGMENTS

Completing a formidable task, such as a PhD, requires not only the steadfast efforts of the candidate, but also the helpful assistance of others. I would like to take this opportunity to acknowledge the efforts of those individuals who contributed to the completion of my Ph.D. degree.

First and foremost I must express my deep appreciation to my supervisor Dr. Gerald Minuk for his invaluable guidance and direction throughout my degree. His broad knowledge in clinical medicine and basic science has taught me a great deal about scientific research. He has shared not only the importance of a critical and complete approach to designing and conducting research experiments, but has also taught me a lot about scientific writing and publishing. In addition to the extensive basic research training I have received, Dr. Minuk provided an excellent learning environment in which interactions between physicians and researchers were fostered. I really appreciated this opportunity of being exposed to the many facets of both basic science and clinical medicine throughout my degree and it has reinforced in my mind the need and importance of translating laboratory research to bedside medicine. In addition to being an accomplished clinician/researcher Dr. Minuk is a wonderful person. He has demonstrated time and time again his genuine concern and desire to see others excel. I am truly fortunate to have had Dr. Minuk as a mentor in my education.

I really enjoyed working with all the members of the Liver Diseases Unit, both present and past. All of the staff was supportive and always willing to collaborate in the research studies conducted in the laboratory. I would especially like to thank Dr. Manna Zhang and Mrs. Duane Li for their technical assistance with the animal experiments, Dr. Gong and his research group for their support and Kim Hawkins, Rachel Gernstein and Rose Bazylewski for their assistance with the clinical study.

I would also like to acknowledge Dr. Jim Peeling and his laboratory for their support and technical assistance in performing the MRS experiments. Special thanks goes out to Vyacheslav Volotovskyy and Richard Buist who played pivotal roles in designing the MR coil and developing the CSI pulse sequence for *in vivo* MRS respectively.

I would like to thank Drs Lawrence Ryner and Valerie Strevens at the Institute for Biodiagnostics and Corinne LeBlanc in the Department of Radiology for their assistance and collaborative efforts which enabled us to perform the human patient study.

I wish to acknowledge the Department of Pharmacology and Therapeutics for their support and help throughout my degree. In addition to providing an excellent graduate studies program they also provided monetary assistance, which was greatly appreciated. Other agencies whose financial support I would like to acknowledge include the Health Science Centre Foundation and the Canadian Liver Foundation.

I must also express a genuine thanks to the members of my advisory committee; Drs. Jim Peeling, Frank Burczynski and Jeremy Lipschitz. Their constructive suggestions and eagerness to act as advisors throughout my degree was greatly appreciated.

Finally, I would like to acknowledge the support of my family. To my parents, Hugh and Wilma, my sister, Esther, and my aunt Miranda I must express a heart felt thank you. It has been through your faithful support and consistent encouragement throughout my education that I have been able to achieve such accomplishments.

TABLE OF CONTENTS

LIST OF ABBREVIATIONS

	angstrom
ADP	adenosine diphosphate
ALT	alanine aminotransferase
AMP	adenosine monophosphate
AST	aspartate aminotransferase
ATP	adenosine triphosphate
B_0	static magnetic field
B_1	radiofrequency magnetic field
^{13}C	carbon-13
CBDL	common bile duct ligation
CCl_4	carbon tetrachloride
CPM	counts per minute
CSI	chemical shift imaging
CT	computer tomography
CTP	cytidine triphosphate
D-galN	D-galactosamine
DNA	deoxyribose nucleic acid
ER	endoplasmic reticulum
FID	free induction decay
FOV	field of view
GPC	glycerophosphocholine
GPE	glycerophosphoethanolamine

GTP	guanosine triphosphate
^{1}H	hydrogen-1
ICG	indocyanine green
IgG	immunoglobulin G
INR	international normalized ratio
ITP	inosine triphosphate
LCAR	liver cell area ratio
MDP	methylene diphosphonic acid
MRI	magnetic resonance imaging
MRS	magnetic resonance spectroscopy
NTP	nucleotide triphosphate
OLT	orthotopic liver transplant
^{31}P	phosphorus-31
PC	phosphocholine
PCNA	proliferating cell nuclear antigen
PCr	phosphocreatine
PE	phosphoethanolamine
PDE	phosphodiesters
PHx	partial hepatectomy
Pi	inorganic phosphate
PME	phosphomonoesters
PPA	phenylphosphonic acid
PPM	parts per million

RF	radiofrequency
ROI	region of interest
SEM	standard error measure
T_1	longitudinal relaxation time
TAA	thioacetamide
TCA	trichloroacetic acid
TE	echo time
TM	mixing time
TR	repetition time
UDP	uridine diphosphate
UTP	uridine triphosphate

LIST OF FIGURES

LIST OF TABLES

ABSTRACT

Adenosine triphosphate (ATP) and other high-energy molecules play a central role in the functional and morphological integrity of cells. During periods when energy levels are low the viability of cells may be compromised as demands may exceed supply. Ultimately these events may result in organ dysfunction. As such, disturbances in cellular energy metabolism have been implicated in the pathogenesis in a variety of diseases. *In vivo* phosphorus-31 magnetic resonance spectroscopy (^{31}P MRS) is a non-invasive method that permits direct assessment of energy levels of tissues *in situ*. The principal aim of the present study was to determine whether differences in energy status of the liver, as determined by ^{31}P MRS, could assess the extent of underlying liver disease.

Partial hepatectomies (PHx) were first employed in rats to determine whether changes in hepatic energy levels in healthy rats reflected the amount of residual liver parenchyma remaining after resection. Following 40%, 70% and 90% PHx hepatic energy levels, as reflected by ATP and ATP/Pi, decreased in proportion to the extent of resection with significantly lower ATP levels occurring following 70% and 90% PHx.

Various animal models of acute and chronic liver disease also displayed reduced energy levels with increasing severity of disease. During acute liver failure lower ATP levels were observed when more than 50% of the liver lobule was destroyed. Similar results were evident in rats subjected to parenchymal and cholestatic forms of chronic liver disease as reductions in hepatic ATP levels were only detected once extensive fibrosis or cirrhosis was established.

Patients with hepatitis C induced chronic liver disease also possessed lower hepatic ATP levels than healthy control subjects. However, these reductions did not occur until decompensated cirrhosis developed.

Taken together, the results from animal and human studies suggest that: 1) reduced hepatocyte numbers, (2) increased energy expenditure due to increased regenerative activity and functional demands, and (3) a decreased capacity to produce energy, all contribute to the reduction of hepatic ATP in advanced liver disease. The results also support the hypothesis that diminished energy reserves within the liver play a central role in the pathogenesis of hepatic dysfunction during liver disease.

CHAPTER I

INTRODUCTION

1.1. The Clinical Problem: An Overview

Liver disease is an important cause of morbidity and mortality in North America.[1] Each year thousands of individuals, from newborns to the elderly, are afflicted with this disease.[1, 2] Some forms of liver disease strike healthy individuals quickly and without warning leading to marked morbidity and incapacitation within weeks. Others evolve slowly and silently causing progressive deterioration of the patient's health. For many with liver disease the outcome is grim. Current statistics indicate that liver disease is now ranked as the fourth most common cause of death by disease among working adults and the tenth leading cause of death overall.[3] This striking statistic highlights the importance of this disease. Once liver disease becomes progressive and is no longer self-limiting there are few treatments available. The disease often charts an insidious course that spirals into liver failure and the only know curative intervention for this end-stage sequelae is orthotopic liver transplant.[4] With the current shortage of donor livers world wide many patients die from their liver disease while waiting for a transplant.[5]

Patients that succumb to liver disease usually die from either i) hepatocellular insufficiency (commonly referred to as "liver failure"), (ii) vascular complications (portal hypertensive variceal bleed) or (iii) hepatic malignancy. Of the three, liver failure is the major cause of mortality among patients with liver disease.[1, 6] Hepatocytes constitute the majority of the liver cell mass and are responsible for carrying out hundreds of essential biochemical processes.[7, 8] In addition, the integrity of many organ systems are dependent upon a well functioning liver, such that liver disease is often accompanied with multiorgan dysfunction.[9, 10] Thus when liver cells are damaged and hepatic function

becomes compromised it is not surprising that the outcome of liver disease can be so morbid.

The need to accurately evaluate the status of the liver (particularly hepatocellular function) is very important for the treatment and management of patients with liver disease. However, the current tests used to assess the liver suffer from many limitations including low sensitivity and poor specificity.[11, 12]

The work outlined in this thesis examines the utility of magnetic resonance spectroscopy (MRS) as a novel means of assessing the health and functional status of the liver. This radiologic technique can provide a direct and non-invasive biochemical evaluation of tissues *in situ*. A modality such as this holds great promise in diagnostic medicine, as valuable information and insights can be acquired on disease processes.[13-15] In this thesis several experiments are designed (involving animal and human subjects) to assess applicability of MRS as a diagnostic tool for liver disease. In the first section of the thesis normal liver physiology will be discussed with respect to hepatic structure and function. From there, further discussions on liver pathophysiology, clinical and laboratory methods for evaluating the liver and fundamental concepts and clinical applications of MRS will follow.

1.2. The Liver: Structure and Function

1.2.1. FUNCTIONAL DIVERSITY

The liver is the largest solid organ in the body accounting for approximately 2-3% of the body weight in adults and 5% in new borns.[16-19] Occupying most of the upper right quadrant of the abdomen this complex and intricate organ is capable of operating as a metabolic, endocrine and exocrine gland. The vast biochemical pathways within liver cells allow them to perform numerous duties. The liver plays a central role in the intermediary metabolism and distribution of carbohydrates, amino acids, lipids and vitamins. Circulating toxins and drugs are also extracted by the liver and metabolized to harmless by-products through an elaborate system of detoxifying enzymes. In addition, the liver is also actively involved in the formation of bile and the synthesis of numerous plasma proteins. Specialized phagocytic cells within the liver play an important role in the body's immune system, as hepatic sinusoidal lining cells are quantitatively the most effective site of phagocytosis of particulate materials. Finally, the liver can act as a vascular reservoir allowing it to participate in the regulation of blood volume and blood flow. Collectively these activities permit the liver to perform well over 500 functions that are essential for life.

1.2.2. STRUCTURAL ORGANIZATION

1.2.2.1. Vascular and Biliary System

Central to the functional diversity of the liver is its structural design. Uniquely situated between the digestive tract and the rest of the body, the liver receives a dual blood supply from the portal vein and hepatic artery. The two sources of blood supplying

the liver differ both quantitatively and qualitatively. Seventy-five percent of the blood supplied to the liver occurs through the portal vein, which is a collection of venous tributaries that drain the intestines, stomach, spleen and pancreas. Thus the portal system conveys blood that is rich with ingested material from the digestive tract. This strategic arrangement positions the liver to act as a fare way between the alimentary tract and the rest of the body. Being the first organ exposed to items from the digestive tract the liver is uniquely situated to extract, process, and sort digested material for subsequent distribution or elimination.

The hepatic artery, which branches off the celiac trunk from the aorta, contributes approximately 25% of the blood supply to the liver. This blood is rich in oxygen and is the primary means whereby liver cells receive oxygenated blood. As such, adequate hepatic arterial flow is essential for the proper functioning of the highly active liver parenchyma.

These two main blood vessels enter the liver from its inferior surface at the *porta hepatis* accompanied by the common bile duct, lymphatic vessels and nerves. Within the liver this tract of vessels split into two branches dividing the liver functionally into right and left lobes. Each lobe operates independently with its own arterial and portal venous supply and its own venous and biliary drainage. However, anatomically the liver is divided into four lobes: right, left, quadrate and caudate lobes. The right and left tracts of vessels undergo further divisions that create interlobar, interlobular and eventually terminal vessels. At this level, the terminal branches of the portal vein and hepatic artery feed directly into the hepatic sinusoid, watershed areas that surround and directly bath the hepatic parenchymal cells. The sinusoids converge towards terminal hepatic venules

which merge to form sublobular veins, sublobar veins, and right and left hepatic veins that form the hepatic vein proper which finally drains into the inferior vena cava.

Running in the opposite direction to the hepatic artery and portal vein is the biliary system. Bile which is formed in hepatic parenchymal cells flows into fine ducts called bile canaliculi, from there it enters intralobular ductules, larger interhepatic ducts, and finally into right and left hepatic ducts, which merge from the liver, at the *portal hepatis*, as the hepatic duct proper.

1.2.3. CELLUAR COMPOSITION

The functional capability of the liver resides within its cellular constituents. The liver is composed of both non-parenchymal and parenchymal cells. The non-parenchymal cells consist of a heterogeneous population of sinusoidal lining cells and bile duct epithelial cells. Conversely, the parenchymal cell population is made up solely of hepatocytes.

1.2.3.1. Sinusoidal Lining Cells

Cells found within the hepatic sinusoid include the endothelial and Kupffer cells. Hepatic endothelial cells, similar to endothelium found in other blood vessels of the body, line the walls of the vascular compartment. However, sinusoidal endothelial cells differ from those in regular vessels in that they contain large fenestrae.[20] These fenestrae, approximately 1000 Å in diameter, are often grouped together in clusters of 10 or more to form networks of sieve plates.[20, 21] This feature permits the endothelium to be highly porous which allows the rapid interchange of blood between the vascular and

perisinusoidal compartments. [22] Kupffer cells are a second class of sinusoidal cells. These cells are resident macrophages within the liver that stretch across the lumen of the sinusoids. In this position Kupffer cells play a key role in the immune system by effectively removing waste and foreign material that enters the liver.

Just outside the hepatic sinusoid, in between the endothial cell and the hepatic parenchyma is the perisinusoidal space commonly called the space of Disse. Hepatic stellates cells occupy this space wrapped around and in close proximity to basal surface of the endothelial wall of the sinusoids. Hepatic stellate cells serve primarily to store vitamin A and maintain a healthy hepatic extracellular matrix. Under pathological conditions stellate cells transform into myofibroblasts and play a major role in liver fibrosis.[23] Collectively, the cells within the sinusoids and the parasinusiodal space make up approximately 14-16% of the cell population within the liver.[24]

1.2.3.2. Bile Duct Epithelial Cells

Bile duct epithelial cells, also known as cholangiocytes, line the entire biliary tree. Although cholangiocytes make up only 4-5 % of the total liver cell population they perform important functions in the biliary system.[25] Cholangiocytes alter the composition of bile by secreting and reabsorbing various metabolites, ions and molecules into the biliary tract.

Other non-parenchymal cell types can also be found in the liver where they serve supportive roles in tissues like blood vessels, connective tissue, lymphatics and nerves.

1.2.3.3. The Parenchymal Cell

The hepatocyte is unrivalled by any other cell type in the liver in terms of cellular mass, functional diversity and complexity. Hepatocytes are estimated to number approximately 250 billion in the normal adult liver and account for about 80% of the total cellular population.[24] Functionally, the hepatocyte also carries the majority of the work load imposed upon this organ and as such is considered the 'work horse' of the liver. Activities ranging from the storage and timely release of metabolic fuels, synthesis and secretion of plasma proteins and the uptake and degradation of endogenous and exogenous compounds are all performed by hepatocytes.[7, 8] Key to the functional diversity of the hepatocyte is the structural arrangement of the hepatic parenchyma.

1.2.3.3.1. The Hepatic Acinus

The organization of hepatocytes within the liver can be described as an acinar arrangement. Rappaport et al. first described the hepatic acinus as a concentric cluster of hepatocytes organized around a terminal portal venule and its accompanying hepatic arterioles, bile ducts, lymphatics and nerve fibers.[26] Located in the periphery, terminal hepatic venules can be found surrounding this arrangement. A typical illustration of the hepatic acinus is presented in Figure 1.

Figure 1. The hepatic acinus, consisting of a concentric cluster of hepatocytes organized around a terminal portal vein (TPV), terminal hepatic arteriole (THA), terminal bile ductule (TBD) and lymphatics (L). The TPV and THA drain directly into the hepatic sinusoids (HS), which run along the outside of the liver cell plates (LCP). The HS drain into the terminal hepatic venules (THV). The hepatocytes within the LCP are located in zone 1, 2 or 3 of the hepatic acinus.[27]

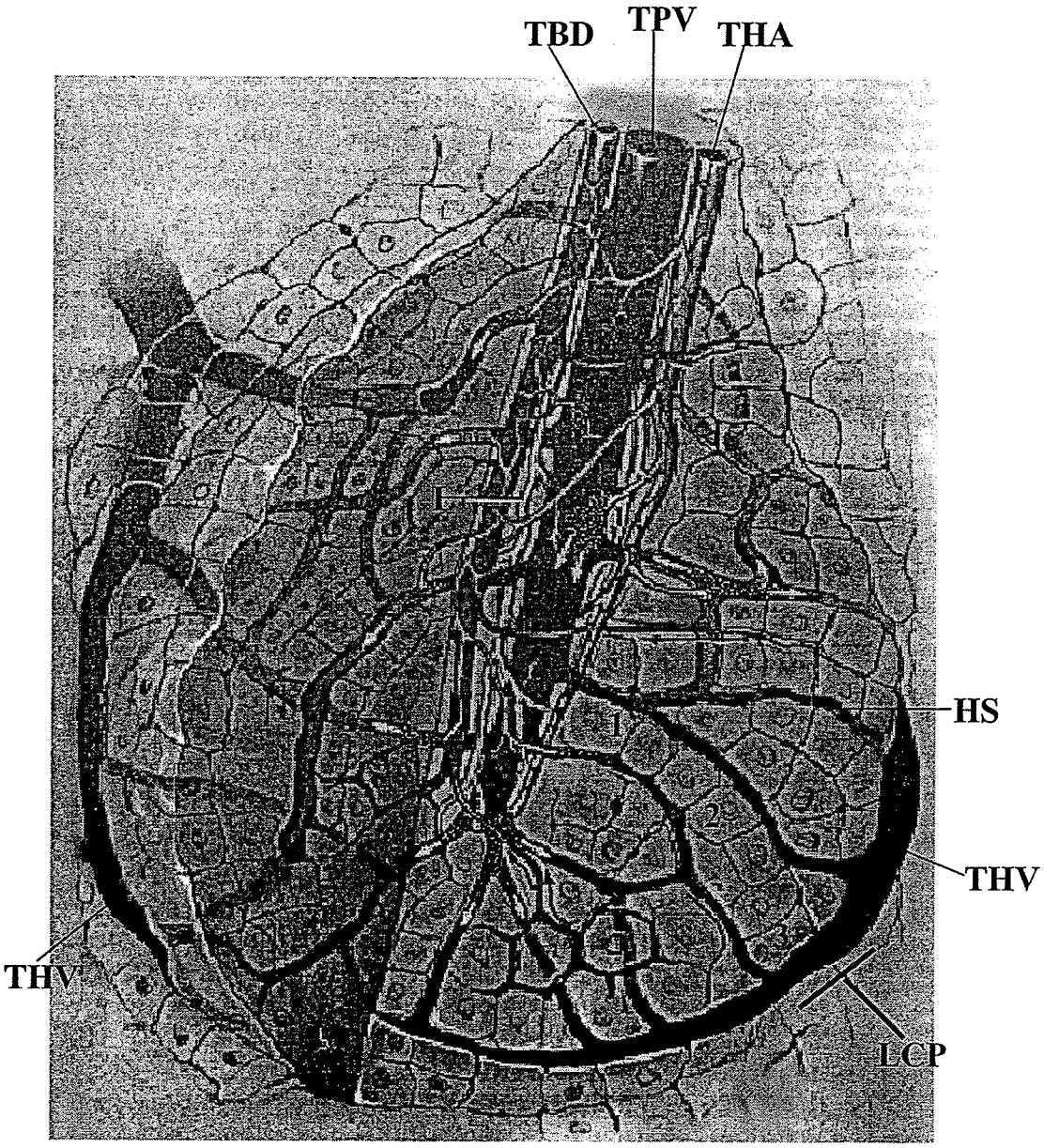
TBD
TPV
THA
HS
THV
THV
LCP

1.2.3.3.2. The Liver Cell Plate

Between the portal tract and the terminal hepatic venule hepatocytes are organized into liver cell plates. Within the liver cell plate, hepatocytes are arranged in single rows one cell thick with approximately 15-25 hepatocytes spanning the distance between the portal triad and terminal venule.[28] Hepatocytes closest to the portal triad are described as periportal or zone 1 hepatocytes, those in the middle of the cell plate are called zone 2 hepatocytes and finally those near the terminal venule are termed perivenous or zone 3 hepatocytes (Fig. 1).

Due to the unique characteristics of sinusoidal endothelium, blood flowing into the hepatic sinusoid readily passes into the space of Disse and perfuses the hepatocytes in the liver cell plate. The flow of blood through the sinusoids and down the liver cell plate is unidirectional. Thus hepatocytes near the proximal end of the sinusoid will be exposed to the highest concentration of incoming solutes, substrates and hormones. As the blood flows down the liver cell plate its composition progressively changes as substances are both extracted from and secreted into the blood. Once this blood reaches the distal end of the liver cell plate (zone 3) it is markedly different from that initially entering the sinusoids. This gradient of solutes and substrates creates heterogenous microenviroments across the liver cell plate such that functional heterogeniety exists among hepatocytes within a single hepatic acinus.[7, 8, 29] Differences in hepatocyte metabolism with respect to oxidative and ammonia metabolism are two common examples of functional herogeneity across the hepatic acinus.

1.2.3.3.3. Hepatocyte Ultrastructure

The morphological features of the individual hepatocyte also facilitate the vast functional capacity of this cell. The hepatocyte is a polyhedral cell with three distinct membrane surfaces, which include the basal, lateral and apical surfaces.[30] The basal surface of the hepatocyte, also called the sinusoidal front, is the membrane area that faces the space of Disse. Most hepatocytes within the plate have two or three contiguous surfaces exposed to the space of Disse and collectively the basal surface accounts for approximately 72% of the total surface area of the hepatocyte.[30] Irregular microvilli present on the basal surface also greatly amplify the surface area available for the exchange of substances between the vascular and parenchymal compartments. In fact electron microscopy studies have demonstrated that hepatocyte microvilla actually project directly into larger endothelial fenestrations permitting more direct and intimate contact with the vascular compartment.[21] The high capacity for exchange across the sinusoidal front is further facilitated by the numerous receptors, secretory vesicles and clathrin-coated pits present on the basal surface of the hepatocyte.

The lateral and apical surfaces of hepatocytes lie between adjacent parenchymal cells. Cell-cell junctions typically line the lateral surface, where tight junctions, zonula adherens, desmosomes and gap junctions may all be found.[30] These junctions allow for closer contact between hepatocytes and more efficient communication between cells. The apical surface is located midway down the lateral surface. This surface is formed from specialized co-joining grooves that are lined with biliary epithelia. When the apical grooves of two adjacent hepatocytes come in contact they form an enclosed segment of

the biliary system called the biliary canaliculus. The canalicular surface is specialized to transport bile acids, products of detoxification, lipids and other solutes into the biliary system. Like the basal surface, microvilli present on the canalicular membrane serve to increase the amount of surface area available for exchange and transport of molecules. The bile canaliculi form a continuous network of channels through-out the liver cell plate which drain into the intralobular ductules.

1.2.4. LIVER REGENERATION

The liver is one of the few tissues in the body with the capacity to undergo regeneration. Unlike other regenerating tissues (bone marrow and skin) which recruit stem cells to divide, in the liver, in the absence of fulminant hepatic failure, only mature hepatocytes proliferate to restore lost liver mass.[31, 32] The process of regeneration follows a complex series of highly synchronized events which involves an initial phase of hepatocyte hypertrophy followed by a subsequent phase of hyperplasia, which is characterized by accelerated rates of DNA synthesis.[33] In the immediate period following hepatic injury the expression of immediate early pro-oncogenes (c-myc and c-ras) increase markedly in hepatocytes to prime the liver for subsequent proliferation.[32, 34] During the pre-replicative phase glycogen levels become depleted and lipids and fluids accumulate causing cell swelling.[31, 32] Circulating levels of growth stimulating hormones, cytokines and growth factors also increase during the pre-replicative phase and remain elevated throughout the replicative phase of regeneration.[32, 35, 36] Some of the more potent mitogenic factors include hepatocyte and epidermal growth factors, transforming growth factor α, interleukin-6 and tumor necrosis factor. During this event circulating co-

mitogens such as estrogen, glucagons and insulin can serve to upregulate the activities of the mitogenic factors.[32] The integration of all these events serves to alter the gene expression and metabolic activity of the cell to promote liver regeneration. The wave of regenerative activity is believed to begin in the periportal cells and proceeds down the liver plate to the perivenous region.[37] Depending on the extent of liver injury most hepatocytes within the residual liver will participate in one to two proliferative cycles.[38] Non-parenchymal cells also proliferate in the regenerating liver, however, their peak proliferative response trails that of hepatocytes.[39, 40] Within the healthy liver the regenerative response is both efficient and complete. Studies have documented that the normal human liver can safely tolerate a 70-80 % resection with complete restitution of liver mass and function within three to five months of the operation.[41, 42]

1.2.5. The Achilles Heel

The discussion thus far has highlighted the importance of the structural and organizational features of the liver; its strategic position between the digestive tract and the body, the unique arrangement of the hepatic acinus, and the accessibility of solute interchange between the parenchymal and sinusoidal compartments. All of these facilitate the many duties carried out by the liver. Equally important to a well functioning liver is a healthy population of hepatocytes. However, the same structural features (described above) that permit the functional success of this organ also leaves it vulnerable to toxins and a host of other harmful compounds. This susceptibility may explain why the liver is one of the few tissues in the body capable of repairing itself by regeneration. Low-grade short-lived injuries to the liver are easily handled by the regenerative

response. However, if an event should occur where the regenerative response is overwhelmed, hindered or even delayed by injurious stimuli dire consequences may ensue due to hepatic insufficiency.[43] This is best exemplified in the setting of liver disease.

1.3. Liver Disease

Hepatocellular injury and varying degrees of hepatic dysfunction are hallmark features common to both acute and chronic forms of liver disease. In acute liver disease the onset of liver injury and functional deficits develop rapidly, while for chronic liver disease the course of the disease is often long and progression slow. Common to both forms of liver disease is the deteriorating status of the liver, which manifests as systemic complications. There are numerous clinical signs and symptoms that reflect impaired hepatic function in the setting of liver disease.

1.3.1. Symptoms of Liver Disease

1.3.1.1. Non-specific Symptoms

Fatigue, malaise, listlessness and gradual weight loss are all non-specific symptoms commonly associated with liver disease. The pathogenesis of these symptoms are unknown, but high levels of circulating cytokines (particularly, interleukin-1 and tumor necrosis factor) associated with liver disease have recently been implicated to induce catabolic and endocrine changes that promote both fatigue and weight-loss.[44-46] In addition, the central role the liver plays in the processing and distribution of metabolic

fuels[47] should not be overlooked, as an improperly functioning liver can disrupt the energy economy within the body leading to some of the symptoms described.

1.3.1.2. Jaundice

There is a constant turn-over of heme proteins within the body. Once slated for degradation the heme moiety of the protein undergoes a two-step conversion to the more lipid soluble compound, bilirubin.[48] The liver is primarily responsible for the uptake and elimination of bilirubin.[49] During this process bilirubin undergoes subcellular translocation to the endoplasmic reticulum where it is modified to a more water soluble form, thus allowing its excretion into bile for fecal elimination. When the liver parenchyma is severely damaged and no longer functions properly, the uptake, metabolism and excretion of bilirubin is hindered. As a result, bilirubin accumulates and settles within tissues such as the skin and sclera.[49] The deposition of bilirubin in these sites cause a yellowish coloration to the eyes and skin, which is a feature referred to as scleral icterus and jaundice respectively.

1.3.1.3. Coagulopathy

The liver plays a key role in the regulation of the coagulation cascade as it synthesizes most of clotting factors and inhibitory modulators necessary for proper hemostasis. Disturbances in liver function due to hepatocellular injury can result in marked impairment of the clotting cascade. The clotting factors most affected by hepatic insufficiency are factors V, VII, VIII and fibrinogen.[50] Decreased levels of the inhibitory modulators (antithrombin III, protein C, heparin cofactor II) have also been documented

in patients with liver disease. Collectively, these defects prolong clotting times and potentiate hemorrhagic events.

1.3.1.4. Ascites

Ascites is a condition characterized by the excessive retention of fluid within the abdominal cavity. While ascites may accompany a number of disease states, liver disease is the leading cause for this condition. In the setting of liver disease, many factors contribute to ascites formation, including peripheral arterial vasodilatation, renal sodium retention and sinusoidal hypertension with marked lymph formation and accumulation. Hepatocellular dysfunction is believed to contribute to the process via impaired hepatic synthesis of serum albumin, which reduces oncotic pressures within the sinusoids. Together with portal hypertension, this causes fluid to accumulate within the peritoneal cavity and further potentiates the formation of ascites. Also relevant is the liver's ability to clear selected compounds from the circulation which is reduced with liver disease, consequently, hormones such as aldosterone acquire an extended half-life and this in turn promotes both sodium and water retention.

1.3.1.5. Encephalopathy

The functional integrity of the central nervous system is highly dependent upon a well functioning liver.[51] The liver acts not only to provide appropriate fuels for the brain, but also to remove endogenous and exogenous neurotoxins from the body. If the hepatic parenchyma is hindered or damaged to the point where it is incapable of removing neurotoxic/inhibitory molecules like ammonia, aromatic amino acids and endogenous

benzodiazepines from the circulation neurological disturbances will develop.[9] Neurological manifestations range from subtle behavioural changes and forgetfulness to delirium, seizures or deep coma depending on the degree and rapidity of the hepatic insufficiency.[51]

1.3.2. Evaluation of Liver Status

Clearly the clinical spectrum of liver disease is vast. Some patients experience only mild nausea and fatigue while others can suffer from life threatening multi-system failure. The severity of the disease is dependent upon the extent in which the structural and functional integrity of the liver is compromised. Providing an accurate assessment of liver disease severity is essential as it influences patient prognosis and decisions regarding therapeutic interventions. However, the task of evaluating the status of the liver is a difficult clinical problem. The liver is not as accessible for evaluation as some other organs; despite this, several modalities can be employed to address this task. Clinical tests used to evaluate the status of the liver can be categorized as methods that monitor: liver function, anatomic structure (imaging studies), and morphology (histologic studies).

1.3.2.1. Liver Function Tests

The term 'liver function test' often refers to a large group of laboratory tests used by physicians to help evaluate and manage patients with liver disease. This term includes i) conventional liver function tests, (ii) quantitative liver function tests and (iii) tests of liver injury.

1.3.2.1.1. Conventional Liver Function Tests

This group of tests routinely performed in the laboratory provide a measure of liver function, however, the assessments are not quantitative.

1.3.2.1.1.1. Bilirubin

Serum bilirubin levels become elevated in settings of increased production, reduced clearance, impaired metabolism and/or decreased excretion. Aside from the setting of increased production, elevated serum bilirubin levels can be interpreted as indicative of liver dysfunction reflecting impaired hepatocyte activity and/or cholestasis. The main limitation of this test is its insensitivity. Serum bilirubin levels do not become elevated until the liver has lost at least one-half of its excretory capacity.[12] The test is also non-specific as hyperbilirubinemia can result from haemolytic conditions.

1.3.2.1.1.2. Ammonia

Blood ammonia levels have also been used as an index of the liver's functional capacity as well as the severity of hepatic encephalopathy. However, hyperammonemia is not specific for liver disease (elevated levels also occur with poor sample preparation and in patients with certain congenital enzyme deficiencies) and blood ammonia levels do not correlate well with presence or stage of hepatic encephalopathy.[12] For these reasons many centres do not routinely use blood ammonia measurements as an index of liver function.

1.3.2.1.1.3. Albumin

Albumin is the major protein synthesized by the liver, as such its blood levels can serve as an index of the synthetic capacity of the liver. When the status of the liver is compromised, hepatic protein synthesis may become impaired and the production of albumin reduced. However, several factors make serum albumin concentrations a difficult parameter to interpret.[52] First, the liver can synthesize albumin at twice the required basal rate, thus high rates of production can compensate for and mask minor impairments in liver function. Secondly, the half-life of albumin is approximately three weeks, therefore, changes in serum albumin levels occur too slowly for it to be informative in settings of acute liver disease. Third, up to two thirds of the body's albumin is distributed into extravascular compartments and movements of albumin across compartments can confound serum measurements. Finally, serum albumin concentrations may decrease as a result of non-hepatic disorders such as proteinuria, malnutrition and inflammatory states like burns, trauma and sepsis.

1.3.2.1.1.4. Prothrombin Time

The synthetic capacity of the liver can also be measured by prothrombin times. The liver synthesizes many of the factors in the clotting cascade, including factor VII which has a half-life of six hours.[12] Hence, prothrombin times are sensitive to rapid changes in liver synthetic function. Similar to other conventional liver function tests, prothrombin times measurements are limited by insensitivity and non-specificity. This test can be normal in mild and early hepatocellular injury, upwards of 80 percent of the

liver's synthetic capacity must be lost before abnormal prothrombin times are detected.[12] Prolongation in prothrombin times may also result from vitamin K deficiency, this can occur with chronic cholestasis, fat malabsorption from diseases of the pancreas or small intestine and prolonged use of antimicrobial agents that alter Vitamin K synthesizing intestinal flora.

1.3.2.1.2. Tests of Liver Injury

Although this group of tests are classified as 'liver function tests' they do not evaluate liver function per se. Rather these tests measure the serum levels of liver enzymes as an indication of hepatocellular damage or impaired bile flow.

The most commonly used markers of hepatocyte injury are the aminotransferases, aspartate aminotransferases (AST) and alanine aminotransferase (ALT). Both enzymes are present in the hepatocyte, the former in both the cytosol and mitochondria while the latter is localized in the cytosol. Both AST and ALT are normally present in the serum at low levels (<30-40 U/L), with hepatocellular injury the integrity of the hepatocyte membrane is lost and these enzymes leak into the circulation. Depending on the degree of hepatocyte necrosis, enzyme levels reaching several thousand units per litre may be detected during liver disease.[53] Although measurements of serum aminotransferase provide a general indication of liver damage, their levels do not directly correlate with the extent of liver damage.[12, 54] Moreover, normal enzyme levels do not exclude the presence of hepatocellular damage.[55, 56] Finally, elevation in serum aminotransferase levels, especially of AST, are not specific for liver injury, as these enzymes may also increase with skeletal muscle injury or cardiac myopathy.

Lactate dehydrogenase has also been used as a maker of heparocellular injury, however, it suffers the same shortcomings as the aminotransferases. Other common enzyme markers of liver injury include alkaline phosphatase, gamma glutamyltransferase and 5'-nucleotidase. Elevations in these enzymes are indicative of cholestasis.

1.3.2.1.3. Quantitative Liver Function Tests

Quantitative liver function tests are a group of assays that measure the liver's ability to clear certain exogenous compounds. The selected compound must be one that is eliminated mainly or exclusively by the liver. During this procedure the test compound is administered to the subject and samples, typically blood, are collected over a given period to calculate hepatic clearance rates. Depending on the test compound selected these tests may reflect liver function, hepatic blood flow or a combination of both processes.

Indocyanine green (ICG), perhaps one of the most popular quantitative liver function tests, is an anionic dye that is taken up solely by the liver and excreted unchanged. Although ICG clearance parameters are best known to provide information on hepatic blood flow, determination of ICG clearance at 15 min or its maximal removal rate have been used to estimate hepatic function.[57, 58] Several studies have demonstrated that the ICG retention times are effective in predicting post-operative liver failure in cirrhotic patients. However, these reports have not been universally transposable to other centres.[59, 60] An additional shortcoming of ICG measurements is that it can not be reliably performed in the presence of marked jaundice since bilirubin and ICG share the same vascular carriers.

Clearance exams involving galactose, caffeine, aminopyrine, antipyrine and trimethadone are alternative test compounds that can be used to assess the metabolic capacity of the liver.[61-63] While all of these tests have proven to accurately assess hepatic microsomal/ metabolic activity, they only provide information on individual detoxifying/ clearance pathways within the liver. Furthermore it is well documented that hepatic microsomal / metabolic activity decreases with age in the absence of hepatocellular dysfunction[64] and that hepatic elimination pathways are not uniformly impaired in liver disease.[65]

In most centres quantitative liver function tests are not included in the general clinical work up for patients with liver disease.[63] Although these tests can provide additional quantitative information regarding specific functional processes, their clinical applicability is limited by inaccuracies, cumbersome data collection and/or difficulties in interpretation. For these reasons quantitative liver function tests have largely remained a research tool.

1.3.2.2. Child's Classification Systems

In an attempt to acquire information about the overall function of the liver a grading system was devised in which several liver function tests and clinical features of liver disease were combined to provide an index of the severity of liver dysfunction. Child first proposed such a system in 1964 to evaluate cirrhotic patients undergoing portal systemic shunt procedures.[66] A modified version of the classification system was later published by Pugh in 1973 where a point system was used to grade the severity of each test variable. Depending on the cumulative score, patients are classified in increasing

severity as either a Child's A, B or C.[67] The grading system is traditionally used to predict overall life expectancy and surgical mortality in patients with cirrhosis. The shortcoming of this system is the fact that it is based on clinical assessments and conventional liver function tests that already have limitations of their own. This may explain the variable successes reported with this classification system.[68]

1.3.2.3. Hepatic Imaging

Several imaging modalities are available for examining of the liver. These include: ultrasound, computer tomography (CT), magnetic resonance imaging (MRI) and scintigraphy (nuclear medicine). With the advent of digital imaging techniques and the development of novel contrast agents these imaging techniques are now able to provide highly detailed anatomical information of the liver. The modality of choice is dictated by the clinical scenario and the objectives of the imaging exam. Typically, ultrasound is indicated as the initial screening modality for most liver disorders due to its low-cost and wide spread availability.[69] When higher sensitivity and resolution is required CT or MRI is employed. Both techniques provide excellent spatial resolution and with the development of triple phase spiral CT both modalities now offer three-dimensional reconstructive imaging capabilities.[70] CT or MRI are indicated in the detection and characterization of focal masses and to a lesser extent, infiltrative lesions and diffuse liver diseases. With the recent advances in ultrasound, CT and MRI, scintigraphy has had a decreasing role in evaluations of the liver. At present, scintigraphy is occasionally used as an adjunctive imaging technique to CT or MRI. The main limitation of scintigraphy is its poor spatial resolution, thus it is rarely used in routine anatomical studies of the liver.

Instead, efforts have focused on the high sensitivity of this technique and the use of radiopharmaceuticals to provide information about targeted receptors or selected metabolic processes in the liver.[71, 72]

1.3.2.4. Liver Biopsy

To date, the liver biopsy remains an important diagnostic procedure in the management of hepatic disorders and the gold standard by which other diagnostic modalities for liver disease are assessed.[73-75] During this bedside procedure mechanical or trigger-enabled devices assist the physician in puncturing the liver parenchyma to obtain a biopsy sample by suction or the sequential release of a needle and cutting cannula.[76] The size of the biopsy specimens obtained from this procedure are typically 1-3 cm in length with a diameter ranging between 1.2 and 2.0 mm.[76] Provided an adequate specimen is obtained (at least six portal tracts present), histologic examination of tissue cores can provide valuable information regarding the diagnosis, grading and staging of liver disease. In spite of its superiority as a diagnostic tool, a number of problems surround the liver biopsy: first and foremost, the procedure is invasive, often painful and feared by most patients. Secondly there is an inherent risk of complications associated with this procedure such as hemorrhage, bile leakage and infection. Approximately 1-3 percent of patients require hospitalization for complications following a liver biopsy and in 0.015% the complication is fatal.[76, 77] Additional steps such as CT or ultrasound guidance can be employed during the biopsy procedure to help reduce the risk of serious complications.[78, 79] Alternatively, transjugular biopsies can be performed, however, this procedure can be technically difficult and requires the patient to be very cooperative.[76] Finally histological

interpretations of liver biopsy samples are subjective and significant interobserver variations can occur.[80]

1.3.2.5. The Problem

Accurate clinical evaluation of the liver is essential for effective management of patients with liver disease. Each of the techniques described above have their particular strengths and weaknesses. The functional assays, although informative, tend to be based on peripheral markers of liver function that are often subjected to extrahepatic influences. Conversely, the imaging modalities and liver biopsy procedures allow one to directly probe the liver; however, mainly structural/histological information is acquired from these methods. A technique that would offer the strengths of both approaches (i.e. a functional assessment of the liver that is both direct and non-invasive) would greatly enhance our capacity to evaluate the liver.

1.4. Magnetic Resonance Spectroscopy

The nuclear magnetic resonance phenomenon was first described in 1946.[81] Since this time there have been strong endeavours to apply this technology to study living systems. From these efforts two major biomedical applications emerged; magnetic resonance imaging (MRI) and magnetic resonance spectroscopy (MRS). The principle difference between the two radiological applications is that MRI generates anatomical images of the tissue under study based primarily on the detection of signals from tissue water, while MRS provides a biochemical profile of tissues based on their metabolite composition. Of the two applications, MRI quickly gained acceptance into the medical

field and has since emerged as a leading imaging modality in clinical radiology.[82] In contrast, MRS has not developed as quickly as MRI and to date is still confined to the research arena. MRS has not yet reached its full potential but active research in this field in ongoing. This technique affords researchers a unique opportunity to examine and quantify the metabolic composition of tissues in a non-invasive manner. Numerous published studies have already demonstrated that MRS has contributed significantly to our understanding of basic physiological as well as pathophysiological mechanisms.[15, 83, 84] Incorporating such a modality into clinical medicine would greatly advance current methods of diagnosing and managing disease.

1.4.1. Fundamental Principles of MRS

The basic principles of MRS are founded upon the intrinsic property of certain nuclei called magnetic spin. Several nuclei of biological importance such as hydrogen-1 (^{1}H), carbon-13 (^{13}C) and phosphorus-31 (^{31}P) exhibit this property. This characteristic causes the nuclei to behave like magnetic dipoles. In the absence of an external magnetic field the orientation of the magnetic dipoles are random and consequently no net magnetization results. If the nuclei are placed in a static magnetic field (B_o), as that found in an MR scanner, their magnetic dipoles will align (parallel or anti-parallel) and produce a net magnetization in the direction of B_o. Introduction of a second magnetic field (B_1) in the form of a radiofrequency (RF) pulse that is perpendicular to B_o and oscillating at an appropriate frequency (the resonance frequency of the considered nuclei) excites the nuclei to a new state causing them to align with the new field. The net magnetization of the nuclei will now be in the direction of B_1. A receiver device, called the MR probe,

located in the plane of B_1, is positioned to detect this signal. Once the RF pulse is removed the excited nuclei will begin to return to their equilibrium orientation in B_o (Fig. 2). During the relaxation period the amount of signal detected in the probe will decrease at a characteristic rate (relaxation time constant). This decreasing signal is called the free induction decay (FID). The FID is composed of signals from a single nuclear species, however, nuclei from different molecules will generate signals of slightly different frequencies due to the shielding effect of their slightly different chemical environment. This phenomenon, called chemical shift, is essential to MRS since it allows different molecules to be identified by their unique resonant frequency. This is visualized through an elaborate mathematical process, called the Fourier transformation, in which the time domain signal of the FID is converted into a spectrum in the frequency domain. In a typical MR spectrum the x-axis is a frequency scale which is usually expressed in parts per million (PPM) and the vertical axis is an intensity scale. Within the MR spectrum are many peaks, which are generated by molecules that contain magnetically active nuclei that resonate at a characteristic frequency. Quantitative information can also be derived from MR spectra as the area under the peaks are directly proportional to the concentration of the corresponding molecules in the studied sample.

Nuclei within living tissues also behave in this manner when placed in the magnetic field of an MRI scanner. Modified RF transmitter/receiver systems and multinuclear hardware would have to be installed into the clinical MRI scanner to permit

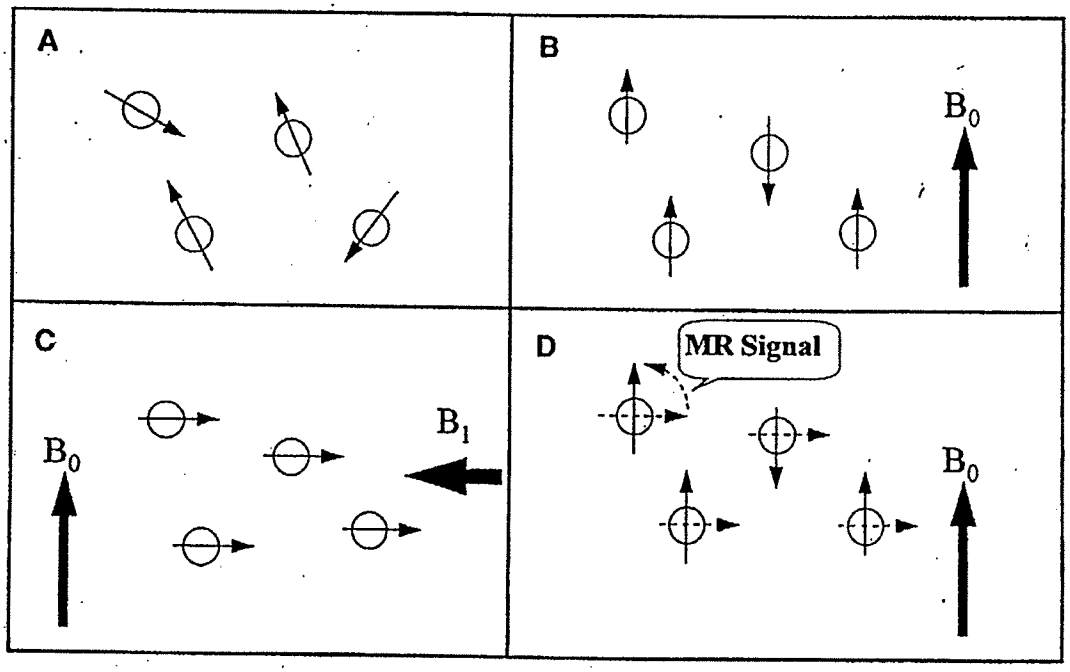

Figure 2. Diagrammatic representation of the behavior of MR-sensitive nuclei when subject to static and oscillating magnetic fields. (A) Nuclei precessing in a random fashion when no magnetic field is present. (B) Nuclei align parallel or antiparallel to the axis of the magnetic field (B_0). (C) Nuclei realign to a different axis upon the application of an oscillating magnetic field (B_1) perpendicular to the original magnetic field (B_0). (D) Nuclei return to their original orientation (along B_0) after termination of the B_1 pulse.[85]

MRS capabilities. This platform would allow the use of elaborate gradient systems of MRI scanners, which would permit the acquisition of localized spectra from specific regions within the body. By incorporating MR imaging into MRS studies one can perform sophisticated MRI guided spectroscopic examination of living organs *in situ*.

1.4.2. MRS and Liver

The majority of *in vivo* MRS studies on liver physiology and disease have utilized ^{31}P MRS. The ^{31}P MR spectrum provides an assessment of energy status, membrane turnover and glycolytic/ gluconeogenic intermediates in tissues. At clinical field strengths six resonances can be identified in ^{31}P MR spectrum of liver; these include: the phosphomonoesters (PME); inorganic phosphate (Pi); phosphodiesters (PDE) and three phosphate groups (α, β and γ) from nucleotide triphosphates (NTP). Several peaks found in the *in vivo* ^{31}P spectrum of liver are multicomponent resonances, hence if the individual components are to be resolved, stronger more homogeneous magnetic fields must be utilized. This can be accomplished by performing high resolution *in vitro* MRS experiments on tissue extracts.[86] The PME resonance is composed of 14 different components.[86, 87] Included in this broad resonance are contributions from intermediates of carbohydrate metabolism: glucose-6-phosphate, glycerol-3-phosphate, glycerol-1-phosphate, 3-phosphoglycerate, ribose-5-phosphate and 2,3-diphosphoglycerate; coenzyme A an important metabolite in fatty acid metabolism; phosphoethanolamine (PE) and phosphocholine (PC,) precursors in membrane synthesis and adenosine monophosphate (AMP).

The PDE signal consists of two overlapping peaks from glycerophosphoethanolamine (GPE) and glycerophosphocholine (GPC).[86] Both metabolites are degradation products of phospholipid catabolism. At clinical magnetic field strengths signal from the endoplasmic reticulum is believed to be the major contributor to the PDE resonance.[88, 89]

The NTP peaks are also multicomponent resonances consisting primarily of adenosine triphosphate (ATP) with minor contributions (10-20% of the signal) arising from the other NTP's like guanosine and uridine triphosphate.[90] Other phosphorylated nucleotides are also associated with some of the NTP resonances. The αNTP resonance contains contributions from αATP along with nicotinamide adenosine dinucleotide (NAD/ NADH) and αADP. Similarly, the γNTP resonance consists of overlapping signals from γATP and βADP. However, the βNTP peak arises solely from βATP. It should be noted that the majority of intracellular ADP is bound to protein; this restricted mobility renders bound ADP MRS invisible.[90] This phenomenon of reduced mobility and MRS invisibility also explains why signals from rigid macromolecules like membrane phospholipids are not present in the *in vivo* ^{31}P spectrum. Likewise the Pi resonance at 5.94 ppm is believed to represent approximately only 40% of intracellular levels of Pi as the remainder is thought to be bound to proteins in the mitochondria.[90]

Normally in most tissues of the body a prominent phosphocreatine (PCr) peak at 0 ppm will be present. The liver, however, does not possess the enzyme creatine kinase and therefore cannot synthesize PCr. Thus the presence of PCr in the *in vivo* ^{31}P spectrum of liver indicates spatial contamination of the spectrum with signals from surrounding muscle.

1.4.3. ^{31}P MRS and Liver Disease

The first reports of MRS of the liver were published approximately fifteen years ago.[91] These early studies involved basic experiments comparing ^{31}P MR spectra of normal liver from neonates, infants and adults.[92, 93] Other studies at this time utilized ^{31}P MRS to document the liver response to various metabolic challenges.[94, 95] Soon after, MRS was being applied to study liver disease, the majority of which involved patients with cirrhosis.[96, 97] A common finding throughout these studies was the increase in PME and decrease in PDE relative to the other hepatic metabolites. Higher levels of hepatic PME/PDE or PME/ATP and lower levels of PDE/ATP were typically reported in patients with hepatitis and cirrhosis compared to healthy controls.[97-100] Elevated ratios of PME are thought to arise from the increased levels of the cell membrane precursors PE and PC.[101] These metabolites are believed to increase as a result of the enhanced cell proliferation occurring in the regenerating cirrhotic liver. Similarly decreased PDE ratios were thought to reflect reduced levels of the cell membrane degradation products GPE and GPC.[101] Complementary *in vitro* studies conducted on liver biopsy samples obtained at liver transplantation reveal that indeed the concentrations of hepatic PE and PC are increased and GPE and GPC decreased in the cirrhotic liver.[100, 102] Subsequent *in vivo* studies went on to show that the relative increase in hepatic PME correlated with the indices of the Child-Pugh classification[97, 103] and the aminopyrine breath test.[97] These findings however have not been consistent, as other groups have reported the PME levels do not change with advanced disease.[104, 105] An alternative approach to assessing the severity of liver disease involved the use of exogenous compounds to measure the liver's metabolic capacity.[106-109] Several studies documented changes within the liver spectrum

following fructose administration. The phosphorylation of fructose results in the formation of fructose-1-phosphate, this can be detected as an increase in the PME resonance. Diminished rates of hepatic fructose metabolism were detected among patients with liver disease, however, investigators of this study raised concerns regarding the interpretation of these findings and the potential for this test to cause adverse affects in selected patient populations.[110]

1.4.3.1. Shortcomings of Previous Studies

Many of the previous studies have provided informative insights into the pathophysiology of liver disease,[14, 96, 100] however, considerably more important information can be acquired from *in vivo* MRS. In most of the published articles, ratios rather than absolute values were used to quantitate metabolite changes in the liver. The short-coming of this method is the uncertainty of not knowing which metabolite is having a greater affect on the changing ratio. The importance of individual metabolite levels to the particular biological process is not provided by ratios and in this regard definitive conclusions cannot be made. While quantitative MRS can provide this information, this method is generally avoided because it is more difficult to perform. Conducting absolute quantitative *in vivo* MRS studies requires that extra steps be performed (calibration experiments) and additional variables be accounted for and controlled (B_1 inhomogeneity and T_1 values), this often translates into longer scan times and more involved data processing. Although challenging, absolute quantitative MRS enables one to report individual metabolite changes with confidence.

Due to the limitations of metabolite ratio quantitation little information has been documented regarding the importance of hepatic ATP levels in liver disease. Central to the viability of all cells, whether healthy or diseased, is the availability of ATP.[111, 112] As the common currency of energy in all cells, ATP hydrolysis is coupled to thermodynamically unfavourable reactions, thereby allowing many biosynthetic, catabolic and transport processes to occur in the cell. Moreover, essential homeostatic processes such as ion regulation and membrane maintenance are governed by ATP availability. The levels of cellular ATP are regulated by a balance between ATP producing and consuming reactions. When the latter prevail intracellular levels of ATP become depleted and the cell is forced to sacrifice less essential acitivies and re-direct its remaining resources to maintaining cell viability. In this setting the functional capacity of the cell becomes compromised[113] and dysfunction becomes evident at the organ level. Hence, it seems reasonable to assume that the direct assessment of hepatic ATP levels would provide a robust measure of the health and functional capacity of the liver.

CHAPTER II

HYPOTHESIS AND OBJECTIVES

2.1. HYPOTHESIS

It is hypothesized that by utilizing ^{31}P MRS, differences in the bioenergetic status of the liver can serve as a valuable and accurate means of assessing the extent of liver disease.

2.2. SPECIFIC OBJECTIVES

To address this hypothesis a series of experiments involving both animal models and human subjects will be performed. In the first set of experiments ^{31}P MRS will be performed on various animals models of liver disease and the association between hepatic energy status and the severity of liver disease will be determined. Following these animal studies, ^{31}P MRS will be performed on a cohort of patients with chronic liver disease of varying severity. The latter study will assess the utility and feasibility of ^{31}P MRS as a diagnostic tool in human liver disease.

The specific objectives of the studies are to determine:

1) Whether ^{31}P MRS can detect changes in the hepatic energy levels of healthy rats following hepatic resection and to determine whether these energy changes reflect the percent of residual hepatic parenchyma remaining after different degrees of partial hepatectomy.

2) Whether the hepatic energy status as documented by ^{31}P MRS can accurately assess the severity of liver damage and is of prognostic value in a rat model of acute liver failure.

3) Whether hepatic energy status as documented by ^{31}P MRS could serve as a non-invasive means of documenting the progression of the liver disease to cirrhosis in a rat model of chronic liver disease.

4) Whether hepatic energy status as documented by ^{31}P MRS reflects differences in the severity of the chronic liver disease in patients with cirrhosis.

CHAPTER III

GENERAL METHODOLOGY

Phosphorus–31 Magnetic Resonance Spectroscopy in the Rat.

3.1. ^{31}P-Magnetic Resonance Spectroscopy

All MRS examinations performed on laboratory rats were conducted at the Health Sciences Centre Magnetic Resonance Laboratory. The laboratory houses a MSLX Bruker Biospec spectrometer equipped with a 7 Tesla 21cm bore horizontal magnet (Bruker, Karlsruhe, Germany). Prior to MR examinations animals were fasted overnight. All MR exams were conducted between 8:00 A.M. and 12:00 noon where animals were anesthetized (isoflurane 2% in N_2O/O_2 2:1 at 1l/min) and placed on their right side on a $^{31}P/^{1}H$ doubly-tunable double ring surface coil (15/40 mm diameter) operating at 121.5/300 MHz. A small vial containing methylene diphosphonic acid (MDP) was placed near the center of the coil to assist with subject positioning during MR imaging, calibration of the RF field strength at the region of interest (ROI), and for quantitation of metabolite concentrations. Snapshot-Flash MR images were acquired in the axial plane with repetition time (TR)/ echo time (TE)= 3.7/2.2 ms, slice thickness of 2 mm, field of view (FOV) 8 cm x 8 cm and a matrix size of 128 x 128. Localized shimming on the liver was performed using a VOSY sequence with a 15x 15x 25 mm^3 (lateral, vertical, and axial dimensions respectively) voxel using TE= 15 ms and a mixing time (TM) of 20 ms. The frequency of the coil was then tuned to phosphorus and the 90° pulse length was determined for the MDP reference vial near the center of the coil. A non-localized fully relaxed spectrum of the MDP reference was acquired for measurements of coil loading. Based on the characteristics of the B_1 field of the surface coil, a 90° pulse length was determined at the center of the ROI for subsequent localized spectroscopy. Localized ^{31}P liver spectra were acquired using two-dimensional chemical shift imaging (2D-CSI) with

a chemical shift selective suppression of the residual MDP resonance. Data acquisition parameters were FOV= 8.85 cm (horizontal) x 6.0 cm (vertical), 14 averages, TR= 3 s, matrix size= 8 x 8 zero filled to 16 x 16, acquisition size= 1K, zero-filled to 2 K, and sweep width= 4840 Hz.

3.2. Data Processing

Data processing was accomplished using WIN-MRI and WIN-NMR software (Bruker-Franzen Analytik GmbH, Bremen, Germany). Briefly, the free induction decay underwent 30 Hz exponential line broadening prior to Fourier transformation, and the resulting spectra were processed with manual phase and baseline correction. Peaks were registered relative to α-ATP resonance (–10 ppm) which served as an internal chemical shift reference. Finally, peak integrals were calculated by gaussian curve-fitting with all signals treated as singlets.

Corrections for minor contributions of metabolite signal arising from overlying skeletal muscle were performed as needed. Based on the percentage of phosphocreatine (PCr) contamination in the liver spectra, relative amounts of muscle signal contributing to each metabolite was calculated according to previous published data.[114, 115] These values were then subtracted from the appropriate integral to give a 'pure' liver reading.

3.3. Quantitation

For quantitation of hepatic metabolites, phantom experiments were performed as described by Meyerhoff et al.[116] A 250 ml flask containing 50 mM sodium phosphate (NaH_2PO_4, pH 7.2) served as a phantom, on which identical MRS examinations were

performed regularly throughout the experiment. The various metabolite concentrations were determined by the equation:

$$\mathbf{C = C_p \times I/I_p \times N_p/N \times S_p/S \times I_{ref(p)}/I_{ref}}$$ [117]

where...

C=	absolute tissue metabolite concentration in mmol/L
C_p=	concentration of phantom (p) solution used for calibration in mmol/L
I,I_p=	corresponding signal integrals (I)
N,N_p=	corresponding number of signal averages (N)
S,S_p=	corresponding saturation factors (S) calculated from measured T_1 times
I_{ref},$I_{ref(p)}$ =	corresponding signal integral of reference sample

Literature T_1 values for liver were used in the calculation for saturation factors.[118] Hepatic ATP levels were determined using the peak area of the β-ATP resonance, which is free of contributions from other phoshorylated adenosine species.[90]

CHAPTER IV

EXAMINATION OF REGENERATIVE ACTIVITY AND LIVER FUNCTION FOLLOWING PARTIAL HEPATECTOMY IN THE RAT UTILIZING ^{31}P MRS

4.1. Introduction

Hepatic resections are now more frequently performed in patients with primary and secondary hepatic malignancies as a result of advances in perioperative care, surgical technique and diagnostics.[119-121] Patients often develop signs or symptoms of liver dysfunction in the immediate post operative period as a result of reduced liver mass, but normal liver function resumes once the resected liver mass is restored.[122-124] However, adequate restoration of the liver mass may not occur when the liver disease is advanced, hence these patients may succumb to hepatic insufficiency.[125-127] The morbidity and mortality which arise as a result of hepatic complications following liver surgery may be reduced with further insight and documentation of the physiological alterations which occur in the liver following partial hepatectomy (PHx). The course of those events involves a complex series of molecular and macroscopic alterations, which are ultimately reflected in the processes of hepatic regeneration and dysfunction. Numerous investigators have used various experimental techniques in animal models of hepatic resection to document and characterize the processes of hepatic regeneration and dysfunction during the post-operative period.[40, 128-130] Although many of these techniques have provided important insights, the majority, by virtue of their invasiveness, have limited applicability to the clinical setting. One technique which provides valuable information and can readily be applied to the clinical setting is phosphorus-31 magnetic resonance spectroscopy (^{31}P-MRS).[13, 131, 132]

Initial animal studies have been performed in which *in vivo* ^{31}P MRS has been used to document metabolic changes in the liver following PHx.[133-136] All studies consistently report changes in the energetic status of the liver, as reflected by the ratio of

ATP/Pi, throughout the post-operative period. These studies, however, failed to elucidate the significance of ATP/Pi in relation to hepatic regeneration or dysfunction, as direct correlations were not performed with either parameter. The aims of the present study were three fold: first, to determine whether ^{31}P MRS-documented alterations in the hepatic energy levels following PHx in the rat best reflect hepatic regeneration or liver dysfunction or a combination of both processes; secondly, to determine whether changes in hepatic energy levels are proportional to the extent of hepatic resection; and finally, to document serial changes in hepatic energy metabolism in hepatectomized rats over a seven-day post-operative period.

4.2. MATERIALS AND METHODS

4.2.1. Animals

Adult male Sprague-Dawley rats weighing (300-350 g) were maintained on Purina rat chow and water ad libitum until the day before surgery when food but not water was withheld. All animals were kept in identical housing units on a 12-hr light and 12-hr dark cycle. This study was approved by the University of Manitoba Animal Ethics Committee.

4.2.2. Surgery

Partial hepatectomies were performed between 9 AM and noon each day while animals were under light ether anaesthesia. Forty and 70% PHx were performed according to the method described by Higgins and Anderson.[137] Ninety percent PHx were performed as described by Zieve et al.[138] Sham operations in which the appropriate portions of the liver were exteriorized and manipulated as in rats undergoing PHx, were also carried out.

Rats (4-6 per group) subjected to a 70% PHx and Sham operations underwent MRS examinations at 24 or 48 hrs following surgeries, while animals allocated to the 40% and 90% PHx groups (5-7 rats) had MRS examinations performed at 48 hrs post surgery. This time interval was selected as previous studies indicate it to be the period at which maximum hepatic regeneration and dysfunction occur,[128, 130, 139] and because the volume of the residual liver makes it more feasible to perform localization spectroscopy

at 48 than at 24 hrs. An additional group of fasted rats not subjected to surgery was also studied, these served as Baseline controls. Finally, serial MRS examinations were performed on a separate group of rats (N=5) preoperatively and at 24, 48, 72, 120 and 168 hrs following 70% PHx.

4.2.3. ^{31}P-Magnetic Resonance Spectroscopy

^{31}P-MRS exams were performed as described in chapter 3.

Immediately following MRS examinations, assays were performed on each animal in the first and second series of experiments to document hepatic regenerative activity and liver function by the following techniques.

4.2.4. Hepatic Regeneration Assays

4.2.4.1. Thymidine Incorporation

Thymidine incorporation assays were performed as described previously.[140] Briefly, rats received ^{3}[H]-thymidine (10 μCi per 200g of body weight) by intraperitoneal injection 1 hr prior to sacrifice. Approximately 0.5 g of each liver specimen obtained at sacrifice was homogenized (1:10 w/v) in a solution of 2.5 mM EDTA and aliquots were precipitated with trichloroacetic acid (TCA). ^{3}[H]-thymidine radioactivity in the precipitates was determined using a liquid scintillation counter (Wallac LKB 1219 Rackbeta, Stockholm, Sweden). Total DNA was measured after reaction with diphenylamine at 37°C, using a UV spectrophotometer at 600nm.[141] Thymidine incorporation was expressed as counts per minute (CPM) incorporated per milligram of DNA.

4.2.4.2. *Proliferating Cell Nuclear Antigen (PCNA) Protein Determinations*

PCNA protein determinations were performed by Western blot analysis.[130] Briefly, cellular proteins were isolated by homogenizing 0.5 g of tissue in 5ml of buffer containing 10 mM tris-HCl, pH 7.5, 1 mM EDTA, 10mM $MgCl_2$, 1 mM KCl, 1mM phenylmethylsulfonyl fluoride. Protein was quantified by the Bio-Rad protein assay. A sample of 100ug of protein was mixed in loading buffer and denatured by boiling for 5 min. The denatured polypeptides were then transferred to nitrocellulose filters. The filters were incubated overnight at 4 °C in a solution of PC-10 mouse antibody specific for PCNA protein (Dako Diagnostics Canada, Mississauga, Ontario, Canada). The secondary antibody (anti-mouse IgG bound to horseradish peroxidase) (Pharmacia Biotech, Baie d'Urfe, Quebec, Canada) was then bound over 1 hr. PCNA bands were visualized by autoradiography following the addition of a commercially available chemiluminescence solution (ECL Western blotting analysis system, Amersham Life Science, Oakville, Ontario, Canada) and quantified using NIH densitometry software for the Macintosh computer.

4.2.5. *Liver Function*

Total serum bilirubin levels were measured using a commercial kit (Sigma, St. Louis, Mo, USA).

4.2.6. *Statistical Evaluation*

Results were expressed as mean ± standard error. An analysis of variance with Fisher's protected least significant difference post hoc testing was used to examine

differences between groups and Spearman correlations to test for associations between test variables. Differences with a P value of less than 0.05 were deemed significant.

4.3. RESULTS

A representative cross-sectional MR image from a normal rat is shown in Fig. 3. Overlayed on the image is a two dimensional spectral grid generated by the CSI pulse sequence. The highlighted voxel located over the liver contains localized spectral information from the liver. Expanded below is the localized hepatic ^{31}P MR spectrum. A typical ^{31}P MR spectrum from liver contains resonances belonging to PME, Pi, PDE and the three phosphate groups (γ, α and β) from nucleotide triphosphates- the majority of which arises from ATP.[90] Small amounts of phosphocreatine may be detected in the *in vivo* spectrum of liver, this is indicative of some spatial contamination of the spectrum with signals arising from muscle.

Table 1 displays the changes in the concentrations of hepatic phosphorylated metabolites at Baseline and 24 and 48hrs after 70% PHx or Sham surgery. At 24 hrs, levels of hepatic ATP among PHx rats were maintained relative to Baseline/Sham levels. The same rats experienced a rise in Pi over Baseline ($P< 0.05$), which was accompanied by a reciprocal drop in hepatic ATP/Pi ($P< 0.05$). At 48 hrs, animals who underwent a 70% PHx displayed a reduction in hepatic ATP ($P< 0.05$), while in Sham operated rats, ATP was equivalent to Baseline. During this time, the levels of Pi in the livers of PHx rats approached Baseline/Sham levels. The more marked decline in the former (ATP levels) led to a more significant reduction in the ratio of hepatic ATP/Pi in PHx rats compared to Baseline/Sham levels ($P<0.001$). Concentrations of the PME resonance remained constant among the various groups, but features of the PDE region varied

Figure 3: A representative hepatic ^{31}P MR spectrum from healthy rat acquired using 2D-CSI. PME, phosphomonoesters; Pi, inorganic phosphate; PDE, phosphodiesters; ATP, adenosine triphosphate. * Small phosphocreatine resonance arising from abdominal wall muscle.

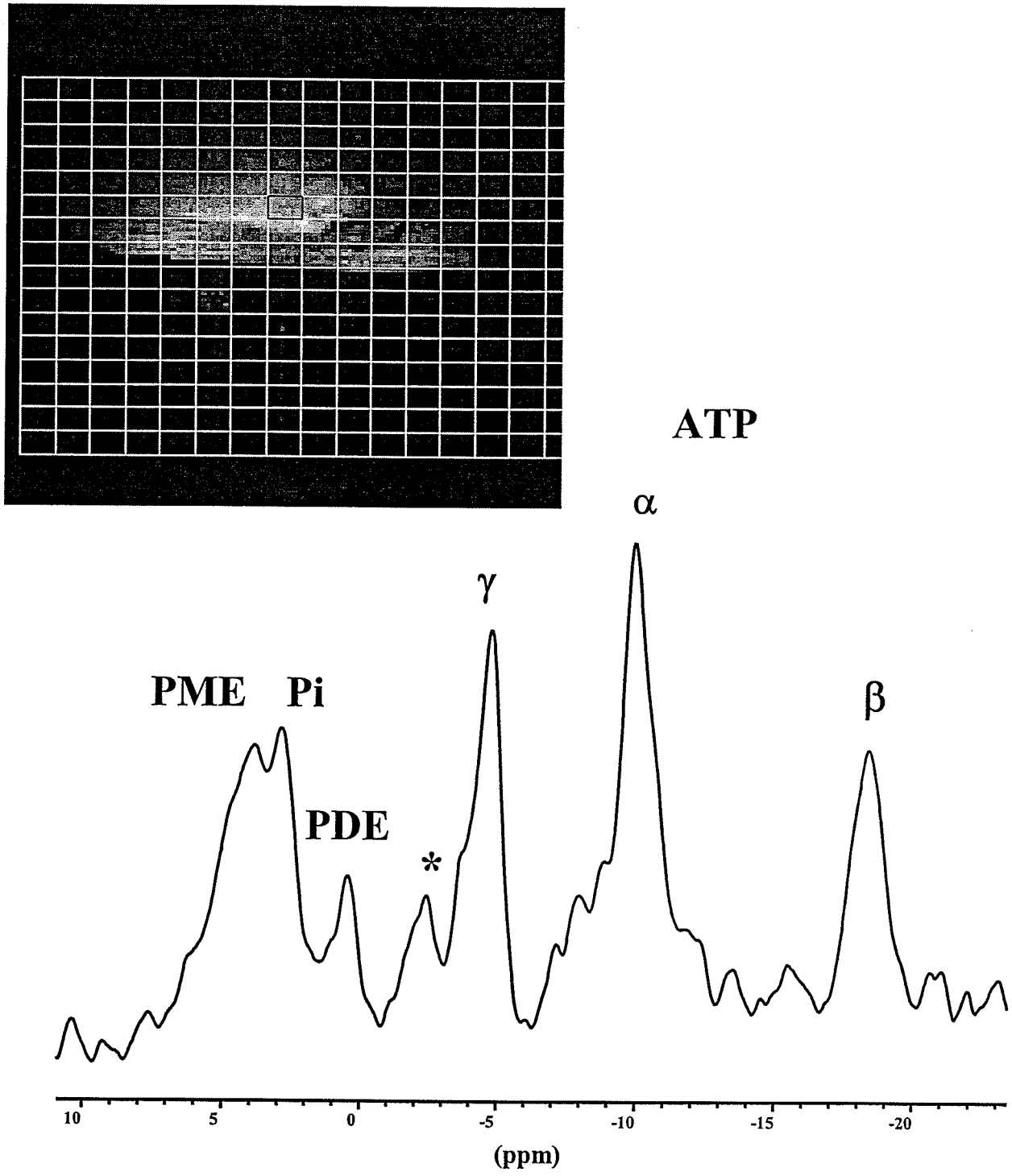
ATP
α
γ
PME
Pi
PDE
*
β
10
5
0
-5
-10
-15
-20
(ppm)

TABLE 1. Concentrations (mM) of phosphorylated metabolites in rat liver before (baseline) and 24 and 48 hrs after 70% partial hepatectomy or sham surgery.

Group	ATP	Pi	ATP/Pi	PME
Baseline❖	3.05 ± 0.23	1.51 ± 0.12	2.07 ± 0.14	3.66 ± 0.29
pHx 24hrs	2.91 ± 0.25	2.12 ± 0.24*	1.46 ± 0.17ξ	3.43 ± 0.29
Sham 24hrs	3.05 ± 0.10	1.66 ± 0.15	1.88 ± 0.19	4.32 ± 0.71
pHx 48hrs	2.37 ± 0.13φ	1.85 ± 0.20	1.32 ± 0.10ξξ	3.38 ± 0.39
Sham 48hrs	3.06 ± 0.20	1.41 ± 0.07	2.17 ± 0.08	3.05 ± 0.18

❖Baseline were concurrently studied rats not subjected to abdominal surgery.
Values are means ± SEM (N=4-6).
ATP, adenosine triphosphate; Pi, inorganic phosphate; PME, phosphomonoesters.
φP < 0.05 vs Baseline and P < 0.05 vs corresponding Sham.
*P < 0.05 vs Baseline.
ξP < 0.05 vs Baseline and P=0.05 vs correspondiing Sham.
ξξP < 0.001 vs Baseline and P < 0.0005 vs corresponding Sham.

considerably between animals. Due to the non-uniformity of this region the PDE peaks underwent curve fitting, but were not further analyzed for inter-group comparisons.

Figures 4, 5 and 6 depict the corresponding non-parametric correlations between hepatic ATP/Pi and changes in regenerative activity (^{3}H-thymidine incorporation and PCNA protein expression) and liver function (serum bilirubin). Correlation coefficients of $r = -0.61$, $P<0.005$; $r = -0.62$, $P<0.005$; $r=-0.49$, $P<0.05$ were observed for ^{3}H-thymidine incorporation, PCNA expression and serum bilirubin respectively.

In the second series of experiments, graded resections were performed and representative spectra from Sham, 40%, 70% and 90% PHx rats are presented in Fig. 7. The corresponding concentrations of hepatic phosphorylated metabolites were documented and are presented in Table 2. Concentrations of hepatic ATP steadily decreased from Baseline/Sham levels at 3.05 ± 0.23 mM, to 2.68 ± 0.17 mM with 40% PHx, reaching significantly lower levels at 2.37 ± 0.13 mM with 70% PHx ($P<0.05$) and 1.22 ± 0.08 mM with 90% PHx ($P<0.001$). Inorganic phosphate tended to increase following 40% and 70% PHx but did not reach statistical significance. ATP/Pi displayed a significant stepwise reduction from Baseline/Sham to 90% PHx. Lower levels of PME were also detected among rats subjected to 90% PHx ($P<0.05$).

Alterations in hepatic ATP/Pi along with corresponding changes in measurements of hepatic regeneration and liver function following graded resections are presented in Fig. 8. ^{3}H-thymidine incorporation and PCNA expression increased over each group, with ^{3}H-thymidine incorporation reaching a maximum at 70% PHx before dropping to lower levels at 90% PHx as described previously.[34] PCNA expression paralleled the

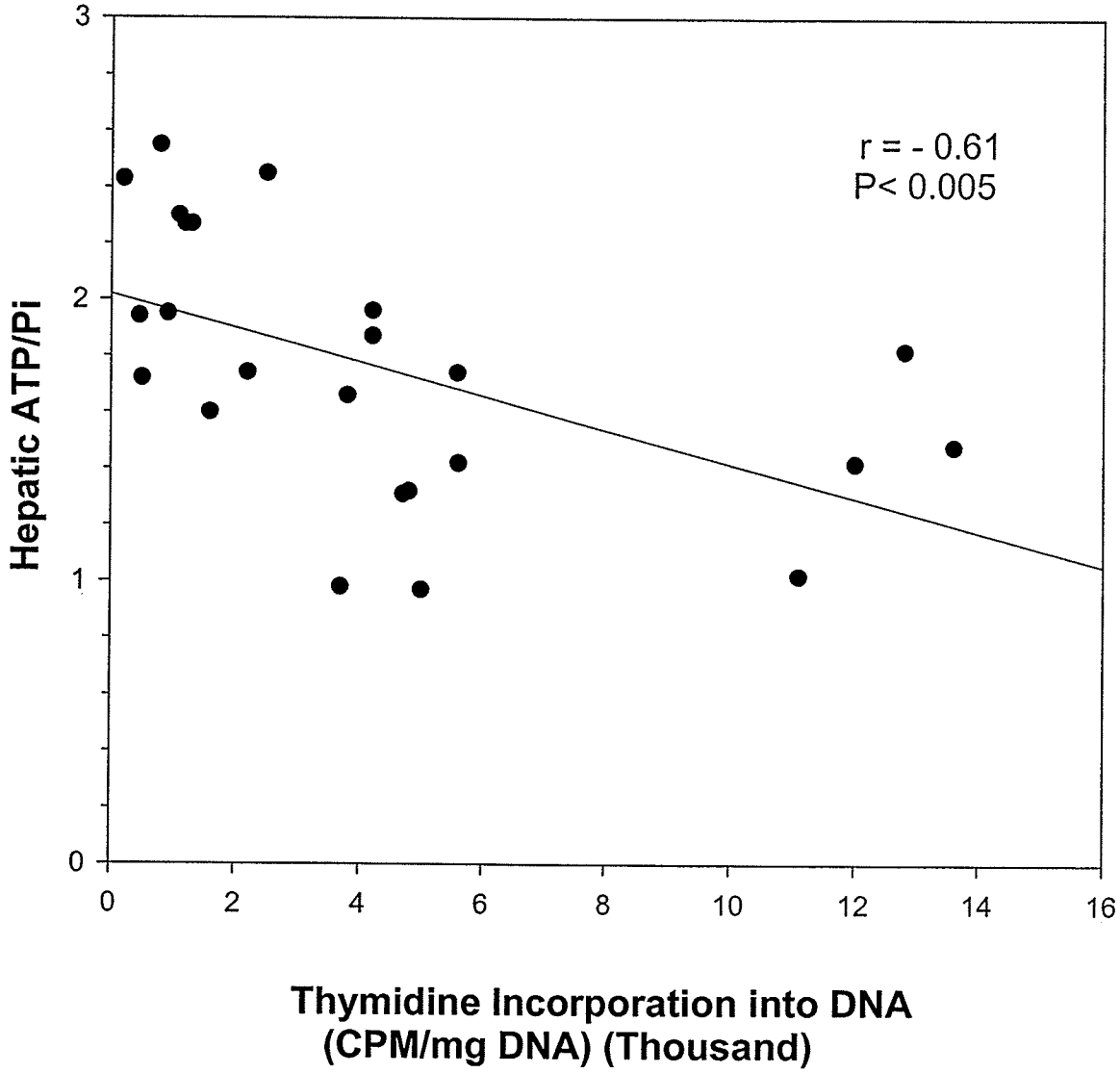

Figure 4: Correlation coefficient and regression line for hepatic ATP/Pi and ^{3}H-thymidine incorporation into hepatic DNA (N=24 rats).

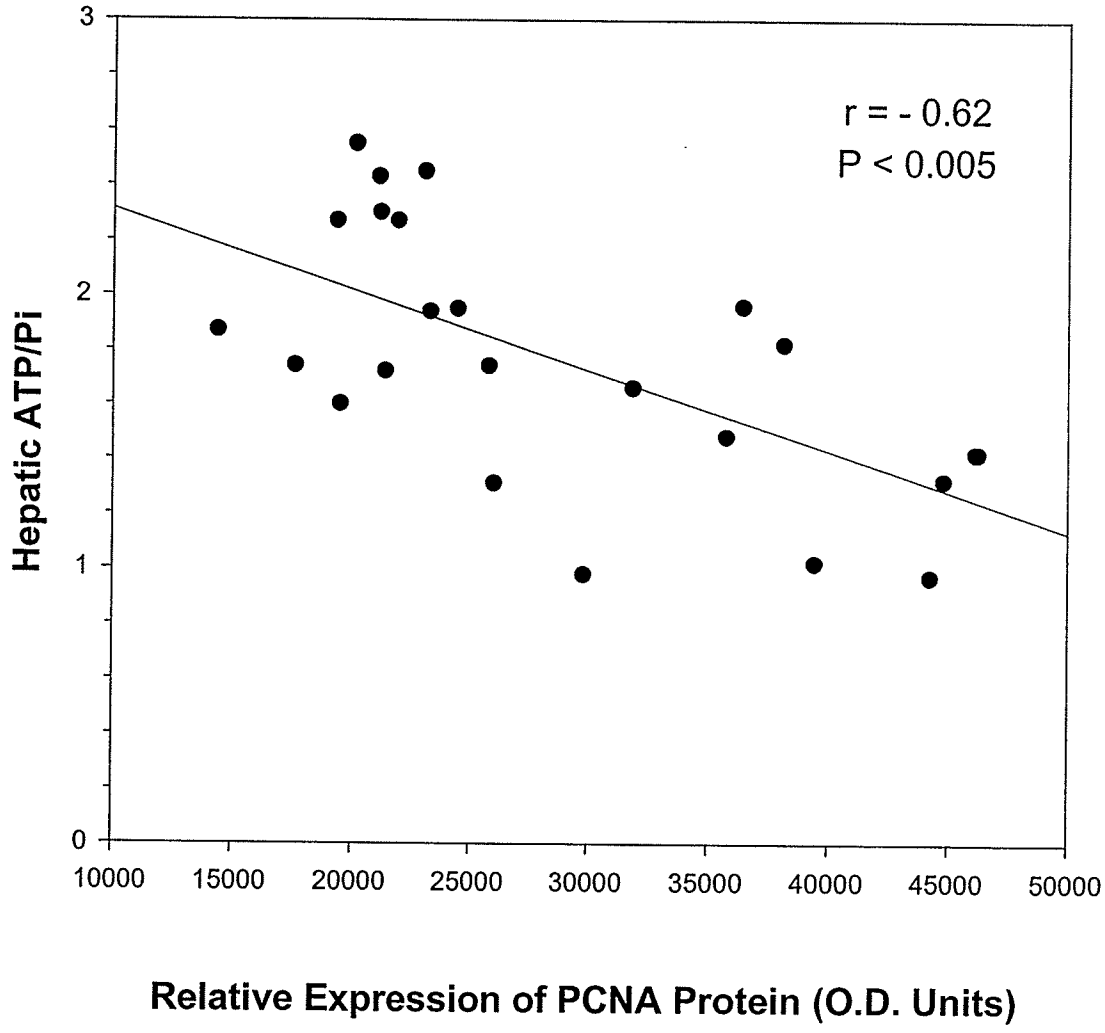

Figure 5: Correlation coefficient and regression line for hepatic ATP/Pi and proliferating cell nuclear antigen (PCNA) protein levels (N=24 rats).

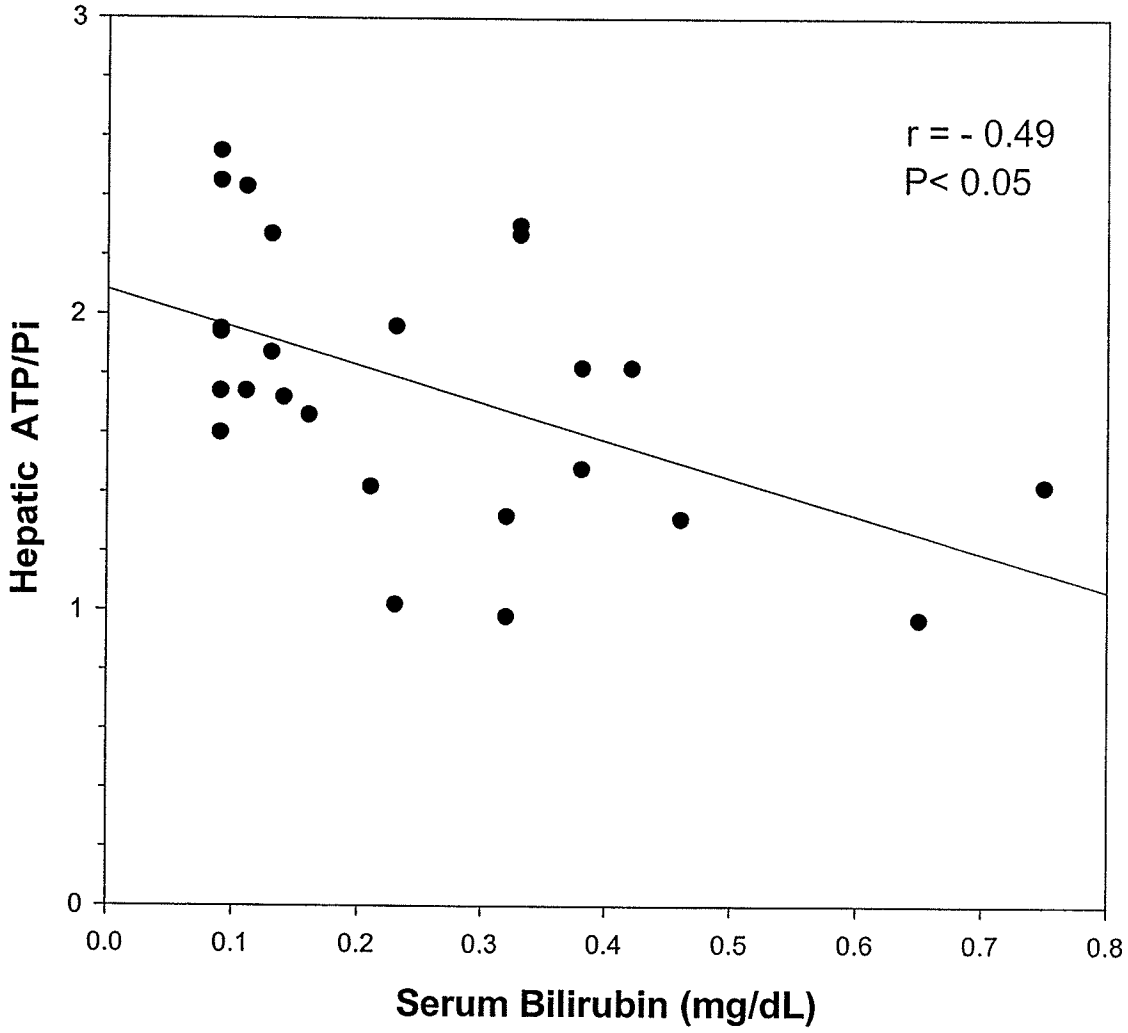

Figure 6: Correlation coefficient and regression line for hepatic ATP/Pi and serum bilirubin (N=24 rats).

Figure 7: Representative hepatic ^{31}P MR spectra from Sham, 40%, 70% and 90% PHx rats. PME, phosphomonoesters; Pi, inorganic phosphate; PDE, phosphodiesters; ATP, adenosine triphosphate. * Small phosphocreatine resonance arising from abdominal wall muscle.

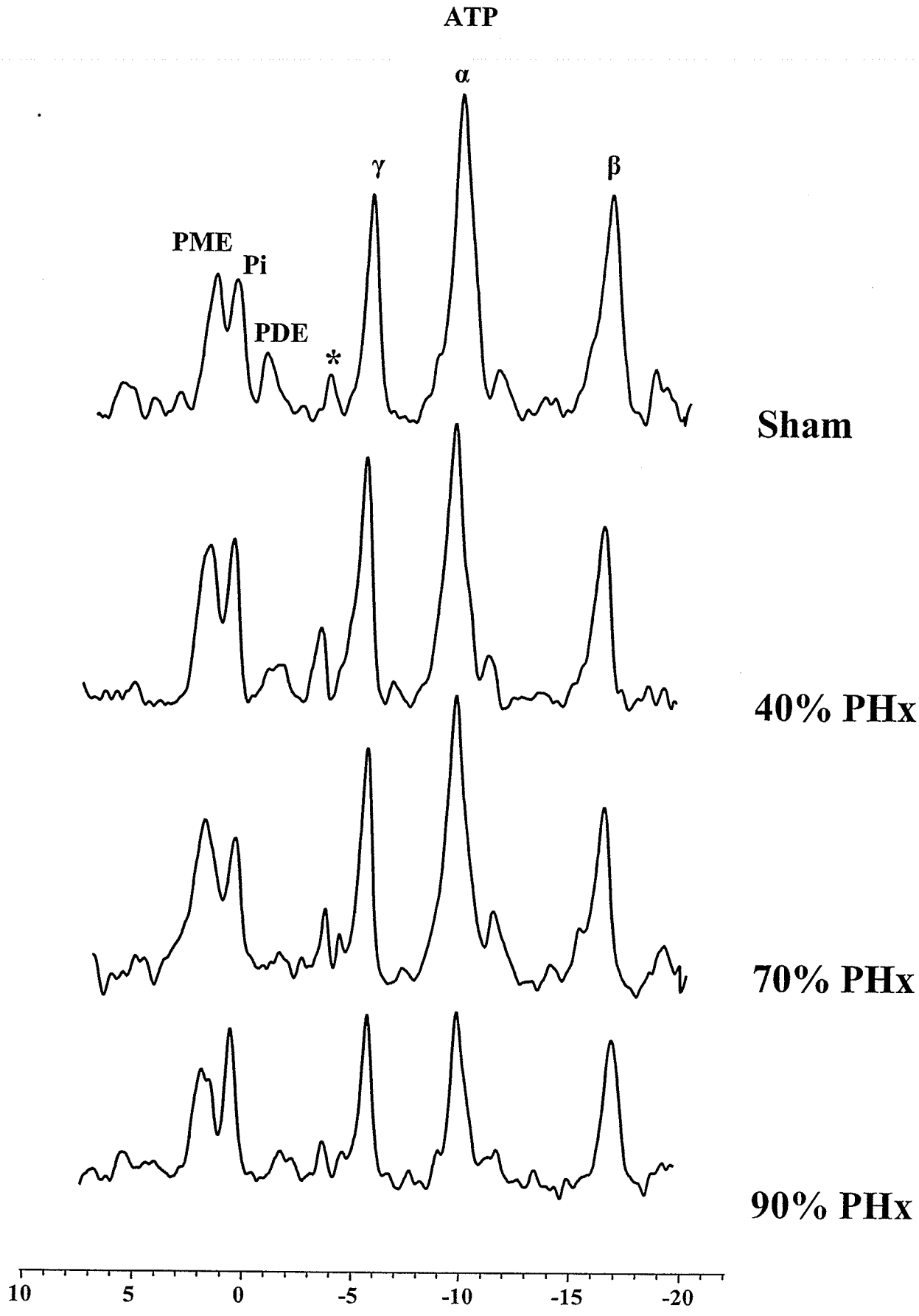
ATP
α
γ
β
PME
Pi
PDE
*
Sham
40% PHx
70% PHx
90% PHx
10
5
0
-5
-10
-15
-20

TABLE 2. Concentrations (mM) of phosphorylated metabolites in rat liver before (baseline) and 48 hours following varying degrees of hepatic resection or sham surgery.

Group	ATP	Pi	ATP/Pi	PME
Baseline*	3.05 ± 0.23	1.51 ± 0.12	2.07 ± 0.14	3.66 ± 0.29
Sham	3.06 ± 0.20	1.41 ± 0.07	2.17 ± 0.08	3.05 ± 0.18
40%	2.68 ± 0.17	1.66 ± 0.07	1.64 ± 0.12*	3.37 ± 0.26
70%	2.37 ± 0.13φ	1.85 ± 0.20	1.32 ± 0.10**	3.38 ± 0.39
90%	1.22 ± 0.08φφ	1.55 ± 0.16	0.81 ± 0.09***	2.35 ± 0.27ξ

*Baseline were concurrently studied rats not subjected to abdominal surgery.
Values are means ± SEM (N=4-6).
ATP, adenosine triphosphate; Pi, inorganic phosphate; PME, phosphomonoesters.
φ P < 0.05 vs Baseline & Sham
φφ P < 0.0001 vs Baseline, Sham, 40% PHx,and 70% PHx
ζ P < 0.05 vs 70% PHx.
*P < 0.01 vs Baseline, P< 0.005 vs Sham.
**P < 0.0001 vs Baseline & Sham, P=0.06 vs 40% PHx
***P < 0.001 vs Baseline, Sham & 40% PHx, P< 0.005 vs 70% PHx
ξ P < 0.001 vs Baseline, P< 0.05 vs 40% PHx, and 70% PHx

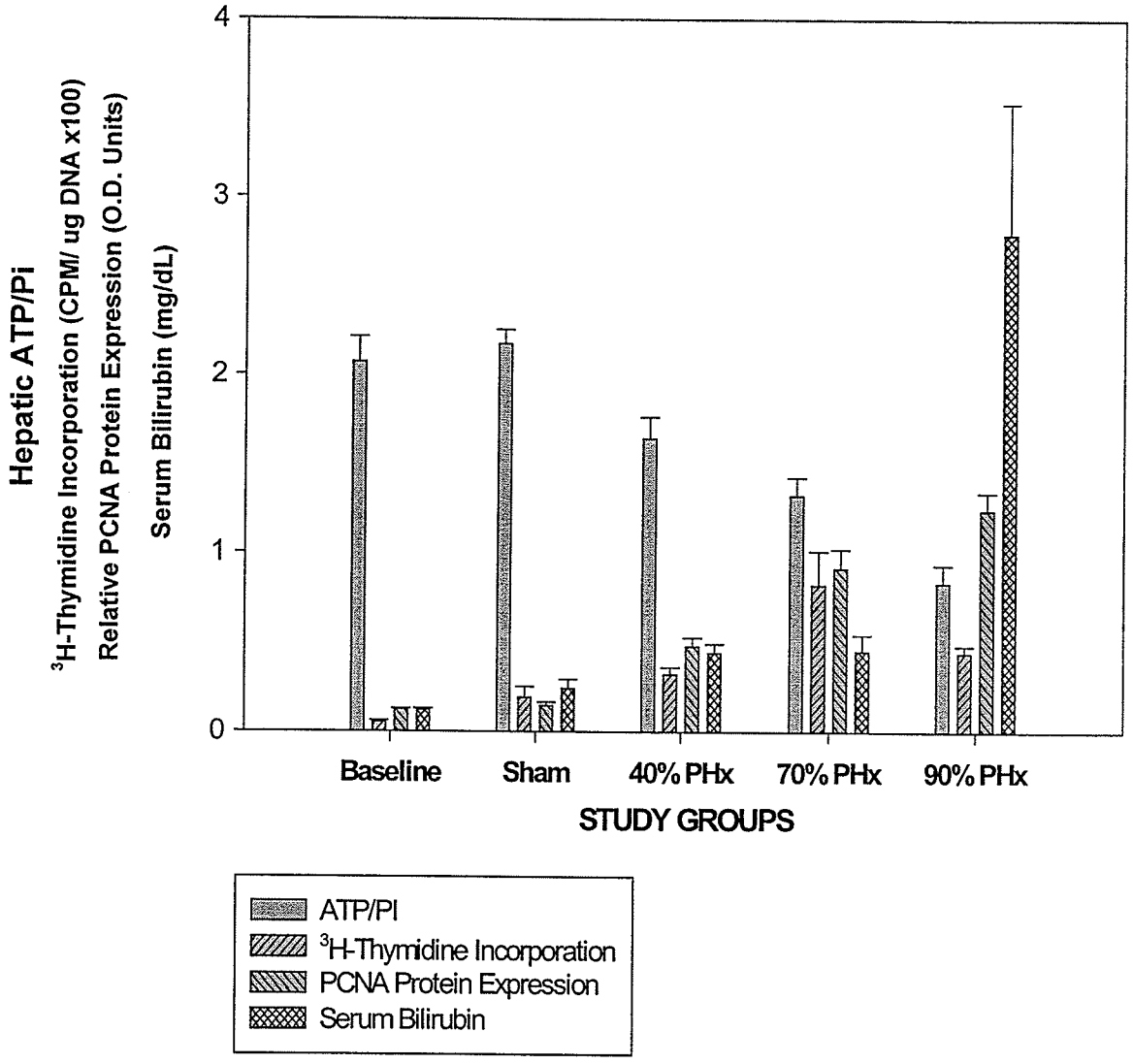

Figure 8: Alterations in hepatic energy status, measures of hepatic regeneration and liver function 48 hours following varying degrees of hepatic resection (N=5-7 rats per group).

increases in ^{3}H-thymidine incorporation but continued to rise, although only marginally, at 90% PHx. Finally, serum bilirubin levels were moderately increased following 40% and 70% PHx and significantly more so (25 fold) following 90% PHx compared to Baseline/Sham.

In the final series of experiments rats underwent MRS examinations before and serially (24 -168 hrs) following a 70% PHx. Changes in hepatic energy status (ATP/Pi) are plotted versus time in Fig. 9. The nadir of hepatic energy status occured at 24-48 hrs following liver resection ($P< 0.001$), the period of maximum regenerative activity in the rat, beyond this point ATP/Pi began to return to pre-operative levels. The increased ratio observed at 120 hrs corresponds with the well documented "rebound" of regenerative activity described in animals and man.[142, 143]

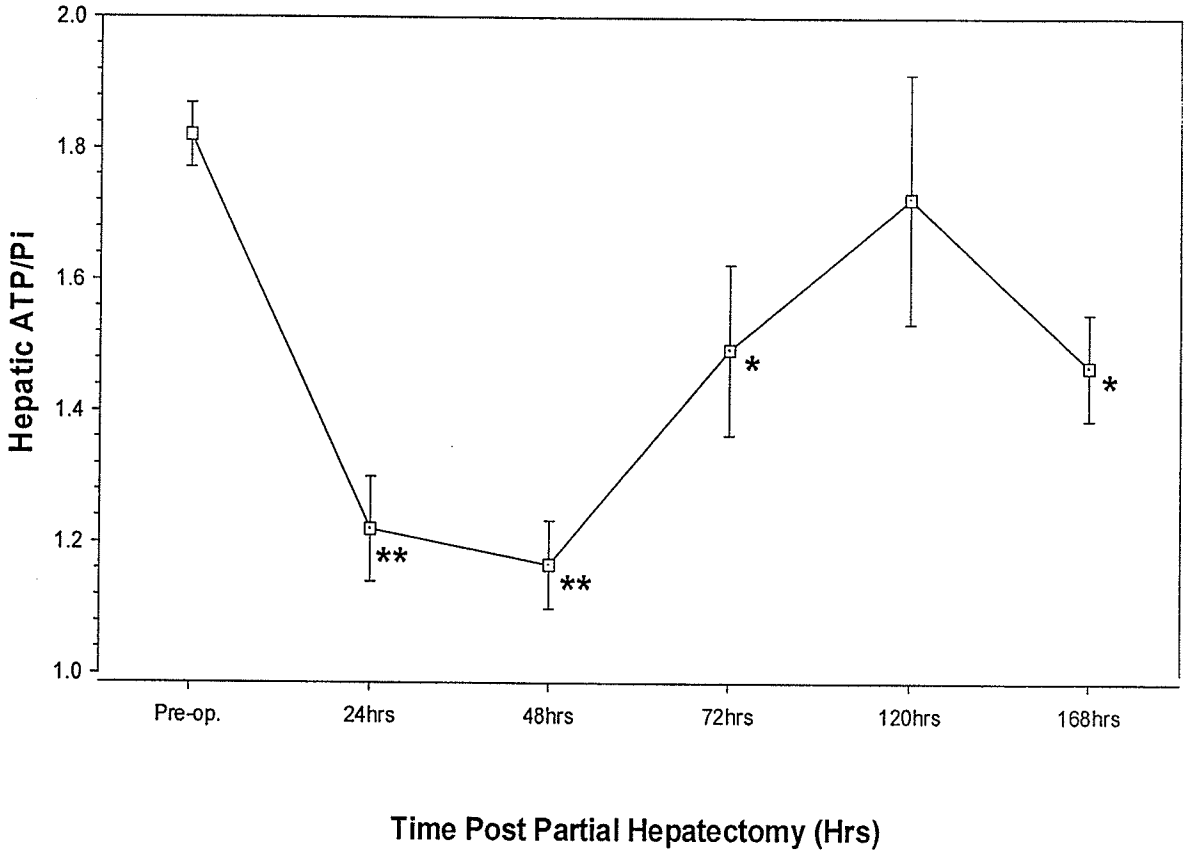

Figure 9: Serial measurements of hepatic energy status in regenerating rat livers after 70% partial hepatectomy. Each point represents the mean ± SEM (N=5 rats). $P<0.05$, ** $P<0.001$ compared to pre-operative values.

4.4. DISCUSSION

Phosphorus-31 MRS provides a unique opportunity to monitor the energy levels of intact tissues in a non-invasive manner.[13, 90, 131] Traditional methods require the excision and subsequent extraction of tissues, after which HPLC or enzyme analyses are performed to quantify adenine and other high energy species.[144, 145] From these methods expressions such as the phosphorylation potential and the adenylate energy charge can be applied to describe the energy status of tissues.[111, 112] Although several studies have been performed in this manner,[146-148]the results must be interpreted with caution, as hydrolysis of ATP and accumulation of Pi are known to occur during tissue collection and processing.[90] Such problems are avoided with *in vivo* ^{31}P MRS. While the phosphorylation potential and adenylate energy charge cannot be measured directly from *in vivo* spectra, the ATP/Pi ratio has been shown to serve as a reliable index of the cytosolic energy status or the phosphorylation potential of tissues.[15, 149]

Following hepatic resection the remnant liver is known to undergo energetic changes as documented by *in vitro* experiments[87, 146-148, 150, 151] and invasive MRS studies, in which laparotomies were performed and a phosphorus surface coil was placed directly upon the liver.[87, 133, 134, 136] To date, the present study along with a report by Kooby *et al.*[135] are the only published reports to have quantitatively documented hepatic energy levels following PHx non-invasively with ^{31}P MRS. Localized spectral data 24hrs following PHx depicted a decrease in hepatic ATP/Pi among hepatectomized rats, but of interest, it arose not because of lowered ATP levels but as a result of increased hepatic Pi. Campbell et al.[136] reported similar findings using invasive MRS techniques. The increase

in hepatic Pi likely resulted from the hydrolysis of phosphorylated species other than nucleotide triphosphates, as levels of the ATP resonance were maintained. Additional explanations for the increased levels of hepatic Pi include increased hepatic uptake and accumulation of phosphate, which would be in keeping with the depletion of serum phosphate levels observed following hepatic resection.[152, 153] The pronounced increase in DNA synthesis which accompanies hepatic regeneration is also known to liberate Pi species,[111] however, whether this process quantitatively contributes to the increase in hepatic Pi is uncertain. Clearly, further studies are required to elucidate the increase of hepatic Pi in the immediate post-operative period.

Data collected at 48 hrs were also consistent with other MRS findings. As reported by Kooby *et al.*,[135] we observed a reduction in ATP/Pi among hepatectomized animals. Quantitative data from both reports reveal that the depletion in hepatic ATP/Pi arose from a reduction in the levels of ATP, while only a trend towards increasing concentrations of Pi was reported. Although the magnitude of the absolute concentration of metabolites differed between the two studies, the patterns of the energetic changes were consistent.

Alterations in the energetic status of the liver following a PHx are believed to result from the enhanced metabolic load placed upon the remnant liver.[146, 147] Following the removal of a portion of liver, the remnant liver must attempt not only to meet metabolic needs formerly placed upon an entire liver, but also undergo regenerative proliferation to restore lost liver mass. The remnant liver possesses only a finite energetic capacity in its attempt to meet homeostatic functions and regeneration. As a result of this metabolic load, increased energy expenditure occurs, and finally the energy levels of the

remnant liver (as reflected by hepatic ATP/Pi and to a lesser extent ATP) become depleted.

While it has been suggested by some that the reduced energy status of the liver following PHx reflects hepatic regenerative activity[135, 136], others maintain that these energetic disturbances reflect altered liver function.[146, 150] Both arguments are plausible, as hepatic regeneration is an energy consuming process[31, 111], and the functional capacity of a cell is directly related to its energy status.[112] Direct correlations performed in this study between ATP/Pi and parameters of regenerative activity and liver function revealed that the energy status of the remnant liver correlated with both hepatic regeneration and liver function. That correlations were found with both hepatic regeneration and liver dysfunction was not surprising as both these processes occur concurrently following liver injury.[34, 122, 123, 128, 138] Hence the energy status of the remnant liver, as reflected by ATP/Pi, provides a robust measure which encompasses both processes of hepatic regeneration and liver function.

Concentrations of the broad multicomponent PME resonance remained constant in the 24 and 48 hrs terminal experiments as well as in the serial examination series (data not shown). Previous high resolution MRS studies of tissue extracts revealed that concentrations of phosphoethaolamine, a phospholipid membrane precursor, were elevated following PHx.[87, 154] The elevated levels of phosphoethanolamine are interpreted to reflect increased phospholipid membrane synthesis during rapid cellular proliferation. Phosphoethanolamine, however, is just one of 14 different metabolites encompassed in the PME resonance and its contribution to the PME region is less then 15%.[86, 87] Therefore, increases in phosphoethanolamine are unlikely to cause significant

changes to the *in vivo* reading of the PME resonance following hepatic resection. While similar findings have been reported by some investigators[87, 135] others have reported increases in PME following PHx.[133, 154] The broad overlapping characteristics of this peak along with the multiple signals contributing to this resonance hinders accurate quantification of the PME peak and likely explains these conflicting findings.

The intensity of the regenerative response and degree of liver dysfunction are known to be dependant upon the amount of liver resected.[31, 130, 138] The present study reports that the magnitude of the energetic disturbance following PHx is also proportional to the extent of hepatic resection. With each incremental grade of resection the divergence between ATP and Pi became more pronounced and the reduction of ATP/Pi more significant. This would suggest that the step-wise reduction of ATP/Pi is reflective of the increasing metabolic load, resulting from enhanced regenerative activity and functional demands, which accompanies the increasing loss of liver mass. The pattern of the energetic changes, however, was slightly different following 90% PHx. Indeed, the ATP/Pi ratio at 90% PHx was significantly lower then that at 70% PHx, reflecting the striking depletion of ATP (Pi levels were maintained relative to Baseline/Sham values). This differing metabolite profile following 90% PHx was accompanied by reduced or minimal increases in regenerative activity as evidenced by ^{3}H-thymidine incorporation and PCNA expression respectively, and a pronounced increase in hepatic dysfunction, as indicated by elevated serum bilirubin. The marked decrease in hepatic ATP, limited regenerative activity and increase in serum bilirubin suggest that following 90% PHx the depletion in hepatic ATP/Pi more likely reflects liver dysfunction than regeneration. At 90% PHx the functional demand upon the remnant liver is so great that a metabolic crisis

ensues, where the regenerative response may be hindered and liver failure eventually occurs. [34, 138, 155, 156] A mortality rate of 17% associated with 90% PHx further supports this argument (data not shown).

Lower levels of PME were also reported following 90%PHx. This may have resulted from the marked metabolic derangement that occurs following such an extensive resection. The PME resonance contains many glycolytic intermediates the detection of which may have been hampered due to the shortened half-lives that accompany increased metabolic flux during this enhanced catabolic state.[155, 157]

Energetic alterations detected over the seven-day postoperative period were also in keeping with MRS data reflecting both hepatic regenerative activity and function. Specifically, the nadir of hepatic ATP/Pi occurred between 24–48hrs post-PHx, which coincides with the period in which maximum DNA synthesis and liver dysfunction occur.[128, 130, 139] Beyond this time point, the ATP/Pi gradually reverted to preoperative levels. These dynamic changes in hepatic ATP/Pi throughout the post-operative period mirror changes in regenerative activity and liver dysfunction which are known to occur following hepatic resection in rats and humans.[128, 130, 132, 137, 138, 147]

In summary, increased energy expenditure following PHx as indicated by lower hepatic ATP/Pi is a robust index that reflects enhanced regenerative activity and functional demands placed upon the remnant liver. As such, valuable information concerning the status of these physiological processes throughout the post-operative period can be documented by repeated determinations of hepatic ATP/Pi levels. Furthermore, the ATP/Pi ratio is a graded index, in that levels decrease in proportion to the extent of PHx. Finally, quantitative MRS is a promising technique to monitor in a

non-invasive manner, hepatic regenerative activity and dysfunction following surgical resection of the liver.

CHAPTER V

UTILITY OF HEPATIC PHOSPHORUS-31 MAGNETIC RESONANCE SPECTROSCOPY IN A RAT MODEL OF ACUTE LIVER FAILURE

5.1. INTRODUCTION

Acute liver failure is a clinical syndrome associated with rapid deterioration of hepatic function in the absence of pre-existing liver disease.[158] The clinical signs accompanying the sudden cessation of normal liver function include jaundice, coagulopathy, ascites, renal impairment, encephalopathy and/or cerebral edema.[159, 160] The course of acute liver failure is variable. For some patients, hepatic dysfunction is short lived and recovery occurs without sequelae, while for others, hepatic function continues to deteriorate, multiorgan failure develops, and death ensues.[159, 160] Mortality rates in the absence of medical treatment can be in excess of 80%.[160]

Orthotopic liver transplant (OLT) has been proposed as the optimal treatment for most patients with acute liver failure.[161, 162 163] This approach, however, is hampered by lengthy transplant waiting lists and a shortage of donor livers worldwide.[164, 165] In addition, there is also a risk of performing OLT in patients who would otherwise recover from an episode of acute liver failure. Were this to happen, recipients could be considered to have undergone unnecessary surgery and are committed to life-long immmunosupressive therapy and the complications thereof. In addition, an inappropriate allocation of a donor liver would have occurred. Thus, an accurate determination of which patients might benefit from OLT is of utmost importance.

In current clinical practice, patients with acute liver failure are selected for transplantation based on various clinical and laboratory prognostic criteria.[166, 167] Traditional liver function tests which measure the functional capacity of the liver, such as prothrombin times, international normalized ratio (INR) and serum bilirubin levels, are commonly used to assess the status of the liver upon presentation of acute liver failure.

However, information provided by such indicators can be misleading, as these markers are subject to extrahepatic influences.[12] Direct assessment of the liver by biopsy may be a strong indicator of prognosis, but for most patients with acute liver failure this procedure is contraindicated.[168-170]

Radiologic examination provides yet another approach with which direct information may be obtained from the liver. Traditional magnetic resonance imaging, computer tomography and ultrasound, however, provide only anatomical information, which is of limited prognostic value.[171, 172] Phosphorus-31 magnetic resonance spectroscopy (^{31}P-MRS) is an alternative radiologic technique that provides biochemical rather than structural information about the tissue under examination. Such information may be of importance when assessing patients with acute liver failure as bioenergetic alterations and disturbances in plasma membrane integrity are known to accompany liver cell injury and acute liver failure.[113, 173] Thus, the aim of the present study was to determine whether hepatic metabolic alterations, as detected by quantitative ^{31}P-MRS, reflect the severity of disease in a rat model of acute liver failure. Secondly, we sought to prospectively determine the prognostic value of ^{31}P MRS for predicting survival following acute liver failure in rats.

5.2. MATERIALS AND METHODS

5.2.1. Animals and Acute Liver Failure

The protocol outlined below was approved by the University of Manitoba Animal Ethics Committee. Adult male Sprague-Dawley rats (240-300 g) were allowed free access to food (Purina rat chow) and water throughout the study. Acute liver failure was induced by a single intraperitoneal injection of the potent hepatotoxin D-galactosamine hydrochloride (D-galN) (Sigma Chemical Co., St. Louis, MO, USA) at a dose of 1.0 g/kg as described by Terblanche and Hickerman.[174] D-galN was dissolved in physiological saline and adjusted to a pH of 7.0 with 1 M NaOH prior to each injection.[174]

5.2.2. Disease Severity Study

Fourteen rats were subject to D-galN exposure, after which in vivo MRS examinations were performed 48hrs following treatment (mean peak of hepatic necrosis).[175] Immediately following MRS examinations, animals were sacrificed at which time blood samples and livers were collected. A portion of each excised liver was fixed in 10% buffered formalin. An additional group of rats not exposed to D-galN was also studied, these served as healthy controls.

5.2.2.1. ^{31}P-Magnetic Resonance Spectroscopy

MRS examinations were performed as outlined in chapter 3.

5.2.2.2. *Liver Function*

Sera were isolated from blood samples collected at the time of sacrifice. Serum aspartate aminotransferase (AST) and total bilirubin were measured using commercial kits (Sigma, St. Louis, MO, USA).

5.2.2.3. *Histology*

Fixed tissue specimens were blocked in paraffin, cut and then stained with hematoxylin and eosin. Slides were graded (0-IV) blindly by two independent investigators (GM and MZ) for hepatic necrosis according to the following scale; grade 0; no necrosis, grade I (mild disease); <25%, grade II (moderate disease); 25-50%, grade III (marked disease); 50-75% and grade IV(severe disease); >75% necrosis of the liver lobule.[176, 177] Concordance was excellent between the two investigators (<10% variability).

5.2.3. *Survival Study*

Twenty-two rats were administered D-galN as described above. Approximately thirty hours post D-galN treatment rats underwent MRS examinations (see above), following which animals were observed and deaths recorded over a 7 day post treatment period.

5.2.4. *Statistical Evaluation*

Results were expressed as mean ± standard error. The Student's t-test was used to examine differences between groups and Spearman correlations to test for associations

between continuous and categorical test variables. Differences with a P value of less than 0.05 were deemed significant. Sensitivity, specificity and positive and negative predictive values were calculated using receiver operating characteristic curves.

5.3. RESULTS

5.3.1. Severity of Disease Study

Presented in Figure 10a is a representative section of normal liver tissue from a control rat and the corresponding localized hepatic ^{31}P MR spectrum. As indicated earlier, a typical ^{31}P MR spectrum from healthy liver contains strong resonances belonging to phosphomonoesters (PME), inorganic phosphate (Pi), phosphodiesters (PDE) and the three phosphate groups (γ, α and β) from nucleotide triphosphates- the majority of which arise from ATP.[90] Shouldering the α-ATP peak is the broad resonance belonging to uridine 5'- diphosphosugar (UDP-sugar) species. Small amounts of phosphocreatine may be detected in the *in vivo* spectrum of liver, indicative of signals arising from adjacent muscle.

As has been described previously with the D-galN model of liver disease,[174] the severity of disease varied considerably with some rats displaying limited evidence of hepatic injury while others died of liver failure. Of the 14 animals receiving D-galN injections, four (29%) died before MRS examinations could be performed. Figure 10b, 10c and 10d depict histological sections and corresponding spectra from other rats with histologic evidence of mild, moderate and severe disease respectively. In those with mild liver disease, inflammatory infiltration was present but confined to the periportal regions

Figure 10: A representative histologic section of liver and corresponding hepatic ^{31}P MR spectrum from (A) healthy rat and rats with acute liver failure (B) mild; (C) moderate and (D) severe. H&E, X20. Abbreviations: PME, phosphomonoesters; Pi, inorganic phosphate; PDE, phosphodiesters; ATP, adenosine triphosphate; PCr, phosphocreatine resonance arising from abdominal wall muscle.

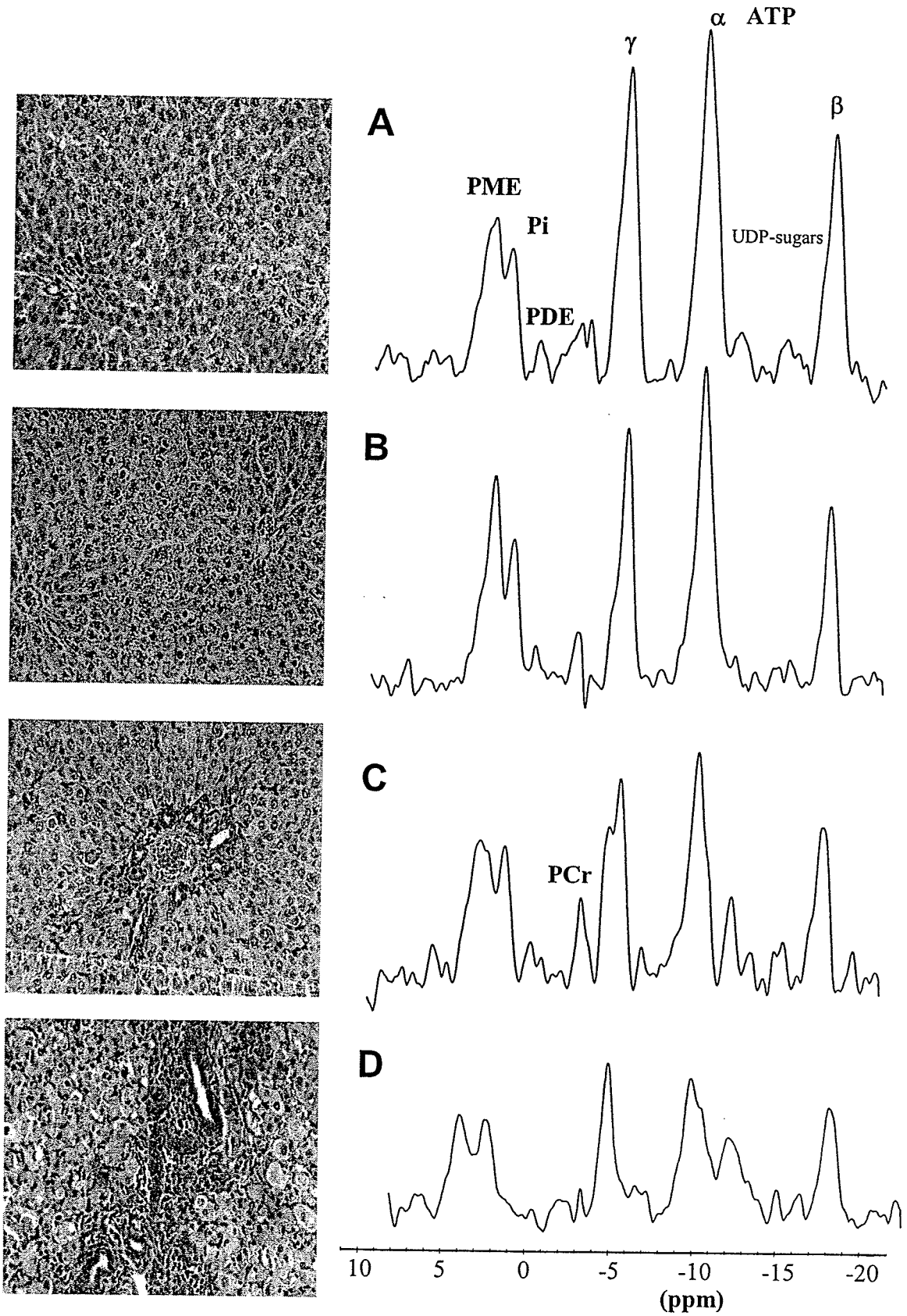
α ATP
γ
β
A
PME
Pi
PDE
UDP-sugars
B
C
PCr
D
10
5
0
-5
-10
-15
-20
(ppm)

(Rappaport zone 1) of the hepatic lobule. A slight decrease in the signal of phosphorylated metabolites in ^{31}P spectrum accompanied mild liver disease. Moderate liver disease was associated with more marked inflammatory infiltration extending into Rappaport zone 2. The signal from MR detectable metabolites continued to decline; in contrast the levels of the UDP-sugars increased. With severe liver failure there was extensive destruction of the liver lobule with a heavy inflammatory cell infiltration. In addition, there was pronounced dilation of the portal venules and bile ductular proliferation. Corresponding spectra displayed a pronounced depletion of phosphorylated metabolites with the exception of UDP-sugars.

The actual concentrations of the various phosphorylated metabolites depicted in the hepatic ^{31} P MR spectra are presented in Table 3. Features of the PDE region varied considerably between animals. Due to the non-uniformity of this region, the PDE peaks underwent curve fitting, but were not further analyzed for inter-group comparisons. Overall, each of the measured phosphorylated metabolites in the livers of D-galN treated rats were significantly lower than in controls. ATP levels displayed the most striking reduction (- 45%), followed by PME (- 32%), and Pi (- 17%).

Table 4 provides the results of correlations between changes in the concentrations of phosphorylated metabolites and biochemical markers of liver injury (AST) and function (bilirubin). Both ATP and PME showed a negative correlation with serum AST ($r=-0.91$, $P< 0.00001$, $r=-0.65$, $P<0.01$ respectively) while correlations with serum bilirubin were $r= -0.74$, $P<0.005$ for ATP and $r=-0.71$, $P<0.005$ for PME. Hepatic Pi did not correlate with these parameters of liver disease.

Table 3. Concentration (mM) of hepatic phosphorylated metabolites in controls and rats with acute liver disease following D-galactosamine exposure.

Group	PME	Pi	ATP
Control (n= 7)	4.02 ± 0.25	1.58 ± 0.09	3.15 ± 0.16
D-galN (n=10)	2.74 ± 0.20[b] (-31.8%)	1.32 ± 0.07[a] (-16.5%)	1.72 ± 0.17[b] (-45.4%)

Values are means ± S.E.M. Numbers in parentheses represent percent changes from control values.
Abbreviations; D-galN, D-galactosamine; PME, phosphomonoesters; Pi, inorganic phosphate; ATP, adenosine triphosphate.
[a] $p < 0.05$ vs Controls
[b] $p < 0.0001$ vs Controls

Table 4. Correlations between hepatic phosphorylated metabolites, serum AST and bilirubin and liver histology

	Serum AST	
	Correlation (r)	P-value
PME	-0.65	<0.01
Pi	-0.38	0.14
ATP	-0.91	<0.00001
	Serum Bilirubin	
	Correlation (r)	P-value
PME	-0.71	<0.0005
Pi	-0.32	0.23
ATP	-0.74	<0.001
	Liver Histology	
	Correlation (r)	P-value
PME	-0.71	<0.005
Pi	-0.40	0.11
ATP	-0.92	<0.00001

Abbreviations; PME, phosphomonoesters; Pi, inorganic phosphate; ATP, adenosine triphosphate.

Correlations were also performed between changes in the concentration of phosphorylated metabolites and histological grade of injury. A strong negative correlation existed between ATP levels and the percentage of hepatocyte necrosis ($r= -0.92$, $P<0.00001$), while a weaker correlation existed for PME ($r= -0.71$, $P<0.005$).

5.3.2. *Survival Study*

In the second series of experiments, all animals (n=22) were alive 30 hrs post D-galN injection for MRS examinations. Between 48 and 72 hrs post D-galN exposure, nine rats (41%) died of liver failure. Based on data from the previous series wherein hepatic ATP levels best reflected the status of the liver during acute liver injury, the ATP level was selected for prospectively predicting survival. Sensitivity, specificities and predictive values are listed in Table 5. When sensitivity and specificity were simultaneously maximized, values of 78% and 62% respectively were found with an ATP cut-off value of 2.01mM. The corresponding positive and negative predictive values were 58% and 80% respectively. When an ATP cut-off value was selected to increase the sensitivity to 100% (ATP = 2.29 mM), specificity dropped to 54% and positive and negative predictive values were 60% and 100% respectively. If specificity was increased to 100% (ATP cut-off = 1.46 mM), sensitivity fell to 22%, the positive predictive value rose to 100%, while the negative predictive value equalled 65%.

Table 5. Sensitivity, specificity and predictive value of hepatic ATP levels with respect to death following D-galN induced acute liver failure

Cut-off value (mM)	Sensitivity	Specificity	Positive Predictive value	Negative Predictive value
1.46	0.22	1.00	1.00	0.65
2.01	0.78	0.62	0.58	0.80
2.29	1.00	0.54	0.60	1.00

5.4. DISCUSSION

Acute liver failure is a potentially life threatening illness which results from a rapid deterioration in liver function.[158-160] Regardless of etiology, the syndrome is characterized by massive hepatocyte necrosis and near complete destruction of the liver parenchyma.[158-160] Oral or intravenous administration of the potent hepatotoxin, D-galN, to laboratory animals produces hepatic lesions similar to those seen in many forms of acute liver failure in humans including extensive hepatocyte necrosis and inflammatory cell infiltration, bile ductular proliferation, and enlargement of portal venules.[175]

The most striking finding in the present study was the significant decrease in the concentration of phosphorylated metabolites detected in the hepatic ^{31}P spectra of D-galN treated rats. This decrease likely reflects reduced hepatocyte mass within the liver.[175, 178-181] As the total amount of viable cells per unit volume of liver decreases, MR detectable signal from that volume of tissue will also decrease.[178-181] The strong correlations between hepatic ATP levels and serum AST ($r=-0.91$, $P<0.00001$) and the histological extent of hepatocyte necrosis ($r=-0.92$, $P<0.00001$) support this interpretation.

Bioenergetic alterations may also explain the reduced levels of hepatic ATP seen among rats with acute liver injury. Indeed, bioenergetic disturbances do occur in acute liver failure.[173] The loss of upwards of 80%-85% of liver cell mass places considerable metabolic demands on the residual liver to maintain life.[182] Not only must the residual liver mass expend energy to maintain normal synthetic and excretory functions but in addition, regenerative activity, another energy demanding process must be undertaken.[31, 183, 184] These homeostatic demands can lead to a metabolic crisis in

which energy stores are depleted and the functional performance of the liver is compromised. This was evident in the hepatic dysfunction seen among rats with acute liver failure and the significant correlations that existed between hepatic ATP and serum bilirubin levels ($r=-0.74$, $P<0.005$). Rats subjected to 90% hepatic resections (chapter 4) further support these findings.

The mechanism of D-galN induced liver damage involves both direct and indirect pathways of injury.[185-187] Free standing D-galN elicits cell injury by binding to membrane structures. Galactosamination of membrane proteins and lipids is thought to promote lipoperoxidation and impair key membrane ion pumps, such as calcium dependent ATPase.[187] Both processes contribute to cellular necrosis by causing membrane dysfunction, the accumulation of intracellular calcium, and irreversible metabolic derangements. While the liver is capable of metabolizing D-galN, this occurs along catabolic pathways that are optimal for galactose and thereby result in the depletion of both glycogen and uridine triphosphate (UTP) stores (Fig. 11).[188] The latter hinders the synthesis of both RNA and glycoproteins, which in turn compromises the integrity of the cell membrane and potentiates cell necrosis.[189] In addition, the numerous uridine-hexose derivatives that accumulate, due to the inefficient metabolism of D-galN, generate intracellular disturbances through defective glycosylation of internal and secreted proteins.[190]

It could be argued that the depletion of hepatic UTP stores following D-galN administration further influenced hepatic ATP levels. The 'ATP' peaks in ^{31}P MR spectrum actually contain resonances from other triphosphate species, e.g. CTP, GTP, UTP and ITP.[90] However, the concentration of these additional species collectively

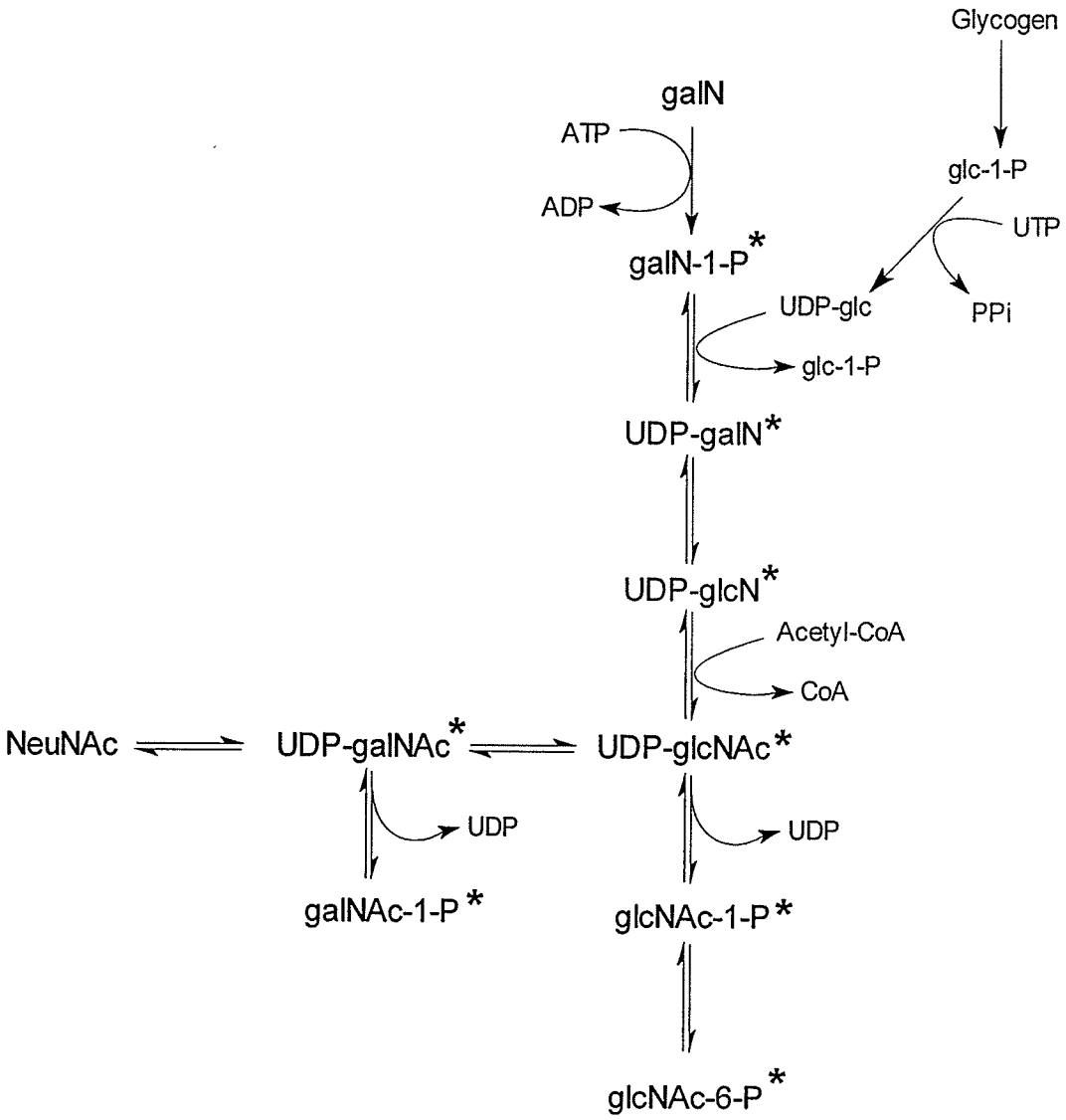

Figure 11: Metabolism of galactosamine. * Indicates MRS detectable catabolites of galactosamine. Galactosamine, galN; Glucose, glc; Glucosamine, glcN; Uridine triphosphate, UTP; Uridine diphosphate, UDP; Phosphate, P; Pyrophosphate, PPi; N-acetyl-glucosamine, glcNAc; N-acetyl-galactosamine, galNAc; N-Acetylneuraminic acid (sialic acid), NeuNAc

only account for approximately 10% of the concentration of 'ATP'.[90] Thus, although significant depletion of UTP stores occurs with D-galN metabolism, its contribution to the reduction of the 'ATP' resonance would be limited.

Hepatic PME levels also correlated with liver histology, but not to the same extent as ATP. The weaker correlation presumably reflects the fact that several metabolites arising from different metabolic pathways contribute to the PME resonance.[86] For example, the metabolism of D-galN produces many phosphorylated intermediates which accumulate to detectable levels in the ^{31}P MR spectrum (Fig. 2).[191, 192] Previous studies using elaborate high resolution MR spectroscopy of liver extracts have described the identity and position of these D-galN catabolites in the ^{31}P MR spectrum.[191, 192] The D-galactosamine catabolites glucosamine-6-phosphate and N-acetyglucosamine-6-phosphate are in fact PME-molecules which increase dramatically following D-galN administration and contribute to the broad PME resonance. In addition, phosphocholine and phosphoethanolamine, the principal metabolites of the PME resonance, are precursor molecules for phospholipid membrane synthesis. As such, their levels, particularly that of phosphoethanolamine, have been reported to increase with liver regeneration following hepatic resection[87, 154] and during the course of chronic liver disease.[98, 100, 102] Similar increases in PME metabolites have been reported in setting of rapid cell proliferation such as lymphomatous infiltration of the liver[193, 194] and during hepatic graft failure in chronic ductopenic rejection.[195] Thus the increased concentrations of metabolites arising from D-galN metabolism and hepatocyte proliferation may have contributed to the weak correlation between PME and the extent of liver damage.

In a similar manner, concentrations of Pi can be altered by the same processes. D-galN intermediates, galactosamine-1-phosphate, N-acetylglucosamine-1-phosphate and N-acetyl-galactosamine-1-phosphate all accumulate and resonate within 0.20 ppm of Pi.[191, 192] The broad lines present in *in vivo* spectroscopy thereby render the 'Pi' resonance a multicomponent peak. In addition to the contributions made from D-galN catabolites, levels of Pi have also been reported to increase during liver regeneration.[87, 196]

Actual evidence of D-galN metabolism was identified by the prominent elevation of the UDP-sugar resonances in the spectra from rats with moderate and severe acute liver failure. Peaks belonging to UDP-galactosamine, UDP-glucosamine and their N-acetylated derivatives all increased dramatically following D-galN exposure, and resonate up-field from α-ATP.[191, 192]

The prognostic outcome from acute liver failure is largely dependent on residual viable liver tissue.[197, 198] Unfortunately, radiologic imaging lacks sensitivity in terms of measuring viable liver tissue and liver biopsies are often avoided and/or contraindicated in most patients with acute liver failure due to coagulopathies.[169, 170] The results of the present study indicate that ^{31}P MRS, via hepatic ATP levels, provides a non-invasive indication of residual viable tissue and thereby helps predict the outcome in this rat model of acute liver failure. When performed 18-20 hrs prior to maximum liver injury MRS clearly demonstrated that rats with hepatic ATP > 2.3 mM would survive the episode of acute liver failure (negative predictive value 1.0), while rats with hepatic ATP <1.5 mM would die (positive predicative value 1.0). Values between these extremes provided a less definitive outcome. When a cut off value of 2.0 mM was selected (both sensitivity and specificity were maximized) the test was able to correctly predict survival and death

with 80% and 60% accuracy respectively. This compares favourably with other purported means of predicting survival.[167]

Regarding the limitations of intermediate hepatic ATP levels and prognosis it should be noted that hepatic ATP is a dynamic variable. Thus, during an episode of acute liver failure the nadir of hepatic ATP (severity of necrosis) is determined by the rate of ATP depletion over the initial course of liver injury. This raises the possibility that repeated measures of hepatic ATP may prove to be of even greater prognostic value than a single ATP measurement at one point in time. However, transporting severely ill patients to the MR unit for multiple scans would be technically difficult. Given these constraints only a single MR scan may be feasible, in which case the prognostic value of a single hepatic ATP measurement must be interpreted in relation to the etiology, time of onset and current clinical features of the episode of acute liver failure.

In summary, we have documented that ^{31}P MRS can non-invasively assess the bioenergetic alterations, hepatocyte necrosis and hepatic dysfunction that accompanies acute liver failure. We have also documented that hepatic ATP levels hold promise as a useful indicator of prognosis in the setting of acute liver failure.

CHAPTER VI

HEPATIC ^{31}P MRS IN RAT MODELS OF CHRONIC LIVER DISEASE: ASSESSING THE EXTENT AND PROGRESSION OF DISEASE

6.1. INTRODUCTION

The majority of chronic liver disorders will eventually progress in an insidious manner to cirrhosis.[9, 10] Cirrhosis is a diffuse condition, characterized by the loss of functioning hepatic mass, extensive fibrosis and reconstruction of hepatic lobules into abnormal nodular patterns.[199] Initially the condition is asymptomatic and associated with normal liver function tests as the residual liver is able to compensate for hepatocyte necrosis and changes in hepatic architecture. Eventually the disease and structural distortions become sufficiently extensive to result in hepatic decompensation and death from liver failure or complications thereof.[9]

The rates of progression of chronic liver diseases to cirrhosis are highly variable. For some patients, cirrhosis can develop within 1 to 2 years while for others, 2 to 3 decades may be required.[200] This variability highlights the importance of being able to accurately document the rate of disease progression, which often impacts on decisions regarding therapeutic interventions. To date, liver biopsies remain the gold standard whereby assessments of liver disease are conducted.[73-75] However, a number of problems surround this procedure, including; 1) it is invasive, occasionally painful and often feared by patients, (2) complications can be life threatening, (3) it is prone to sampling error and (4) the histological interpretation is subjective.[76, 77, 201] Alternative means of documenting the extent of chronic liver disease and dysfunction include traditional blood tests (serum aminotransferases, bilirubin and albumin levels and plasma prothrombin times) and classification systems such as Child-Pugh scores.[12] Quantitative liver function tests can also be employed. These include various measurements of hepatic blood flow, clearance

rates and hepatic metabolism of exogenous agents.[63] Unfortunately, the applicability of these tests is limited by inaccuracies, cumbersome data collection and/or difficulties in interpretation.[11, 12]

Chapters 4 and 5 have demonstrated that hepatic ATP levels in particular accurately reflect the extent of hepatic disease and dysfunction following graded surgical resections and in animal models of acute liver disease. Reports by other groups have suggested that changes in the PME resonance may also be indicative of the extent of acute or chronic disease.[97, 100, 102] The aim of the present study was to determine whether levels of hepatic metabolites (ATP, Pi, PME and/or PDE), as detected by quantitative ^{31}P-MRS, reflects the severity and progression of chronic liver disease to cirrhosis in rats.

6.2. MATERIAL AND METHODS

6.2.1. Experimental Animals

Adult male Sprague-Dawley rats were maintained on Purina rat chow and water ad libitum until initiation of the study. All animals were kept in identical housing units on a 12-hr light and 12-hr dark cycle. The number of rats assigned to each experimental group was based on published data regarding the consistency of the model employed, anticipated death rates and number of analyses outlined in the experimental protocol. This study was approved by the University of Manitoba Animal Ethics Committee.

6.2.1.1. Thioacetamide-Induced Liver Cirrhosis

Thioacetamide (TAA) cirrhosis was induced in 35 rats (150-250g) by administering TAA (Sigma Chemicals, St. Louis, Mo, USA; 30 mg/ 100 ml) in their drinking water over a period of 6 months.[202, 203] Serial MRS examinations were performed at baseline and at 2, 4 and 6 months during TAA exposure. Following MRS examinations at each time, a subset of rats (4-12 per group) was sacrificed and blood and livers samples were collected. For animals which underwent serial examinations (n=10) over the entire six month period, percutaneous liver biopsies were performed following each MRS exam.

Twelve isocaloric-fed rats not exposed to TAA served as controls. Serial MRS examinations were also performed on this group. However, subsets of these rats were only sacrificed at baseline and at 6 months.

6.2.1.2. Carbon Tetrachloride-Induced Liver Cirrhosis

This group consisted of 27 rats weighing 100-120g. All animals had free access to water containing 0.35g/l phenobarbital (Abbott Laboratories Canada) starting two weeks prior to and continuing throughout carbon tetrachloride (CCl_4) administration.[204] CCl_4 (Sigma Chemicals, St. Louis, Mo, USA) was given intragastrically twice a week to 21 rats for 8 to 9 weeks. CCl_4 was diluted in 0.5 ml of corn oil and doses were continuously adjusted on the basis of individual body weight as described by Dupin et al.[205] Six control rats underwent the same procedure, but received only corn oil intragastrically.

MRS examinations were performed on all animals 10-14 days after their last CCl_4 or corn oil treatment. Following each MRS exam, animals were sacrificed and blood and liver samples were collected.

6.2.1.3. Common Bile Duct Ligation-Induced Cirrhosis

Common bile duct ligation (CBDL) was used to produce secondary biliary cirrhosis in ten rats (240-270g).[206] Briefly, under ether anaesthesia a 4 cm incision was made just below the xiphoid process. The bile duct was isolated, a double ligation of the common bile duct was performed, and then the bile duct was severed between the ligatures. The abdomen was subsequently closed and the animal allowed to recover.

Serial MRS examinations and blood sample collections were performed on each rat at baseline (preoperatively), and on days 12, 27 and 46 post-surgery. Following the measurements on day 46, animals were sacrificed and liver samples were collected.

MRS examinations, blood and liver sample collections were also performed on day 46 on an additional group of age-matched rats (n=4) not subjected to surgery.

6.2.2. ^{31}P-Magnetic Resonance Spectroscopy

MRS examinations were performed as outlined in Chapter 3.

6.2.3. Liver Function

Sera were isolated from collected blood samples and serum aspartate aminotransferase (AST) and albumin were measured using commercial kits (Sigma, St. Louis, MO, USA). Albumin was selected because it accurately reflects hepatic dysfunction in the setting of chronic liver disease and serum bilirubin levels tend to be disproportionatly elevated in cholestatic liver disorders.

6.2.4. Histology and Quantitative Morphological Analysis of Liver Tissue.

Fixed tissue specimens were blocked in paraffin, cut and stained with hematoxylin and eosin and van Gieson (collagen) stains. Slides were staged (0-IV) by a pathologist (blinded to the study groups) for hepatic fibrosis according to the following scale: stage 0; no fibrosis, stage I (mild fibrosis); fibrous expansion around portal tracts or central veins, stage II (moderate fibrosis); septa extending into the liver lobule, stage III (moderate fibrosis); bridging fibrosis (portal-portal, central-central or portal-central linkage) and stage IV (cirrhosis); parenchymal noduals surrounded by fibrous septa and disturbed hepatic architecture.

Images of the van Gieson stained sections were captured with a Spot Cooled Color Digital Camera and Spot Software v2.2 (Diagnostic Instruments, Inc., Sterling Heights, MI, USA). A 40x power microscopic field of the liver tissue was displayed on a colour monitor as an 800x 600 pixel image. Proportional areas of liver tissue and fibrosis were determined using a computerized image analysis system (Image Pro Plus Software Package, Silver Spring, MD, USA) and the liver cell area/ whole tissue area ratio was then calculated. The procedure was carried out over 10-15 fields of view on each tissue section excluding large vessels and large portal tracts. The mean value from all fields was expressed as a percentage defined as the 'liver cell area ratio' (LCAR), which represents the liver cell volume per unit of liver tissue.

6.2.5. Statistical Evaluation

Results were expressed as mean ± standard error. An analysis of variance with Tukey-Kramer correction was used to examine differences between groups. Spearman correlations were performed to test for associations between nonparametric test variables, with a P value of less than 0.05 considered significant.

6.3. RESULTS

6.3.1. TAA Model

Animals in the TAA series tended to gain weight over the course of the disease as rats at stages 2, 3 and 4 weighed more than those at stage 0 and 1 (Table 6). Liver weights were also greater at stages 3 and 4 than at the preceding stages.

Table 7 provides the results of serum AST and albumin determinations at various stages of disease. Similar to the reports of others, levels of serum AST and albumin did not differ with the stage of disease.[207, 208] However, LCAR decreased with progressive disease reaching significantly lower levels at stages 2, 3 and 4.

Representative sections of liver tissue and corresponding localized ^{31}P MR spectra from rats with normal livers (stage 0) and those with stages 2, 3 and 4 of TAA induced chronic liver disease are provided in Fig.12. In addition to the fibrosis and cirrhosis traditionally described for late stages of chronic liver disease, regions of ductular cholangiocellular proliferation were frequently present in TAA-treated rats with stages 3 and 4 disease.

Hepatic ^{31}P MR spectra from rats with normal livers (stage 0), and stages 1 and 2 disease were similar. Once disease progressed to stages 3 and 4, a significant decrease in the signal of phosphorylated metabolites was seen in the ^{31}P MR spectra. The concentrations of the various phosphorylated metabolites are presented in Table 8. Hepatic ATP levels decreased with progression of the disease such that significantly lower levels were documented once rats progressed to stages 3 and 4. Levels of Pi fluctuated with progression of the disease, but significantly lower levels were detected at

Table 6. Rat Body and Liver Weights At Various Stages of Chronic Liver Disease

Thioacetamide Series

Group	n	Body Weight (g)	Liver Weight (g)
Stage 0	9	341 ± 15	14.8 ± 0.9
Stage 1	4	270 ± 9.0	11.1 ± 0.6
Stage 2	4	410 ± 15*	15.0 ± 1.6
Stage 3	7	423 ± 15*	19.1 ± 1.5**
Stage 4	9	415 ± 15*	19.7 ± 1.6**
Carbon Tetrachloride Series			
Stage 1	6	433 ± 12	11 ± 0.5
Stage 4	10	413 ± 11	13 ± 1.0
Common Bile Duct Ligation Series			
Baseline	8	283 ± 7.0	-
Cholestasis			
11 days	9	295 ± 7.0	-
26 days	9	344 ± 10$^{\perp}$	-
46 days	7	376 ± 24$^{\perp\perp}$	20.0 ± 2.1
Age Matched Controls	4	461 ± 12	14.1 ± 0.9

Values are means ± S.E.

*p<0.05 vs Stage 0 and 1. **p<0.05 vs Stage 1

$^{\perp}$p<0.05 vs Baseline. $^{\perp\perp}$p<0.05 vs Baseline and Age matched controls

Table 7. Serum AST and albumin levels and liver cell area ratio (LCAR) in control rats and rats at various stages of thioacetamide-induced chronic liver disease

Stage	Serum AST (U/L)	Serum Albumin (g/L)	LCAR (%)
0	65.7 ± 14.4	38.5 ± 0.9	98.5 ± 0.2
1	72.4 ± 24.0	42.6 ± 2.6	98.2 ± 0.1
2	59.2 ± 10.0	40.6 ± 1.8	93.6 ± 2.0$^{\varphi}$
3	76.5 ± 15.0	40.6 ± 1.0	90.1 ± 2.5$^{\varphi\varphi}$
4	89.1 ± 14.4	42.0 ± 0.8	86.4 ± 2.5$^{\varphi\varphi\varphi}$

Abbreviations; AST, aspartate aminotransferase; LCAR, liver cell area ratio.

$^{\varphi}p< 0.05$ vs Stages 0 and 4
$^{\varphi\varphi}p<0.05$ vs Stages 0 and 1
$^{\varphi\varphi\varphi}p<0.05$ vs Stages 0,1 and 2

Figure 12: A representative histologic section of liver and corresponding hepatic ^{31}P MR spectrum from (A) a healthy rat (stage 0) and rats with TAA-induced chronic liver disease (B) stage 2; (C) stage 3 and (D) stage 4. Van Gieson, X20. See methods for description of histologic staging. Abbreviations: PME, phosphomonoesters; Pi, inorganic phosphate; PDE, phosphodiesters; ATP, adenosine triphosphate. PCr, small phosphocreatine resonance arising from abdominal wall muscle.

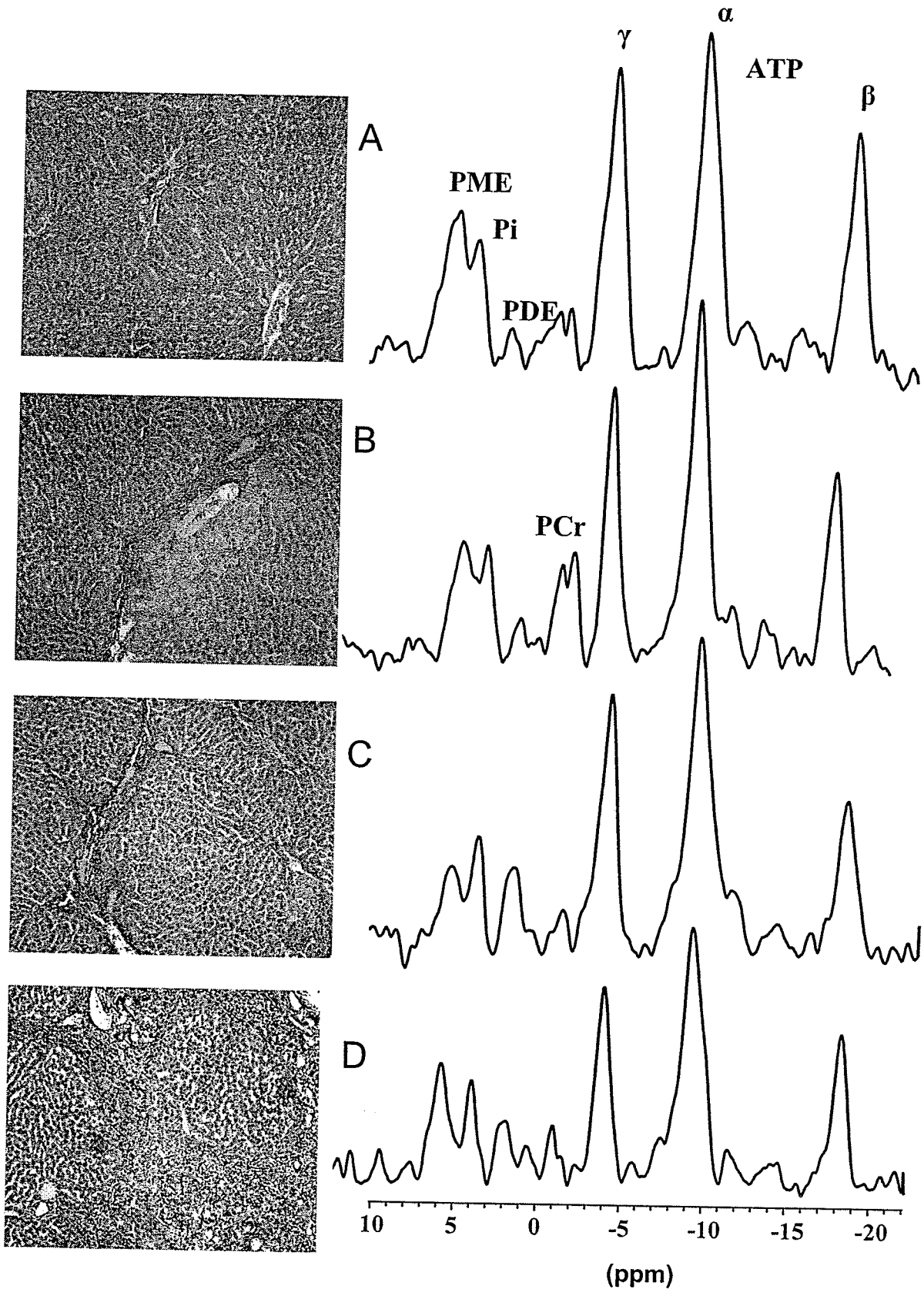
α
γ
ATP
β
A
PME
Pi
PDE
B
PCr
C
D
10
5
0
-5
-10
-15
-20
(ppm)

Table 8. Concentrations (mM) of hepatic phosphorylated metabolites in control rats and rats at various stages of thioacetamide-induced chronic liver disease

Stage	PME	Pi	PDE	ATP
0	3.68 ± 0.17	1.55 ± 0.07	1.05 ± 0.09	3.04 ± 0.12
1	3.63 ± 0.40	1.90 ± 0.28	1.13 ± 0.15	2.82 ± 0.04
2	3.05 ± 0.17	0.91 ± 0.07*	1.23 ± 0.11	2.61 ± 0.14
3	3.03 ± 0.88	1.21 ± 0.08*	1.28 ± 0.12	2.21 ± 0.17**
4	2.55 ± 0.17	0.94 ± 0.06*	1.11 ± 0.09	2.18 ± 0.15**

Values are means ± S.E. Abbreviations; PME, phosphomonoesters; Pi, inorganic phosphate; PDE, phosphodiesters; ATP, adenosine triphosphate.
*$p<0.05$ vs Stage 0 and 1. **$p<0.05$ vs Stage 0

stages 2, 3 and 4 compared to stage 0 and 1 levels. PME levels displayed a downward trend with disease progression but did not achieve statistical significance , while PDE levels remained unchanged.

Correlation analysis (Table 9) revealed no significant associations between these hepatic phosphorylated-metabolite levels and serum AST, however, Pi levels did correlate with serum albumin concentrations ($r=-0.48$, $P<0.004$). Significant correlations also existed between the LCAR index and hepatic ATP ($r=0.56$, $P<0.001$) and PME ($r=0.46$, $P<0.01$) levels.

6.3.2. CCl_4 Model

Body and liver weights among rats exposed to CCl_4 were similar to those of controls (Table 6) as were serum AST concentrations (Table 10). However, serum albumin concentrations in rats with stage 4 disease were significantly lower than in rats with stage 1 disease (30.2 ± 0.6 versus 35.2 ± 1.2 g/L, $P<0.05$ respectively). Stage 4 livers also had a lower LCAR index than those at stage 1 ($83.9 \pm 1.2\%$ vs $98.6 \pm 0.2\%$, $P<0.05$, respectively).

Animals treated for 8-9 weeks with CCl_4 had cirrhosis (stage 4) while those treated with corn oil alone displayed non-specific histologic changes. Presented in Fig. 13 are representative histological sections and hepatic ^{31}P MR spectra from cirrhotic and control rats. Table 11 shows the concentrations of hepatic phosphorylated metabolites in CCl_4 treated rats and controls. Similar to TAA experiments, animals with stage 4 disease had decreased hepatic ATP levels compared to rats with stage 1 disease. Hepatic Pi and PME levels demonstrated a trend towards lower levels with increasing severity of disease but these did not reach statistical significance. PDE levels remained unchanged.

Table 9. Correlations between hepatic phosphorylated metabolites, serum AST and albumin levels and liver cell area ratio (LCAR) in thioacetamide-induced chronic liver disease

	Serum AST	
	Correlation (r)	P-value
PME	0.01	0.97
Pi	-0.02	0.92
PDE	-0.10	0.59
ATP	0.01	0.95
	Serum Albumin	
	Correlation (r)	P-value
PME	-0.21	0.24
Pi	-0.48	0.004
PDE	0.09	0.65
ATP	-0.25	0.15
	LCAR	
	Correlation (r)	P-value
PME	0.46	0.01
Pi	0.29	0.14
PDE	-0.12	0.52
ATP	0.56	0.001

Abbreviations; PME, phosphomonoesters; Pi, inorganic phosphate; PDE, phosphodiesters; ATP, adenosine triphosphate; AST, aspartate aminotransferase.

Table 10. Serum AST and albumin levels and liver cell area ratio (LCAR) in control rats and rats with carbon tetrachloride-induced chronic liver disease

Stage	Serum AST (U/L)	Serum Albumin (g/L)	LCAR (%)
1	60.98 ± 10.70	35.23 ± 0.63	98.56 ± 0.21
4	75.14 ± 13.07	30.23 ± 1.20*	83.86 ± 1.22*

Abbreviations; AST, aspartate aminotransferase;
*$p < 0.05$ vs Stage 1

Table 11. Concentrations (mM) of hepatic phosphorylated metabolites in control rats and rats with carbon tetrachloride-induced chronic liver disease

Stage	PME	Pi	PDE	ATP
1	3.61 ± 0.39	0.94 ± 0.11	0.90 ± 0.16	3.33 ± 0.20
4	3.35 ± 0.18	1.09 ± 0.06	0.81 ± 0.08	2.71 ± 0.10*

Values are means ± S.E. Abbreviations; PME, phosphomonoesters; Pi, inorganic phosphate; PDE, phosphodiesters; ATP, adenosine triphosphate.
*$p < 0.05$ vs Stage 1

Figure 13: A representative histologic section of liver and corresponding hepatic ^{31}P MR spectrum from (A) a control rat and (B) a rat with carbon tetrachloride-induced cirrhosis. Van Gieson, X20. See methods for description of histologic staging. Abbreviations: PME, phosphomonoesters; Pi, inorganic phosphate; PDE, phosphodiesters; ATP, adenosine triphosphate. PCr, small phosphocreatine resonance arising from abdominal wall muscle.

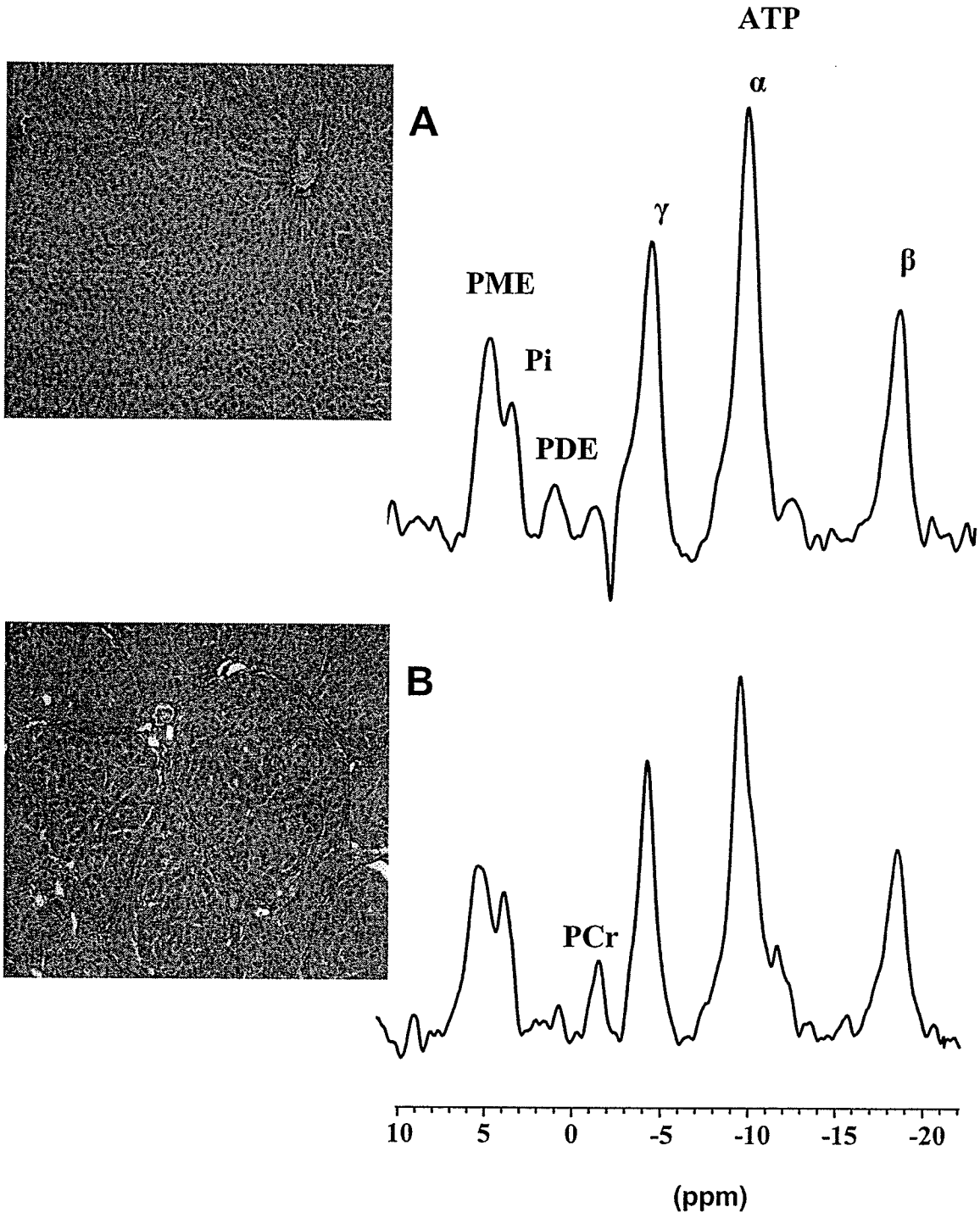
ATP
α
A
γ
β
PME
Pi
PDE
B
PCr
10
5
0
-5
-10
-15
-20
(ppm)

Correlations between hepatic phosphorylated metabolites, serum AST and albumin concentrations and LCAR in CCl_4 treated rats are presented in Table 12. Hepatic ATP levels correlated with both serum albumin ($r=0.53$, $P<0.02$) and LCAR ($r=0.63$, $P<0.006$).

6.3.3. CBDL Model

As shown in Table 6, animals in the CBDL series followed a similar trend to that described for the TAA group in that rats with more advanced disease (days 26 and 46) weighed more than those at baseline or with early disease (day 12). Aged-matched controls weighed more than their day 46 cholestatic counterparts. Liver weights were similar between the two groups (Table 6).

As shown in Table 13, significant elevations of serum AST and reductions in serum albumin concentrations and the LCAR index occurred in cholestatic rats over the course of the disease.

Representative sections of liver tissue and the corresponding liver ^{31}P MR spectra from a control rat and rat with chronic cholestasis are displayed in Fig. 14. At 46 days post bile duct ligation, hepatic lesions which included marked hepatocyte necrosis, inflammation, bile duct proliferation and fibrosis, were in keeping with biliary cirrhosis. A summary of the levels of hepatic phosphorylated metabolites documented during the course of the chronic cholestatic liver disease is presented in Table 14. Hepatic ATP levels progressively decreased, with significantly lower levels occurring at 47 days post surgery (Fig. 12). Correlation analysis (Table 15) revealed that hepatic ATP levels

Table 12. Correlations between hepatic phosphorylated metabolites, serum AST and albumin levels and liver cell area ratio (LCAR) in rats with carbon tetrachloride-induced chronic liver disease

	Serum AST	
	Correlation (r)	P-value
PME	0.04	0.86
Pi	0.13	0.62
PDE	0.01	0.95
ATP	0.26	0.30
	Serum Albumin	
	Correlation (r)	P-value
PME	0.00	0.99
Pi	-0.34	0.17
PDE	0.19	0.35
ATP	0.53	0.02
	LCAR	
	Correlation (r)	P-value
PME	0.25	0.32
Pi	-0.24	0.35
PDE	0.29	0.17
ATP	0.63	0.006

Abbreviations; PME, phosphomonoesters; Pi, inorganic phosphate; PDE, phosphodiesters; ATP, adenosine triphosphate; AST, aspartate aminotransferase.

Table 13. Serum AST and albumin levels and liver cell area ratio (LCAR) in control rats and rats with chronic cholestatic liver disease following common bile duct ligation

Time	Serum AST (U/L)	Serum Albumin (g/L)	LCAR (%)
Baseline	73.9 ± 18.4	48.2 ± 1.4	-
12 days	237 ± 29*	42.0 ± 2.3	-
27 days	217 ± 38*	33.5 ± 2.8$^{\perp}$	-
46 days	325 ± 98**	27.5 ± 1.9**	70.7 ± 5.8*
Aged matched Controls	33.0 ± 5.4	39.4 ± 1.1$^{\gamma}$	96.0 ± 0.7

Abbreviations; AST, aspartate aminotransferase.
*p< 0.05 vs Aged matched
**p< 0.05 vs Baseline, 12 days and Aged matched Controls
$^{\perp}$p< 0.05 vs Baseline, 12 days
$^{\gamma}$p< 0.05 vs Baseline, 46 days

Figure 14: A representative histologic section of liver and corresponding hepatic ^{31}P MR spectrum from (A) a control rat and (B) a rat with cholestatic (common bile duct ligation) induced cirrhosis. Van Gieson, X40. See methods for description of histologic staging. Abbreviations: PME, phosphomonoesters; Pi, inorganic phosphate; PDE, phosphodiesters; ATP, adenosine triphosphate. PCr, small phosphocreatine resonance arising from abdominal wall muscle.

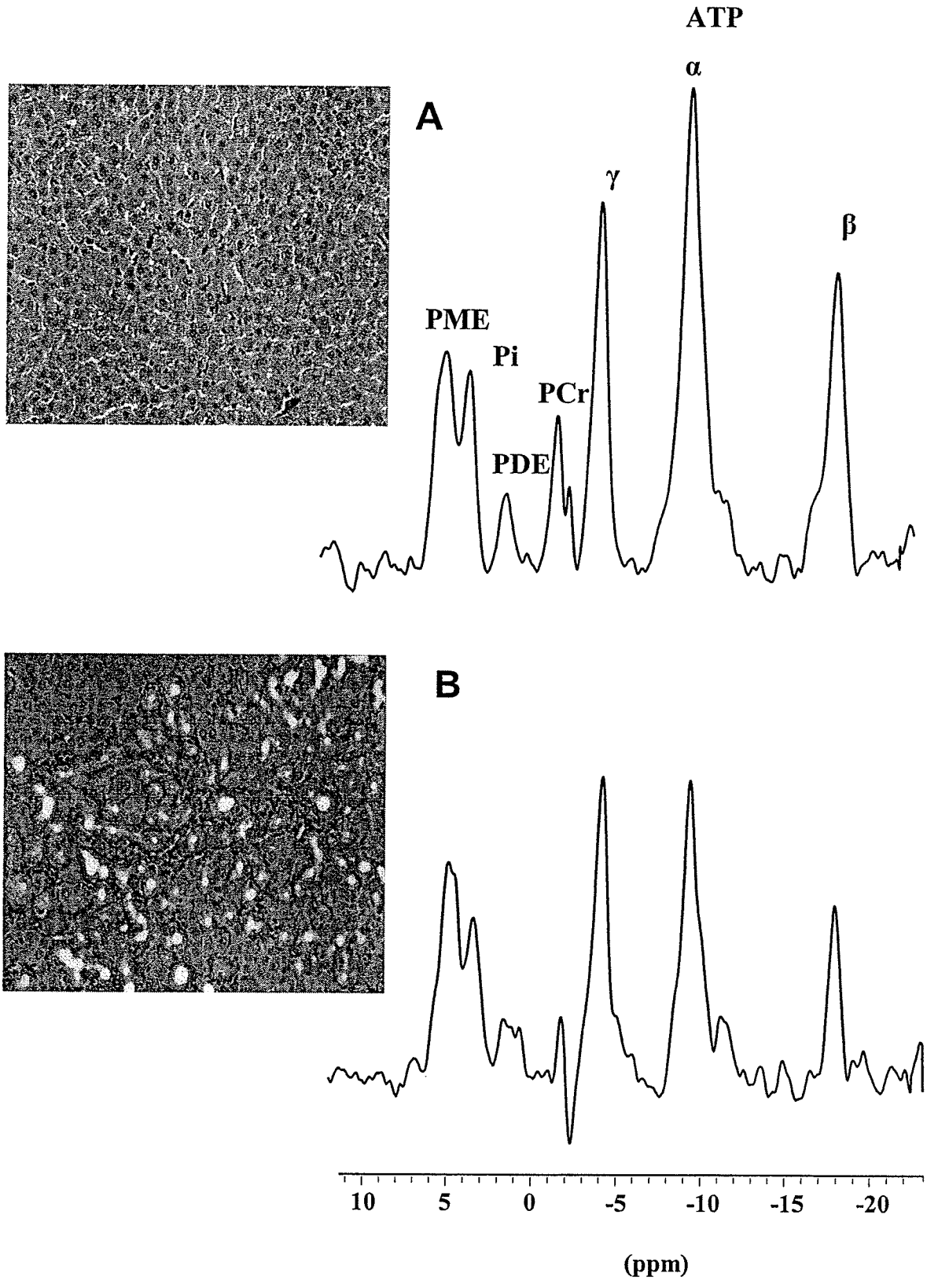
ATP
α
A
γ
β
PME
Pi
PCr
PDE
B
10
5
0
-5
-10
-15
-20
(ppm)

Table 14. Concentrations (mM) of hepatic phosphorylated metabolites in control rats and rats with chronic cholestatic liver disease following common bile duct ligation.

Time	PME	Pi	PDE	ATP
Baseline	3.05 ± 0.24	1.64 ± 0.11	0.94 ± 0.15	3.13 ± 0.22
12 days	3.21 ± 0.19	1.56 ± 0.10	1.01 ± 0.07	2.69 ± 0.22
27 days	3.20 ± 0.28	1.72 ± 0.16	0.98 ± 0.09	2.60 ± 0.30
46 days	2.64 ± 0.30	1.43 ± 0.17	0.97 ± 0.19	1.66 ± 0.13*
Age matched Controls	3.04 ± 0.13	1.30 ± 0.03	1.49 ± 0.37	3.28 ± 0.34

Values are means ± S.E. Abbreviations; PME, phosphomonoesters; Pi, inorganic phosphate; PDE, phosphodiesters; ATP, adenosine triphosphate.
*$p < 0.05$ vs Baseline, Aged matched Controls, 12 day and 27 day cholestatic rats

Table 15. Correlations between hepatic phosphorylated metabolites, serum AST and albumin levels and liver cell area ratio (LCAR) in rats with common bile duct ligated induced cholestatic liver disease

	Serum AST	
	Correlation (r)	P-value
PME	-0.08	0.70
Pi	0.14	0.50
PDE	-0.36	0.11
ATP	-0.57	0.002
	Serum Albumin	
	Correlation (r)	P-value
PME	-0.23	0.19
Pi	-0.02	0.91
PDE	0.13	0.52
ATP	0.42	0.01
	LCAR	
	Correlation (r)	P-value
PME	0.24	0.51
Pi	0.39	0.26
PDE	0.53	0.14
ATP	0.71	0.02

Abbreviations; ATP, adenosine triphosphate; AST, aspartate aminotransferase.

correlated with serum AST ($r=-0.57$, $P<0.002$) and albumin ($r=0.42$, $P<0.01$) concentrations and LCAR ($r=0.71$, $P<0.02$).

6.4. DISCUSSION

Chronic liver disease can result from various causes which operate through different pathophysiological pathways and elicit distinct patterns of hepatic injury.[9, 10, 113] However, the general course and outcome of chronic hepatic injury as described by progressive fibrosis and eventually cirrhosis remains constant.[9, 74] In a similar manner, the present study reports consistent alterations in hepatic metabolism throughout the course of hepatocellular and cholestatic chronic liver diseases to cirrhosis. Animals subjected to TAA-, CCl_4- and CBDL- induced chronic liver disease all displayed progressive reductions in hepatic ATP levels with disease progression.

Although the mechanism(s) responsible for the decline in hepatic ATP levels remains to be determined, as in the case of acute liver failure, the loss of viable hepatocytes is likely to be an important contributing factor. As the total amount of these cells per unit volume of liver decreases, MR detectable signal from that volume will also decrease. Indeed, image analysis of tissue sections taken at various stages of disease revealed a progressive decrease in the LCAR index that correlated with decreases in hepatic ATP levels. Thus, during early phases of disease, when hepatocyte loss is offset by active hepatic regeneration only minor changes in hepatic ATP were detected.[209, 210] Once more advanced disease was established, and when regenerative activity becomes impaired,[211] hepatic ATP levels decreased and the decrease was proportional to the loss of functional hepatic tissue.

Another possible explanation relates to altered hepatic bioenergetics, namely increased energy expenditure as liver disease progresses.[212] With the reduction in total volume of viable liver tissue, residual hepatocytes must expend more energy to maintain

normal hepatic function and engage in compensatory liver regeneration. Eventually, the remnant hepatocyte population is incapable of meeting the increasing demands and both energy depletion and hepatic insufficiency ensue. Supporting this explanation were the decreases in serum albumin concentrations and hepatic ATP levels in CCl_4-treated and CBDL rats. That serum albumin concentrations were maintained during TAA-induced chronic liver disease is in keeping with the findings of other investigators who reported no or few changes in liver function tests in TAA-treated animals.[207, 208, 213] Further studies are required to examine the compensatory mechanism that exists in this model.

Disturbed hepatic bioenergetics has also been ascribed to the capillarization of hepatic sinusoids during the development of cirrhosis.[214] In normal livers, the sieve-like structure of the sinusoidal endothelium and the freely accessible perisinusoidal space allow for rapid and high exchange of substrates and nutrients between the vascular compartment and hepatocytes. During fibrogenesis and the development of cirrhosis, a barrier of connective tissue and extracellular matrix is deposited in the perisinusoidal space.[65, 215] By limiting hepatocyte access to nutrients, high energy substrates and oxygen, this barrier may impair hepatic energy metabolism.[214, 216]

The levels of hepatic ATP at end stage disease varied considerably between the models of chronic liver disease, being highest in CCl_4-treated rats (ATP= 2.71 mM), lowest in CBDL rats (1.66 mM) and intermediate in TAA-treated rats (ATP=2.18 mM), despite similar levels of LCAR in each model. This disparity may be explained by the different histological features present. Specifically, CCl_4 administration produced the typical pattern of cirrhosis with bridging fibrotic septa, disorganized parenchymal architecture, regenerative nodules and mild periportal bile ductual proliferation.

Although the same features were present in the TAA model, TAA-exposed rat livers also contained multiple cholangiofibromas. In the CBDL model, a different pattern of cirrhosis was present where extensive bile ductual proliferation extended beyond periportal regions and replaced much of the normal parenchyma. Given that the LCAR index includes both parenchymal and non-parenchymal cells and bile ductual cells are luminal cells, the disparity observed in the hepatic ATP levels could reflect differences in viable hepatocyte populations. It is important to note that the differences between the various models would not affect the results of serial examinations within the same model or individual subjects within the group.

An alternative explanation for the differences in absolute ATP levels relates to the heterogeneity of the liver lobule and the patterns of zonal injury induced by the various models. Periportal hepatocytes within zone 1 of the liver lobule have sufficiently high oxygen tension that they are capable of generating energy by both glycolytic and oxidative metabolism, whereas the less aerobic perivenous hepatocytes predominantly utilize glycolytic pathways of energy generation.[8, 29] Having access to both aerobic and anerobic pathways, and thereby a selection of fatty acid and carbohydrate substrates, periportal hepatocyte are capable of generating more energy on a per mole basis than those in the perivenous region.[7, 217] Hence, one would predict that lesions specific to zone 1 of the liver lobule would create a greater bioenergetic disturbance than lesions localized in zone 3. The results from the present study support this hypothesis as CBDL injury predominantly involves zone 1, while CCl_4 involves zone 3 and TAA is a more diffuse injury, involving zones 1-3 hepatocytes.

Inorganic phosphate, another marker of tissue bioenergetics, displayed a trend towards lower levels with more advanced stages of chronic liver disease. However, significant decreases were only detected among TAA-treated rats. As with hepatic ATP, lower levels of hepatic Pi likely result from reduced hepatocyte mass. However unlike ATP, these changes are attenuated by certain metabolic activities within the functioning remnant liver. Specifically, increased energy expenditure perpetuates the hydrolysis of high energy phosphate bonds which in turn liberates inorganic phosphate species. Accumulation of Pi due to enhanced metabolic activity and reduced recycling back to purine/ pyrimidine moieties would in turn contribute to the Pi signal. Indeed, increases in Pi have been observed during high energy activities such as liver regeneration following partial hepatectomy.[136, 196]

Contrary to previous reports, in this study the PME resonance did not increase in any of the models employed. As discussed earlier, the PME peak is difficult to interpret because it is a multicomponent resonance with numerous metabolites contributing to its broad signal.[87] These include membrane phospholipid precursors, phosphoenthaolamine (PE) and phosphocholine (PC), and several phosphorylated glycolytic intermediates. Moreover, in the previous reports, PME findings were reported as ratios of PME/ATP and PME/PDE[97, 98] which could also reflect decreases in hepatic ATP and/or PDE levels, as was observed in the present study, rather than increases in PME.[104] Finally, biological processes can influence the components of the PME resonance in a dissimilar manner. While the loss of viable liver cells likely contributes to a decrease in PME, other processes favour an increase in the PME signal. High resolution MRS experiments performed on tissue extracts demonstrate significant elevations of hepatic PE and PC in

cirrhosis.[100] High levels of these membrane precursors are assumed to reflect enhanced cell turnover as the cirrhotic liver attempts to regenerate. PE and PC, however, only contribute approximately 15% to the total PME signal[87] and thus are unlikely to cause a significant effect on the *in vivo* PME resonance. This may explain why we and others have not found significant changes in the absolute levels of PME in cirrhosis or following partial hepatectomy.[135]

Levels of the PDE resonance also remained constant over the course of chronic liver disease in each animal model. Like the PME signal, PDE is a multicomponent resonance with contributions from several metabolites. Signals arising from degradative phospholipid metabolites GPC and GPE and the phospholipid bilayer of the endoplasmic reticulum contribute to this peak.[87-89] These components are not resolved in *in vivo* spectra. Thus, difficulties interpreting the state of these metabolites remain as diverging alterations in individual components may cancel, leaving total PDE levels unchanged. The interpretation of the PDE resonance is further complicated by its magnetic field dependence, hence caution must be exercised when comparing studies performed at different field strengths.[88, 89]

In summary, the results of the present study indicate that hepatic ATP levels correlate well with biochemical evidence of hepatic dysfunction and histological evidence of loss of functioning hepatocytes and progressive disease. The results also support the concept that regardless of the etiology, progressive liver disease has a significant effect on hepatic bioenergetic integrity. Given these observations, hepatic ^{31}P MRS holds promise as a non-invasive means of documenting the extent and progression of chronic liver disease.

CHAPTER VII
QUANTITATIVE HEPATIC PHOSPHORUS-31 MAGNETIC RESONANCE SPECTROSCOPY IN PATIENTS WITH COMPENSATED AND DECOMPENSATED CIRRHOSIS

7.1. INTRODUCTION

Cirrhosis and its associated complications is a major cause of morbidity and mortality worldwide.[218] The clinical spectrum of cirrhosis is broad, including patients who are asymptomatic and unaware of their condition to those who require hospitalization for life threatening emergencies.[9, 10] Between these extremes is an insidious clinical course in which compensated cirrhosis progresses to a decompensated state. During the early stages of cirrhosis the large functional reserve of the liver is able to compensate for changes in tissue architecture brought about by bridging fibrosis and abnormal nodular formation. Hence, patients may only experience non-specific symptoms such as fatigue, weakness and general malaise. Eventually the disease progresses to the point where the hepatic reserve is unable to compensate for hepatocyte loss and structural distortions in the liver. At this late stage, signs of hepatic dysfunction ensue which include jaundice, ascites, variceal hemorrhage, and/or portal systemic encephalopathy. The development of these complications marks the transition from compensated to decompensated cirrhosis and affords the patient a poor prognosis.

The clinical features and gross pathophysiology surrounding hepatic decompensation are well described,[9, 10] however, little is known regarding cellular events in end–stage liver disease. Functionally, in decompensated cirrhosis the synthetic and excretory capacity of the liver is compromised as low levels of albumin, long clotting times (INR) and high levels of bilirubin are commonly documented.[12] Several quantitative liver function tests convey a similar message in that the decompensated cirrhotic liver has a reduced capacity to metabolize/detoxify exogenous compounds.[219] To date, few studies have attempted to document the cellular events that exist in

compensated and decompensated cirrhosis, largely because most methods require invasive tissue sampling which is generally avoided in this group of ill patients with coagulopathies. In the present study we employed ^{31}P MRS to document and compare the metabolic status of the livers of patients with compensated and decompensated cirrhosis.

7.2. Material and Methods

7.2.1. Subjects

The study population consisted of 17 chronic hepatitis C patients. Their mean age was 51 years (range 28-73 years) and 13 were male. The presence of cirrhosis was documented histologically and/or by CT or ultrasound features of cirrhosis including irregular, nodular liver surfaces with accompanying signs of portal hypertension such as the presence of ascites, esophageal varices and/or splenomegaly. Patients were classified as having either compensated or decompensated cirrhosis based on clinical and radiologic findings. Decompensated cirrhosis was defined as patients with persistent jaundice, hepatic encephalopathy, clinically or radiologically apparent ascites and/or endoscopically documented variceal bleeding secondary to cirrhosis. Nine patients with compensated and eight with decompensated cirrhosis were studied.

Eight volunteers (6 males, 2 females, mean age 51 years [range 41-60 years]) with no history or evidence of liver disease served as healthy controls.

7.2.2. MR Examination

Prior to each MR scan, subjects were required to fast for four hours. MR examinations were performed on a 1.5 T General Electric Signa whole body magnetic resonance system. Subjects were positioned supine within the scanner, and a 15 cm transmit/receive phosphorus surface coil, tuned and matched to 25.85 MHz, was placed directly above the subject's liver. A small vial containing 0.5 M phenylphosphonic acid (PPA) was placed

at the center of the coil to assist with subject positioning during proton imaging, calibration of the RF field strength at the region of interest (ROI), and for quantitation of metabolite concentrations. Proton signal was used for shimming and localizer images in the coronal and axial planes were then obtained with the body coil to ensure correct coil positioning. Further automated and manual localized shimming on the ROI within the liver was performed using a STEAM sequence with a typical voxel size of 70mm x 70mm x 40 mm (lateral, vertical, and axial dimensions respectively). For ^{31}P spectroscopy at 25.85 MHz, the transmit power to obtain a 90° flip angle was determined for the PPA reference vial at the center of the coil using a 900 μs slice selective gaussian RF pulse. A fully relaxed spectrum (TR= 7s) of the entire 4-cm axial slice was acquired and the area of the PPA peak at 14.3 ppm was used for measurements of coil loading. Based on the characteristics of the B_1 field of the surface coil, the transmit power for a 45° flip angle was determined at the center of the ROI (typically at a depth of 7cm) for subsequent localized spectroscopy. Localized ^{31}P liver spectra were acquired using two-dimensional chemical shift imaging (2D-CSI). Data acquisition parameters were as follows: FOV= 48 cm (horizontal) x 48 cm (vertical), 8 averages, TR= 1.5 s, matrix size= 12 x 12, an acquisition size of 1024 pts, zero-filled to 2048 pts, and a sweep width of 2500 Hz.

7.2.2.1. Data Processing

Data processing was accomplished using SAGE software (General Electric Ltd.). Briefly, the free induction decay underwent 10 Hz exponential line broadening prior to Fourier transformation, and the resulting spectra were processed with manual phase and

cubic spline baseline correction. Peaks were registered relative to α-ATP resonance (–10 ppm) which served as an internal chemical shift reference. Finally, spectra were analyzed with a frequency domain fitting function where peak integrals were calculated with gaussian curves. The PME, Pi, PDE and PCr (when necessary) signals were treated as singlets, γ and α-ATP peaks as doublets, and the β-ATP resonance as a triplet. Corrections for minor contributions of metabolite signal arising from overlying skeletal muscle were performed. Based on the percentage of PCr in the liver spectra, relative amounts of muscle signal contributing to each metabolite were calculated according to previous published data.[114, 115] These values were then subtracted from the appropriate integral to give a 'pure' liver reading.

7.2.2.2. Quantitation

For quantitiation of hepatic metabolites, simulated phantom experiments were performed as described by Meyerhoff et al.[116] A 20 L plastic carboil containing 50 mM sodium phosphate served as a phantom on which identical MR examinations were performed regularly throughout the experiment. The various metabolite concentrations were determined by the equation:

$$\mathbf{C = C_p \times I/I_p \times N_p/N \times S_p/S \times I_{ref(p)} / I_{ref}}$$ [117]

Where…

C=	absolute tissue metabolite concentration in mmol/L
C_p=	concentration of phantom (p) solution used for calibration in mmol/L
I,I_p=	corresponding signal integrals (I)
N,N_p=	corresponding number of signal averages (N)
S,S_p=	corresponding saturation factors (S) calculated from measured T_1 times
$I_{ref},I_{ref(p)}$ =	corresponding signal integral of reference sample

Literature T_1 values reported for liver were used in the calculation for saturation factors.[118]

Hepatic ATP concentration was based upon the peak area of the β-ATP resonance, which is free of other phosphorylated adenosine species.[90]

7.2.3. Liver Function

Liver enzyme and function tests were performed on the day of or within one month of the date of the MR examination.

7.2.4. Statistical Evaluation

Results were expressed as mean ± standard error. An analysis of variance with Tukey-Kramer correction was used to examine differences between groups. P values < 0.05 were considered significant.

7.2.5. Ethics Approval

The research ethics boards at the Institute for Biodiagnostics National Research Council and the University of Manitoba approved the above study. All subjects provided written informed consent before entering the study.

7.3. RESULTS

Four patients (three compensated and one decompensated) receiving ribavirin therapy for their hepatitis C were excluded from the study post-hoc due to hepatic formation of the activated ribavirin metabolite-ribavirin triphosphate.[220] Once phosphorylated in hepatocytes, these nucleotide triphosphate analogues prevented determinations of hepatic ATP levels.

A summary of liver enzyme and function tests and Child-Pugh scores in the remaining 13 patients with compensated and decompensated cirrhosis are presented in Table 16. As predicted, patients with compensated cirrhosis tended to have earlier, more active liver disease (higher liver enzymes) while those with decompensated cirrhosis had more advanced hepatic dysfunction and a higher Child-Pugh's score (P=0.01). However, only serum albumin concentrations were significantly lower in those with decompensated cirrhosis (P=0.02).

Figure 15 provides a typical axial image from a healthy volunteer. Indicated on the image is a two-dimensional voxel generated by the CSI pulse sequence from which localized spectral information from the liver is acquired. Expanded below is the localized hepatic ^{31}P MR spectrum. A typical ^{31}P MR spectrum from liver contains resonances belonging to PME, Pi, PDE and the three phosphate groups (γ, α and β) from nucleotide triphosphates- the majority of which arise from ATP.[90] PCr may also be detected in the *in vivo* spectrum of liver. This is indicative of signals arising from adjacent muscle and its contribution is deducted from the final data output.

Representative ^{31}P MR spectra obtained from a healthy control (panel A) and patients with compensated (panel B) and decompensated cirrhosis (panel C) are shown in

Table 16. Liver function tests and Child-Pugh's scores in healthy individuals and HCV patients with compensated and decompensated cirrhosis

	Normal Range	Compensated cirrhosis (n=7)	Decompensated cirrhosis (n=6)	P-value
Serum alanine amino transaminase (U/L)	0-30	97.4 ± 29.5	49.83 ± 12.5	0.18
Serum aspartate aminotransferase (U/L)	10-32	95.7 ± 38.4	55.7 ± 8.7	0.37
Serum alkaline phosphatase (U/L)	30-120	113.4 ± 10.7	143.3 ± 30.7	0.34
Serum albumin (U/L)	35-50	36.0 ± 1.4	28.5 ± 2.5	0.02
Serum bilirubin (μmol/L)	3-18	13.8 ± 2.2	29.5 ± 10.9	0.19
INR	0.9-1.1	1.1 ± 0.04	1.3 ± 0.10	0.10
Child-Pugh's score		5.6 ± 0.33	8.2 ± 0.9	0.01

Figure 15: An axial proton image of the liver and corresponding hepatic ^{31}P MR spectrum from a healthy volunteer. PME, phosphomonoesters; Pi, inorganic phosphate; PDE, phosphodiesters; ATP, adenosine triphosphate. * Phosphocreatine resonance arising from abdominal wall muscle.

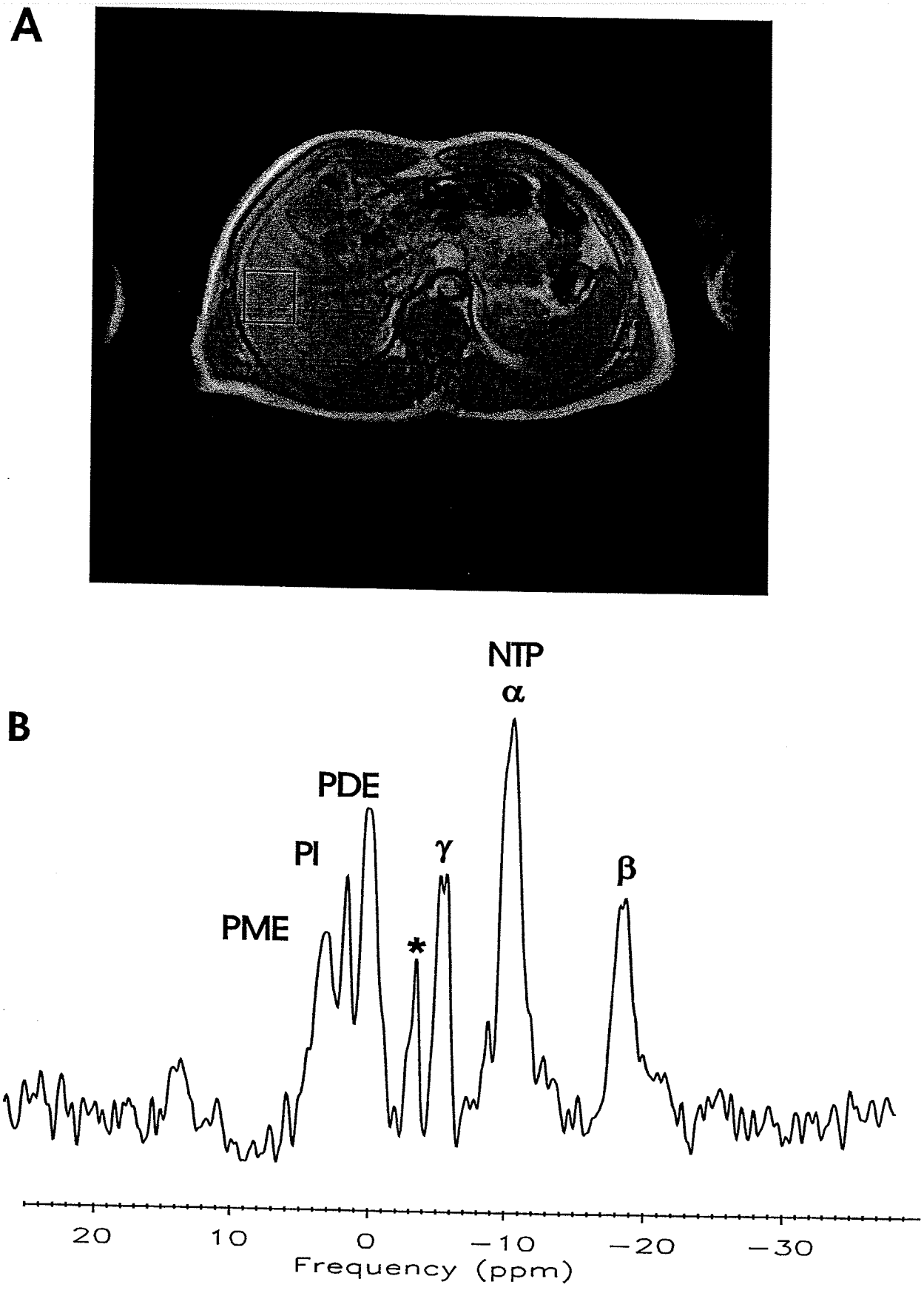
A
B
NTP
α
PDE
PI
γ
β
PME
*
20
10
0
−10
−20
−30
Frequency (ppm)

Fig. 16. Hepatic ^{31}P MR spectra from patients with compensated cirrhosis were equivalent to those seen in healthy controls. However, as indicated in Table 17, significant metabolic derangements were evident in patients with decompensated cirrhosis compared to those with compensated cirrhosis and healthy controls, including lower levels of hepatic ATP ($P<0.02$ and $P<0.009$, respectively) and a higher PME/PDE ratio ($P<0.003$ versus healthy controls).

Figure 16: Representative hepatic ^{31}P MR spectra from (A) healthy control and patients with compensated (B) and decompensated (C) cirrhosis. PME, phosphomonoesters; Pi, inorganic phosphate; PDE, phosphodiesters; ATP, adenosine triphosphate. *Phosphocreatine resonance arising from abdominal wall muscle.

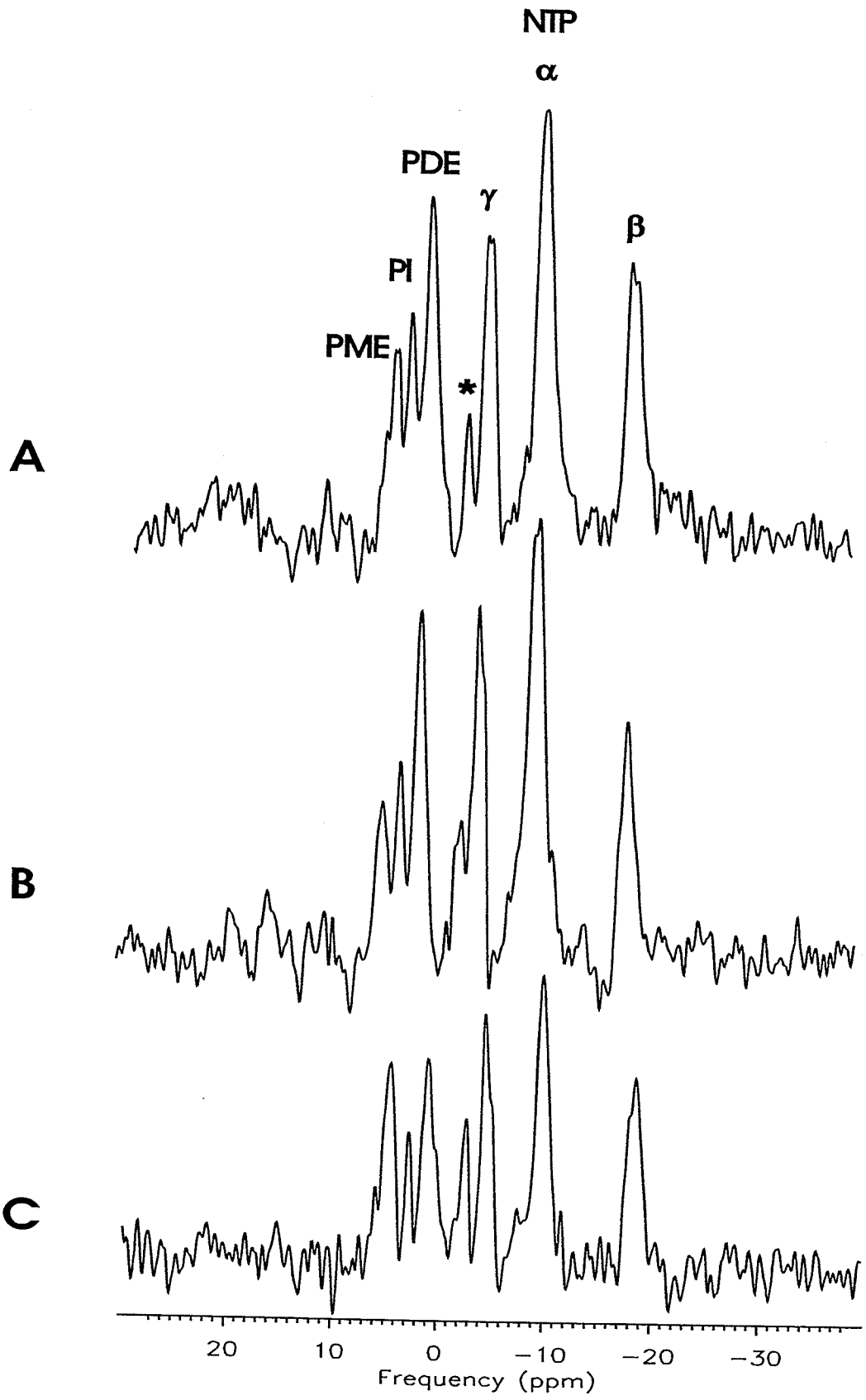
NTP
α
PDE
γ
β
PI
PME
*
A
B
C
20
10
0
−10
−20
−30
Frequency (ppm)

Table 17. Concentrations (mmol/L) of Hepatic Phosphorus Metabolites in Healthy Controls and HCV Patients with Compensated and Decompensated Cirrhosis

Metabolite	Control Subjects (n=8)	Compensated cirrhosis (n=7)	Decompensated cirrhosis (n=6)
PME	3.69 ± 0.56	4.74 ± 0.39	4.06 ± 0.49
Pi	1.18 ± 0.07	1.15 ± 0.20	0.69 ± 0.21
PDE	7.64 ± 0.70	7.55 ± 1.08	4.53 ± 0.98
β-NTP	3.20 ± 0.15	3.11 ± 0.29	2.28 ± 0.20*
PME/PDE	0.47 ± 0.04	0.72 ± 0.12	1.07 ± 0.20**

Values are means ± S.E. Abbreviations; PME, phosphomonoesters; Pi, inorganic phosphate; PDE, phosphodiesters; NTP, nucleotide triphosphate.
*Significant difference $P<0.05$ vs Controls and compensated cirrhosis
**Significant difference $P<0.05$ vs Controls

7.4. DISCUSSION

To date few studies have been performed that examine at a cellular level hepatocyte differences in patients with compensated versus decompensated cirrhosis. In the present study ^{31}P MRS was utilized to non-invasively assess the hepatic metabolic profile of such patients. Our findings suggest that hepatocytes within the decompensated cirrhotic liver have depleted energy stores and altered phospholipid metabolism compared to those within the livers of patients with compensated cirrhosis and healthy controls.

The mechanism whereby hepatic ATP levels become depleted in the decompensated state remains to be determined. Two possible explanations include; (1) the loss of a critical amount of viable hepatocyte mass and/or (2) altered hepatic bioenergetics. With regards to the former, it has been well documented that the formation of cirrhosis involves repeated cycles of hepatic injury and repair that ultimately result in the deposition of fibrous tissue throughout the liver. When hepatocyte necrosis persists in the setting of inadequate liver regeneration (as occurs in decompensated cirrhosis) and extensive fibrosis extends across liver lobules, a significant loss of viable hepatocytes within the liver will occur.[221-223] As the total amount of these cells per unit volume of liver decreases, MR detectable signal from that volume will also decrease. Results from chapters 5 and 6 demonstrated that reduced levels of hepatic ATP detected in animal models of acute and chronic liver disease are proportional to the diminished volume of viable liver tissue.

Bioenergetic alterations may also influence hepatic ATP levels as energy expenditure has been shown to increase with increasing severity of cirrhosis. [212] This explanation is not incompatible with the diminished hepatocyte mass hypothesis as

disturbances in hepatic bioenergetics can arise from a diminished hepatocyte population within the cirrhotic liver. As the total volume of viable liver tissue decreases, residual hepatocytes must expend more energy to maintain hepatic function and engage in compensatory liver regeneration. Eventually, the remnant hepatocyte population is incapable of meeting these increasing demands resulting in both energy depletion and hepatic insufficiency. Supporting this explanation are the results of rat studies wherein hepatic ATP levels correlated with the extent of hepatic dysfunction.[196]

As discussed in relation to animal models of chronic liver disease, further alterations to hepatic bioenergetics would be predicted from capillarization of liver sinusoids. [214] By limiting hepatocyte access to nutrients, high energy substrates and oxygen, this process is likely to impair hepatic energy metabolism.[214, 216] The magnitude of bioenergetic alterations would depend upon the degree of sinusoidal defenestration and impairment of substrate and oxygen transport (i.e. the severity of the disease), thus patients with decompensated cirrhosis would be more likely to be affected by these processes than those with compensated cirrhosis.

Altered hepatic bioenergetics have long been implicated as contributing to the disturbances associated with cirrhosis.[224-226] However, the present study is the first to report *in vivo* that hepatic ATP levels are significantly lower in patients with decompensated cirrhosis. Although previous quantitative ^{31}P MRS studies have described decreased concentrations of hepatic ATP among alcoholic cirrhotics,[105, 227] patients in these studies were not stratified according to disease severity. In addition, concerns exist regarding the cause of ATP depletion in these individuals as diminished levels were also detected in alcoholics with hepatitis who had not yet developed

cirrhosis.[105] To avoid such confounding variables, we selected a cohort of hepatitis C patients with cirrhosis and no alcohol intake for a minimum of one month and off all medications that might adversely affect hepatocyte mitochondria and respiratory chain function.

The ratio of PME to PDE resonance in the ^{31}P MR spectrum has traditionally been viewed as an index of cell membrane turnover.[101] PME and PDE are both multicomponent resonances, which contain contributions from metabolites involved in membrane synthesis (phosphocholine [PC]; phosphoethanolamine [PE]) and degradation (glycerophosphocholine [GPC]; glycerophosphoethanolamine [GPE]) respectively.[87, 89, 154] Rapidly proliferating cells are likely to have high levels of PME relative to PDE. Indeed, high levels of PME/PDE have been reported in hepatic tumors[228] and in regenerating livers following hepatic resection.[132] Several studies have documented elevations in hepatic PME/PDE with increasing severity of cirrhosis.[98-100] In these studies, the increase has commonly been attributed to elevations in PME with concomittant reductions in PDE levels. While *in vitro* MRS has confirmed that the concentration of phosphocholine and phosphoethanolamine increase in cirrhosis,[100, 102] it is uncertain whether these elevations are sufficient to cause an increase in the total concentration of the PME resonance. In fact, increases in the absolute concentration of hepatic PME have not been reported in the cirrhotic liver.[105, 227] In the present study, levels of hepatic PME were similar in the two study populations and controls. However, consistent with other reports, hepatic PME/PDE ratios were significantly elevated in those with decompensated cirrhosis. Hence, the increase in the ratio likely stemmed from lower levels of PDE, rather than increased PME. Although the drop in hepatic PDE only approached

significance (P=0.05) in patients with decompensated cirrhosis, it was sufficient to cause a significant shift in the PME/PDE ratio ($p<0.003$).

The mechanism(s) whereby hepatic PDE levels fall in patients with decompensated cirrhosis is unclear. The two principle components of the PDE resonance include the degradative metabolites of phospholipid metabolism (GPC and GPE) and contributions from endoplasmic reticulum (ER).[88, 89] High resolution *in vitro* analysis has demonstrated that GPC and GPE concentrations are low in the cirrhotic liver,[100, 102] however, these metabolites are only minor contributors to the PDE resonance at low magnetic field strengths.[88] Thus signal arising from the ER phospholipid membrane would be the major contributor to the PDE resonance at clinical field strengths. As such, changes detected in the PDE resonance are likely to reflect disturbances in the ER. Indeed, electron microscopy studies have documented a striking decrease in the quantity of ER in hepatocytes from patients with decompensated cirrhosis compared to those with compensated disease.[100]

Given the above, caution must be exercised when interpreting changes in the PME/PDE ratio. In settings where PME levels are increased, an elevation in the PME/PDE ratio is likely to be indicative of enhanced cell proliferation. In the present study, hepatic PME/PDE levels were increased in patients with decompensated cirrhosis, however, this increase may not have reflected enhanced cell proliferation (regeneration), but rather disturbances in the hepatic ER pool. The latter explanation would be more in keeping with the pathophysiology of decompensated cirrhosis, as smaller hepatic ER pools may help explain the diminished drug clearing capacity seen in decompensated

cirrhosis. That the increased PME/PDE reflects enhanced regenerative activity is also unlikely given the high death rate from liver failure in these patients.[229]

It is important to note that the present study is not without caveats of its own. Absolute quantitation of tissue metabolites by MRS is a challenging task as many experimental variables must be controlled. The relaxation time of each metabolite, T_1, is an important variable as it governs the metabolite peak area in the MR spectrum. Unfortunately, T_1 values are difficult to determine in population studies, because 1) T_1 may change in disease states and (2) long scan times are required for definitive measurements of T_1. In the present study, T_1 values from normal individuals were used for all subjects. This introduces a source of error to the calculated values of some metabolites, since certain metabolite T_1s change with cirrhosis.[98, 99] Menon et al. documented that T_1s of hepatic PME and Pi increase in cirrhosis while PDE T_1s decrease.[98] As a result, saturation effects would cause calculated concentrations of PME and Pi to be underestimated and PDE to be overestimated. Such errors may explain the discrepancy between the *in vivo* and *in vitro* reports discussed earlier. Interestingly, β-ATP T_1 values remain unchanged between normal individuals and cirrhosis patients,[98, 99] hence one can safely assert that the most striking change detected in the present study, the reduction in hepatic ATP levels among patients with decompensated cirrhosis, is both real and accurate.

In summary, the results of this study indicate that hepatic ATP and PDE levels are reduced in patients with decompensated but not compensated cirrhosis. The results also indicate that ^{31}P MRS examination of the liver is a valuable tool for documenting the metabolic status of hepatocytes in patients with advanced liver disease.

CHAPTER VIII

CONCLUSIONS

8.1. CONCLUSIONS

8.1.1. Hepatic ATP Measurements

The premise of this thesis introduces hepatic energy levels as a new index with which to evaluate the status of liver. In the liver resection study absolute levels of ATP and the ratio of ATP/Pi were used to reflect hepatic energy levels. Following liver resection ATP levels dropped while Pi levels rose concomitantly. This inverse relationship permitted ATP/Pi to be used as an addition index of hepatic bioenergetic derangement brought about by increased functional demands and regenerative activity. However, this relationship was not consistently observed in the settings of acute and chronic liver disease. For this reason ATP levels were used as the sole index of hepatic energy levels in the remaining studies.

Quantitative MRS showed that the concentration ATP within the livers of healthy rats and humans is approximately 3.2 mmol/litre, ranging between 2.8 and 3.6 mmol/litre. These findings are in keeping with previous published *in vivo* data.[115, 230, 231] The results in this thesis also suggest that reductions in hepatic ATP are indicative of damage and/or functional disturbances within the liver. If measurements of hepatic ATP are to be recognized as new test of liver health and functional capacity, confounding variables that may give a lower ATP reading in the absence of liver injury or disease must be identified and appropriately controlled.

8.1.2. Additional Considerations

The fasted versus fed state of the subject is an obvious variable that should be controlled. During the post-prandial state when the supply fuel substrates are readily available to the liver, it is assumed that hepatic ATP production would be high. While in the fasted state, resources to the liver would be at a minimum and consequently, rates of hepatic ATP synthesis would be less. This issue is particularly important for patients with liver disease as these individuals often have depressed appetites and in more severe cases, may be malnourished. Initial MRS experiments performed on rats fasted for 48 hours reported that food restriction did indeed deplete hepatic ATP stores.[232] However, studies performed in humans indicated that fasting does not have as profound an affect on hepatic ATP levels.[233] At this point it is unclear what affect the fasted/fed state of the subject has on hepatic ATP measurements, but this can be controlled by standardizing the subject's nutritional intake or by having the subjects fast for 3-6 hours prior to his/her MRS examination, as was outlined in both the animal and human studies.

From all accounts in the literature there do not appear to be any gender difference in hepatic ^{31}P MR spectra, likewise differences in the quantitation of hepatic ATP by this method would seem unlikely. More importantly, medications or drugs that are taken by the subject that are known to uncouple or disrupt mitochondria function should be noted. In this case the subject can be asked (if possible) to refrain from taking these medication prior to the MRS exams. Alcohol consumption is another important factor that should be carefully documented and restricted before spectroscopic evaluations of the liver. Ethanol is known to have a direct effect on liver mitochondria and has been shown to alter hepatic energy levels.[234]

When taken in moderation many of these medications/drugs can potentially reduce hepatic ATP levels towards the lower end of its normal range. However, if these agents cause hepatic ATP levels to drop beyond this range it is likely that significant hepatocyte damage or severe metabolic derangements have occurred and in this case reductions in hepatic ATP would be reflecting true disturbances within the liver.

Finally, it should be noted that medications that artificially increase the hepatic ATP reading are equally important and should be appropriately controlled. Drugs that are similar in structure to ATP, such as nucleotide triphosphate analogues (a class of antivirals and chemotherapeutic agents), may accumulate in the liver to levels detectable by MRS. This is important to note as many patients with viral induced liver disease or tumors of the liver are prescribed antiviral and chemotherapeutic medications. Indeed, this was the case in the human study where patients with cirrhosis who were receiving ribavirin therapy had markedly elevated β-NTP readings when compared to controls. Once again, knowledge of and/or restricted intake of such medication should be considered prior to MRS exams.

8.1.3. The Verdict

The studies in this thesis have demonstrated that disturbances in hepatic ATP levels occur during liver injury and disease. Regardless of the nature (surgical or disease induced), duration (acute or chronic) or etiology (parenchymal or cholestatic) of hepatocellular damage the response of the liver is uniform, hepatic ATP is reduced. Although ATP depletion is a general response, the interpretation of this finding can be complex. Following hepatic resection ATP levels are lowered within the residual liver

mass as a result of increased energy expenditure arising from increased functional demands and enhanced regenerative activity. During acute liver failure severe hepatocyte necrosis results in a reduced mass of viable hepatic parenchyma. With less hepatocytes there are fewer cells to generate the MRS detectable signal and those that do remain are exposed to increased metabolic demand. Finally, in chronic liver disease the interpretation is most complex as lower ATP levels can result from reduced cell numbers, increased energy utilization or reduced ATP synthesis. Similar to the setting of acute liver failure, reduced ATP signal may arise from hepatocyte necrosis, however, in chronic liver disease, fibrosis which replaces viable hepatic parenchyma also serves as a means whereby less hepatocyte ATP signal may be detected. As described above, increased energy expenditure due to enhanced functional and regenerative demands on the residual liver can also contribute to decreased hepatic ATP levels in chronic liver disease. Finally, capillarization of hepatic sinusoids has been shown to limit substrate and nutrient supply to hepatocytes,[22] and reduced access to these substances (particularly oxygen) can undoubtly hinder hepatocyte ATP production and lower hepatic ATP levels.[216, 235]

Taken together, hepatic ATP, as measured by *in vivo* ^{31}P MRS, is a robust measure of the functional hepatocyte mass. The index reflects both the quantity and bioenergetic integrity of the hepatocyte population within the liver. A disturbance in either of these components could thereby alter this measurement.

Theoretically, such an index should provide physicians with a valuable tool to accurately assess the extent and progression of liver disease in their patients. However, this test has one major limitation, it is insensitive. Levels of hepatic ATP, as detected by ^{31}P MRS, do not decrease until a large fraction of the hepatocyte mass is lost either

through surgery or advanced disease. Following PHx, at least 70% of the liver must be removed before ATP levels drop. In disease states in rats, hepatic ATP levels do not decline until in excess of 50% of the liver lobule is destroyed (acute liver failure) or until extensive fibrosis or cirrhosis is established (chronic liver disease). Moreover, during chronic liver disease in humans, significant reductions in hepatic ATP do not occur until hepatic decompensation is evident.

Collectively these findings suggest that the liver retains healthy ATP levels until advanced disease and functional deficits occur. In hindsight this makes teleological sense. In the absence of disease or metabolic challenge, the healthy liver maintains normal ATP levels due to a metabolic milieu that favours ATP production over ATP consumption. During the initial stages of disease the magnitude of hepatic injury is not great and both the number of viable hepatocytes and their energetic capacity are sufficient to maintain hepatic ATP levels and thus the functional integrity of the organ. Even with more advanced liver disease, when injury to the liver is more pronounced, the remaining hepatocyte mass may still be able to compensate to maintain normal ATP levels and preserve liver function. It is not until the liver has reached end-stage disease that residual hepatocytes are either too few in number and/or metabolically overwhelmed that ATP levels decline and consequently, liver insufficiency and decompensation ensue. A graphic representation of the association between hepatic ATP levels and the course of liver disease is presented in figure 17. If the quantity and bioenergetic integrity of hepatocytes continue to decline along this path a threshold of irreversible damage will be surpassed and the organ will cease to function at a level compatible with life. Based on the findings from the previous chapters this critical point occurs below hepatic ATP levels of 1.0 mM,

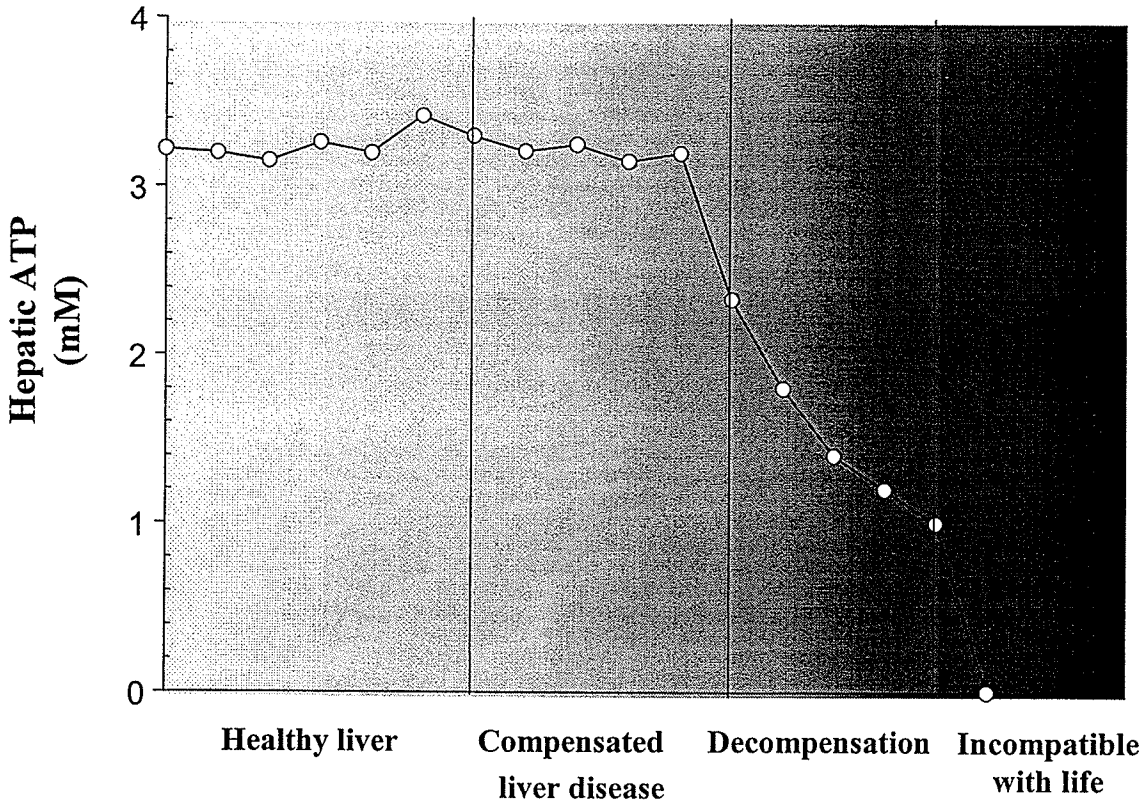

FIG.17 A dynamic view of hepatic ATP levels throughout the course of liver disease

where hepatocytes are too few in number to sustain minimal organ function and/or intracellular ATP levels are severely depleted to the point where ion regulation and membrane integrity can no longer be maintained. Studies performed on tissue slices and cell cultures have reported that irreversible cell injury occur when ATP levels drop below 15-10% of normal.[236-239] The higher critical ATP levels identified in the present study are likely related to the determinations being performed *in vivo*.

The utility of hepatic ATP measurements like many of the conventional liver function tests is limited by the large functional reserve of the liver. Hepatocytes are capable of functioning well above their healthy basal states, thus by simply increasing metabolic, synthetic and/or excretory rates the liver is able to compensate and obscure deficits which may occur. This explains why conventional indicators of liver function, such as levels of albumin and bilirubin and prothrombin times, do not become abnormal until a large percentage of the liver's functional capacity is lost. Adaptive strategies that increase the hepatocyte's capacity to produce ATP, such as increasing mitochondrial content through mitochondrial proliferation has been described in animal models and humans with liver disease.[240-243] Thus, as a result of the liver's large functional reserve, hepatic ATP levels, as measured by ^{31}P MRS, afford the physician little additional information until end-stage liver disease has developed.

8.1.4. Reflections: Hepatic Functional Reserve-Friend or Foe?

The task of accurately assessing liver function has frustrated many. The large functional reserve of the liver continues to arise as an obstacle that obscures our capacity to accurately measure liver function. Although this attribute has thwarted the efforts of

many researchers/clinicians it remains an important feature in liver physiology. Considering how important proper liver function is to the integrity of other organ systems and the overall heath and well being of the individual it is crucial that the liver have a large functional reserve. As discussed earlier, the same anatomical and structural features that permit the liver to perform such a diverse array of functions also leaves it vulnerable to injury from a number of toxic and noxious agents. The liver's large functional reserve, like its regenerative capacity, is an ingenious strategy designed to safeguard the functional viability of an organ that is both essential for life and prone to injury.

8.2. Future Studies

8.2.1. Diagnosis and Prognosis

The need to accurately evaluate liver function to determine the progression and extent of liver disease still remains an unanswered clinical problem. The closest current tests available that may address this issue are the quantitative liver function tests. Although these tests may be difficult to perform and only provide data on selected microsomal pathways, they remain the only class of tests that are sensitive enough to distinguish different stages of disease comparable to the liver biopsy.[122, 244, 245]

Future efforts of developing an improved liver function test should first focus on identifying a more global and robust indicator of liver function. This would circumvent the inconsistent results various microsomal pathways (quantitative liver function tests) provide during liver disease. Secondly, given the large hepatic reserve, the test should attempt to measure the liver's compensatory efforts rather than end products of certain

hepatic processes. By determining the degree of compensation one in fact obtains a measure of the liver's functional reserve. This enables one to determine how much of the liver's resources are exhausted and how much remains. Thus by determining the extent the liver must work over basal rates to maintain homeostasis one can assess how functionally 'challenged' the liver is, which in turn provides a sensitive and accurate measure of the extent of liver disease.

Future applications of quantitative ^{31}P MRS in liver disease should focus on its potential role as a prognostic indicator of liver failure. Figure 17 illustrates that over the course of liver disease hepatic ATP levels are maintained until the onset of hepatic decompensation. Central to this paradigm is the assumption that hepatocyte ATP depletion precedes hepatic dysfunction. If this is true then reductions in hepatic ATP levels among patients with late stage compensated liver disease should predict the onset of hepatic insufficiency. To address this hypothesis a longitudinal prospective study should be performed in patients with compensated cirrhosis. Serial MRS exams would be performed on this patient population at specific intervals from the time of enrolment until the first signs of hepatic decompensation. If hepatic ATP levels begin to decline prior to clinical evidence of decompensation, then ^{31}P MRS would represent a new and very valuable prognostic tool. Such information would greatly improve the selection of patients awaiting liver transplantion.

8.2.2. Therapeutics

The results of this thesis highlight the importance of hepatic ATP levels in the pathophysiology of liver failure. Specifically, when hepatic ATP levels become depleted

as a result of disease or surgical resection, the functional capacity of the liver deteriorates and liver insufficiency soon follows. Given this paradigm, several therapeutic strategies can be introduced during the course of liver disease or preoperatively to prevent ATP depletion and the downward spiral to liver failure. The various ATP preserving strategies include i) increasing the content of hepatic ATP by direct infusion of ATP or nucleotide mixtures; (ii) enhancing the capacity of the liver to generate ATP via oxygen supplementation; and (iii) buffering/reducing the loss of hepatic ATP by introducing the creatine kinase gene to the liver.

Several studies have demonstrated that administration of exogenous ATP or ATP precursors can correct intracellular disturbances of ATP within the liver.[246, 247] In addition to the increase in hepatic ATP levels, marked improvements in the subject's health and liver condition was also observed following this therapy.[247, 248] Patients with advanced nonsmall-cell lung cancer are reported to have decreased levels of liver ATP and experience significant weight loss.[249, 250] Recent studies have demonstrate that intravenous infusion of ATP restores hepatic energy levels and prevents the deterioration of body weight, muscle strength and serum albumin concentrations that occur in cancer patients without ATP infusions.[247, 251, 252] Beneficial results may also be attained when ATP precursors are administered in the setting of liver disease. Animal studies performed by Torres et al. demonstrated that by supplementing the diet of TAA-cirrhotic rats with a mixture of nucleotides required for ATP synthesis, significant histological improvements in cirrhosis (reduced fibrosis and steatosis and increased hepatic regeneration) could be detected.[253, 254]

Although several of these studies have documented that exogenous ATP and ATP precursors increase intracellular levels of ATP,[247, 248] the extracellular effects of these molecules must not be overlooked. Indeed ectonucleotidases limit the availability of these molecules within the extracellular environment, however, only submicromolar levels are required for these nucleotides to exert their physiological effects.[255] As such extracellular ATP can act on cell's purinergic (P2) receptors to enhance glycogenolysis, blood flow and microcirculation within the liver, while systemically adverse effects which include general discomfort, deep and frequent breathing, headaches, nausea, chest pain, sinus bradycardia and atria fibrillation may be experienced.[255]

Oxygen supplementation is an alternative means whereby depleted hepatic ATP levels may be restored. The oxygen limitation theory proposes that the sinusoidal capillarization associated within cirrhosis induces hepatocyte hypoxia, which elicits metabolic disturbances.[235] Studies performed by Harvey et al. demonstrated that by providing oxygen supplementation to cirrhotic rats, reductions in hepatic ATP and energy levels could be reversed.[216] Oxygen supplementation has also been shown to temporarily improve oxidative drug metabolism in patients and rats with cirrhosis.[256, 257] Froomes et al., however, noted a limitation of this therapy, namely oxygen delivered to human patients, via a face mask, did not produce the full therapeutic requirements for changes in arterial and portal pO_2 as was demonstrated in rats.[256-258] To achieve this, studies are examining the feasibility of selectively increasing hepatic artery perfusion through the administration of oral vasodilators.[259, 260]

The final and most complex therapeutic approach to preserving hepatic ATP levels in liver disease and surgical resection would be to introduce the creatine kinase

gene to the liver. While absent in the liver, creatine kinase functions in other tissues to catalyze the formation of phosphocreatine. This high energy metabolite donates its phosphate group to hydrolyzed ATP moieties to buffer reductions in ATP and preserve energy levels during enhanced ATP utilization.[111] Studies performed in transgenic mice expressing liver creatine kinase reported that following 70% PHx, liver phosphocreatine both preserved hepatic ATP levels and enhanced regenerative activity.[261] Hepatic PCr has also been shown to buffer ATP losses and help protect the liver during periods of hypoxia and ischemia.[262] Liver gene therapy using viral and non-viral delivery systems would have to be used to introduce creatine kinase to human patients. To date such technology has been applied to congenital deficiency of various enzymes, metabolic diseases and liver malignancies, thus it should be technically feasible to perform *in vivo* gene transfer of creatine kinase to the liver.[263-265] However, numerous problems associated with gene therapy (low efficacy gene transfer, non-specific interactions, safety issues and ethical concerns), currently limit its use in clinical medicine

Each therapeutic strategy has its strengths and shortcoming, depending on the clinical setting some strategies may be more practical and effective then others. The first two strategies provide only temporary solutions and thus would be limited to the setting of fulminant liver failure where the goal would be to preserve liver ATP, function and integrity until a suitable donor liver would be available for transplantation. Alternatively if difficulties surrounding gene therapy can be overcome, stable transfection of creatine kinase may provide a more long term solution for patients with chronic liver disease.

8.3. Closing Remarks

To date *in vivo* MRS has made few inroads into clinical medicine.[13, 131] The author still believes that MRS is a valuable tool with immense clinical potential. However, at this time, it remains a sophisticated technique in search of an appropriate clinical application. It is my hope that the experiments and discussion outlined in this thesis have not only provided further insights into the pathophysiology of liver disease but on a much larger scale, have also advanced efforts to one day establish MRS as a diagnostic tool in clinical medicine.

REFERENCES

1. Kim WR, Brown RS, Jr., Terrault NA, El-Serag H. Burden of liver disease in the United States: summary of a workshop. Hepatology 2002; 36(1):227-42.
2. Bell BP, Navarro VJ, Manos MM, Murphy RC, Leyden WA, St. Louis TE, Kunze K. The epidemiology of newly-diagnosed chronic liver disease in the United States: findings of population-based sentinel surveillance [Abstract]. Hepatology 2001; 34(Part 2):468A.
3. Murphy S. Deaths: final data for 1998. National vital statistics reports. National Center for Health Statistics 2000.
4. Starzl TE, Iwatsuki S, Van Thiel DH, Gartner JC, Zitelli BJ, Malatack JJ, Schade RR, et al. Evolution of liver transplantation. Hepatology 1982; 2(5):614-36.
5. Anonymous. 2000 Annual Report of the U.S. Scientific Registry for Transplant Recipients and the Organ Procurement and Transplantation Network: Transplant Data:1990-1999. U.S. Department of Heaalth and Human Services, Health Resources and Services Administration, Office of Special Programs, Division of Transplantation; United Network of Organ Sharing 2000.
6. Anonymous. Compressed Mortality File (http://wonder.cdc.gov).: Centers of Disease Control and Prevention. (Accessed on March 10, 2002).
7. Jungermann K, Katz N. Functional hepatocellular heterogeneity. Hepatology 1982; 2(3):385-95.
8. Katz NR. Metabolic heterogeneity of hepatocytes across the liver acinus. J Nutr 1992; 122(3 Suppl):843-9.

9. Chung RT, Jaffe DL, Friedman LS. Complications of chronic liver disease. Crit Care Clin 1995; 11(2):431-63.

10. Williams EJ, Iredale JP. Liver cirrhosis. Postgrad Med J 1998; 74(870):193-202.

11. McIntyre N. The limitations of conventional liver function tests. Semin Liver Dis 1983; 3(4):265-74.

12. Johnston DE. Special considerations in interpreting liver function tests. Am Fam Physician 1999; 59(8):2223-30.

13. Cox IJ. Development and applications of in vivo clinical magnetic resonance spectroscopy. Prog Biophys Mol Biol 1996; 65(1-2):45-81.

14. Meyerhoff DJ, Karczmar GS, Weiner MW. Abnormalities of the liver evaluated by 31P MRS. Invest Radiol 1989; 24(12):980-4.

15. Gadian DG. NMR and its Application to Living Systems. 2 ed. Oxford: Oxford University Press, 1995.

16. Furbank RA. Conversion data, normal values, nomograms and other standards. *In* Simpson K, ed. Modern Trends in Forensic Medicine, Vol. 2. New York: Appleton-Century-Crofts, 1967. pp. 344-364.

17. Ludwig J. Current Methods of Autopsy Practice. Philadelphia: WB Saunders, 1972.

18. Schulz DM. Weights of organs of fetuses and infants. Arch Pathol 1962; 72:244.

19. Sunderman FW, Boerner F. Normal Values in Clinical Medicine. Philadelphia: WB Saunders, 1950.

20. Wisse E, De Zanger RB, Charels K, Van Der Smissen P, McCuskey RS. The liver sieve: considerations concerning the structure and function of endothelial

fenestrae, the sinusoidal wall and the space of Disse. Hepatology 1985; 5(4):683-92.

21. Lemasters JJ. Biology of the sinusoidal endothelial cell and implications for liver disease. In Liver Injury Update: Clinical Implications and Mechanistic Role of Cells of the Liver. American Association for the Study of Liver Diseases. Chicago, 1997. pp. 283-292.

22. Martinez-Hernandez A, Martinez J. The role of capillarization in hepatic failure: studies in carbon tetrachloride-induced cirrhosis. Hepatology 1991; 14(5):864-74.

23. Alcolado R, Arthur MJ, Iredale JP. Pathogenesis of liver fibrosis. Clin Sci (Lond) 1997; 92(2):103-12.

24. Gates GA, Henley KS, Pollard HM, Schmidt E, Schmidt FW. The cell population of the human liver. J Lab Clin Med 1961; 57:182-184.

25. Desmet VJ. Organizational Principles. *In* Arias IM, Boyer JL, Fausto N, et al., eds. The Liver: Biology and Pathobiology. New York: Raven Press, Ltd., 1994. pp. 3-14.

26. Rappaport AM, Borowy ZJ, Longheed WM, Lotto WN. Subdivision of hexagonal liver lobules into a structural and functional unit. Role in hepatic physiologyand pathology. Anat Recl 1954; 119:11-33.

27. Rappaport AM, Wanless IR. Physioanatomic Considerations. *In* Schiff L, Schiff ER, eds. Diseases of the Liver. Philadelphia: Lippincott Company, 1993. pp. 1-41.

28. Gumucio JJ, Bilir BM, Moseley RH, Berkowitz. The Biology of The Liver Cell Plate. *In* Arias IM, Boyer JL, Fausto N, et al., eds. The Liver: Biology and Pathobiology. New York: Raven Press, Ltd., 1994. pp. 1143-1166.

29. Gumucio JJ, Miller DL. Functional implications of liver cell heterogeneity. Gastroenterology 1981; 80(2):393-403.

30. Hubbard AL, Barr VA, Scott LJ. Hepatocyte surface polarity. *In* Arias IM, Boyer JL, Fausto N, et al., eds. The Liver: Biology and Pathobiology. New York: Raven Press, Ltd., 1994. pp. 189-213.

31. Bucher NL. Regeneration of Mammalian Liver. In: International Review of Cytology. Vol. 15. New York: Academic Press, 1963.

32. Michalopoulos GK, DeFrances MC. Liver regeneration. Science 1997; 276(5309):60-6.

33. Bucher NL, Schrock TR, Moolten FL. An experimental view of hepatic regeneration. Johns Hopkins Med J 1969; 125(5):250-7.

34. Moser MJ, Gong Y, Zhang MN, Johnston J, Lipschitz J, Minuk GY. Immediate-early protooncogene expression and liver function following various extents of partial hepatectomy in the rat. Dig Dis Sci 2001; 46(4):907-14.

35. Kren BT, Trembley JH, Fan G, Steer CJ. Molecular regulation of liver regeneration. Ann N Y Acad Sci 1997; 831:361-81.

36. Fausto N, Laird AD, Webber EM. Liver regeneration. 2. Role of growth factors and cytokines in hepatic regeneration. Faseb J 1995; 9(15):1527-36.

37. Rabes HM, Wirsching R, Tuczek HV, Iseler G. Analysis of cell cycle compartments of hepatocytes after partial hepatecomy. Cell Tissue Kinet 1976; 9(6):517-32.

38. Stocker E, Heine WD. Regeneration of liver parenchyma under normal and pathological conditions. Beitr Pathol 1971; 144(4):400-8.

39. Widmann JJ, Fahimi HD. Liver Regeneration after Experimental Injury. New York: Stratton Intercontinental Medical Book Corp., 1975.

40. Grisham J. A morphologic study of deoxyribonucleic acid synthesis and cell proliferation in regenerating rat liver: autoradiography with H-3 thymidine. Cancer Res 1962; 22:842-849.

41. Jansen PL, Chamuleau RA, van Leeuwen DJ, Schipper HG, Busemann-Sokole E, van der Heyde MN. Liver regeneration and restoration of liver function after partial hepatectomy in patients with liver tumors. Scand J Gastroenterol 1990; 25(2):112-8.

42. Lin TY, Lee CS, Chen CC, Liau KY, Lin WS. Regeneration of human liver after hepatic lobectomy studied by repeated liver scanning and repeated needle biopsy. Ann Surg 1979; 190(1):48-53.

43. Leevy CB. Abnormalities of liver regeneration: a review. Dig Dis 1998; 16(2):88-98.

44. Flores EA, Bistrian BR, Pomposelli JJ, Dinarello CA, Blackburn GL, Istfan NW. Infusion of tumor necrosis factor/cachectin promotes muscle catabolism in the rat. A synergistic effect with interleukin 1. J Clin Invest 1989; 83(5):1614-22.

45. Gershenwald JE, Fong YM, Fahey TJ, 3rd, Calvano SE, Chizzonite R, Kilian PL, Lowry SF, et al. Interleukin 1 receptor blockade attenuates the host inflammatory response. Proc Natl Acad Sci U S A 1990; 87(13):4966-70.

46. Hellerstein MK, Meydani SN, Meydani M, Wu K, Dinarello CA. Interleukin-1-induced anorexia in the rat. Influence of prostaglandins. J Clin Invest 1989; 84(1):228-35.

47. Hellerstein MK, Munro HN. Interaction of the liver, muscle, and adipose tissue in the regulation of metabolism in response to nutritional and other factors. *In* Arias IM, Boyer JL, Fausto N, et al., eds. The Liver: Biology and Pathobiology. New York: Raven Press, Ltd., 1994. pp. 1169-1192.

48. Chowdury JR, Chowdury NR, Wolkoff AW. Heme and bile pigment metabolism. *In* Arias IM, Boyer JL, Fausto N, et al., eds. The Liver: Biology and Pathobiology. New York: Raven Press, Ltd., 1994. pp. 471-504.

49. Crawford JM, Gollan JL. Bilirubin metabolism and pathophysiology of jaundice. *In* Schiff ER, Schiff L, eds. Diseases of the Liver. Philadelphia: J.B. Lippincott Company, 1994. pp. 42-84.

50. Carr JM. Hemostatic disorders in liver disease. *In* Arias IM, Boyer JL, Fausto N, et al., eds. The Liver: Biology and Pathobiology. New York: Raven Press, Ltd., 1994. pp. 1061-1076.

51. Conn HO. Hepatic encephalopathy. *In* Schiff L, Schiff ER, eds. Diseases of the Liver. Philadelphia: J.B. Lippincott Company, 1993. pp. 1036-1060.

52. Rothschild MA, Oratz M, Schreiber SS. Serum albumin. Hepatology 1988; 8(2):385-401.

53. Neuschwander-Tetri BA. Common blood tests for liver disease. Which ones are most useful? Postgrad Med 1995; 98(1):49-56, 59, 63.

54. Siconolfi LA. Clarifying the complexity of liver function tests. Nursing 1995; 25(5):39-44; quiz 46.

55. Haber MM, West AB, Haber AD, Reuben A. Relationship of aminotransferases to liver histological status in chronic hepatitis C. Am J Gastroenterol 1995; 90(8):1250-7.

56. Healey CJ, Chapman RW, Fleming KA. Liver histology in hepatitis C infection: a comparison between patients with persistently normal or abnormal transaminases. Gut 1995; 37(2):274-8.

57. Moody FG, Rikkers LF, Aldrete JS. Estimation of the functional reserve of human liver. Ann Surg 1974; 180(4):592-8.

58. Inage F, Furuhama K. Application of maximal removal rate of indocyanine green to the determination of hepatic functional mass in conscious rats. J Vet Med Sci 1997; 59(5):335-40.

59. Miyagawa S, Makuuchi M, Kawasaki S, Kakazu T. Changes in serum amylase level following hepatic resection in chronic liver disease. Arch Surg 1994; 129(6):634-8.

60. Suehiro T, Sugimachi K, Matsumata T, Itasaka H, Taketomi A, Maeda T. Protein induced by vitamin K absence or antagonist II as a prognostic marker in hepatocellular carcinoma. Comparison with alpha-fetoprotein. Cancer 1994; 73(10):2464-71.

61. Garello E, Battista S, Bar F, Niro GA, Cappello N, Rizzetto M, Molino G. Evaluation of hepatic function in liver cirrhosis: clinical utility of galactose elimination capacity, hepatic clearance of D-sorbitol, and laboratory investigations. Dig Dis Sci 1999; 44(4):782-8.

62. Merkel C, Gatta A, Zoli M, Bolognesi M, Angeli P, Iervese T, Marchesini G, et al. Prognostic value of galactose elimination capacity, aminopyrine breath test, and ICG clearance in patients with cirrhosis. Comparison with the Pugh score. Dig Dis Sci 1991; 36(9):1197-203.

63. Bircher J. Quantitative assessment of deranged hepatic function: a missed opportunity? Semin Liver Dis 1983; 3(4):275-84.

64. Stolz A, Kaplowitz N. Biochemical tests for liver disease. *In* Zakim D, Boyer TD, eds. Hepatology: A textbook of liver disease. New York: Saunders, 1990. pp. 637-667.

65. Morgan DJ, McLean AJ. Clinical pharmacokinetic and pharmacodynamic considerations in patients with liver disease. An update. Clin Pharmacokinet 1995; 29(5):370-91.

66. Child CG, Turcotte JG. Surgery and portal hypertension. *In* Child CG, ed. The Liver and portal Hypertension. Philadelphia: Saunders, 1964. pp. 50-62.

67. Pugh RN, Murray-Lyon IM, Dawson JL, Pietroni MC, Williams R. Transection of the oesophagus for bleeding oesophageal varices. Br J Surg 1973; 60(8):646-9.

68. MacIntosh EL, Minuk GY. Hepatic resection in patients with cirrhosis and hepatocellular carcinoma. Surg Gynecol Obstet 1992; 174(3):245-54.

69. Killi RM. Doppler sonography of the native liver. Eur J Radiol 1999; 32(1):21-35.

70. Cheng YF, Lee TY, Chen CL, Huang TL, Chen YS, Lui CC. Three-dimensional helical computed tomographic cholangiography: application to living related hepatic transplantation. Clin Transplant 1997; 11(3):209-13.

71. Adam WE. A general comparison of functional imaging in nuclear medicine with other modalities. Semin Nucl Med 1987; 17(1):3-17.

72. Iozzo P, Osman S, Glaser M, Knickmeier M, Ferrannini E, Pike VW, Camici PG, et al. In vivo imaging of insulin receptors by PET: preclinical evaluation of iodine-125 and iodine-124 labelled human insulin. Nucl Med Biol 2002; 29(1):73-82.

73. Degos F, Benhamou JP. Liver Biopsy. Oxford: Oxford University Press, 1999.

74. Desmet VJ, Gerber M, Hoofnagle JH, Manns M, Scheuer PJ. Classification of chronic hepatitis: diagnosis, grading and staging. Hepatology 1994; 19(6):1513-20.

75. Perrillo RP. The role of liver biopsy in hepatitis C. Hepatology 1997; 26(3 Suppl 1):57S-61S.

76. Bravo AA, Sheth SG, Chopra S. Liver biopsy. N Engl J Med 2001; 344(7):495-500.

77. Piccinino F, Sagnelli E, Pasquale G, Giusti G. Complications following percutaneous liver biopsy. A multicentre retrospective study on 68,276 biopsies. J Hepatol 1986; 2(2):165-73.

78. Gervais DA, Gazelle GS, Lu DS, Han PF, Mueller PR. Percutaneous transpulmonary CT-guided liver biopsy: a safe and technically easy approach for lesions located near the diaphragm. AJR Am J Roentgenol 1996; 167(2):482-3.

79. Smith BC, Desmond PV. Outpatient liver biopsy using ultrasound guidance and the Biopty gun is safe and cost effective. Aust N Z J Med 1995; 25(3):209-11.

80. Intraobserver and interobserver variations in liver biopsy interpretation in patients with chronic hepatitis C. The French METAVIR Cooperative Study Group. Hepatology 1994; 20(1 Pt 1):15-20.

81. Bloch F, Hansen WW, Packard ME. Nuclear induction. Physics Rev 1946; 69:127.

82. Beavers KL, Semelka RC. MRI evaluation of the liver. Semin Liver Dis 2001; 21(2):161-77.

83. Radda GK. The use of NMR spectroscopy for the understanding of disease. Science 1986; 233(4764):640-5.

84. Cohen SM. Application of nuclear magnetic resonance to the study of liver physiology and disease. Hepatology 1983; 3(5):738-49.

85. Davidson BR, Barnard ML, Changani KK, Taylor-Robinson SD. Liver transplantation: current and potential applications of magnetic resonance spectroscopy. Liver Transpl Surg 1997; 3(5):481-93.

86. Bell JD, Cox IJ, Sargentoni J, Peden CJ, Menon DK, Foster CS, Watanapa P, et al. A 31P and 1H-NMR investigation in vitro of normal and abnormal human liver. Biochim Biophys Acta 1993; 1225(1):71-7.

87. Morikawa S, Inubushi T, Kitoh K, Kido C, Nozaki M. Chemical assessment of phospholipid and phosphoenergetic metabolites in regenerating rat liver measured by in vivo and in vitro 31P-NMR. Biochim Biophys Acta 1992; 1117(3):251-7.

88. Murphy EJ, Bates TE, Williams SR, Watson T, Brindle KM, Rajagopalan B, Radda GK. Endoplasmic reticulum: the major contributor to the PDE peak in

hepatic 31P-NMR spectra at low magnetic field strengths. Biochim Biophys Acta 1992; 1111(1):51-8.

89. Murphy EJ, Rajagopalan B, Brindle KM, Radda GK. Phospholipid bilayer contribution to 31P NMR spectra in vivo. Magn Reson Med 1989; 12(2):282-9.

90. Iles RA, Stevens AN, Griffiths JR, Morris PG. Phosphorylation status of liver by 31P-n.m.r. spectroscopy, and its implications for metabolic control. A comparison of 31P-n.m.r. spectroscopy (in vivo and in vitro) with chemical and enzymic determinations of ATP, ADP and Pi. Biochem J 1985; 229(1):141-51.

91. Oberhaensli RD, Galloway GJ, Taylor DJ, Bore PJ, Rajagopalan B, Radda GK. First year experience with 31-P magnetic resonance studies of human liver. Magn Reson Med 1986; 4:413-416.

92. Schmidt HC, Gooding CA, James TL, Gonzalez-Mendez R, James JL. Comparison of in vivo 31P-MR spectra of the brain, liver, and kidney of adult and infant animals. Pediatr Radiol 1986; 16(2):144-9.

93. Iles RA, Cox IJ, Bell JD, Dubowitz LM, Cowan F, Bryant DJ. 31P magnetic resonance spectroscopy of the human paediatric liver. NMR Biomed 1990; 3(2):90-4.

94. Oberhaensli RD, Galloway GJ, Taylor DJ, Bore PJ, Radda GK. Assessment of human liver metabolism by phosphorus-31 magnetic resonance spectroscopy. Br J Radiol 1986; 59(703):695-9.

95. Radda GK, Oberhaensli RD, Taylor DJ. The biochemistry of human diseases as studied by 31P NMR in man and animal models. Ann N Y Acad Sci 1987; 508:300-8.

96. Cox IJ, Menon DK, Sargentoni J, Bryant DJ, Collins AG, Coutts GA, Iles RA, et al. Phosphorus-31 magnetic resonance spectroscopy of the human liver using chemical shift imaging techniques. J Hepatol 1992; 14(2-3):265-75.

97. Munakata T, Griffiths RD, Martin PA, Jenkins SA, Shields R, Edwards RH. An in vivo 31P MRS study of patients with liver cirrhosis: progress towards a non-invasive assessment of disease severity. NMR Biomed 1993; 6(2):168-72.

98. Menon DK, Sargentoni J, Taylor-Robinson SD, Bell JD, Cox IJ, Bryant DJ, Coutts GA, et al. Effect of functional grade and etiology on in vivo hepatic phosphorus- 31 magnetic resonance spectroscopy in cirrhosis: biochemical basis of spectral appearances. Hepatology 1995; 21(2):417-27.

99. Jalan R, Sargentoni J, Coutts GA, Bell JD, Rolles K, Burroughs AK, Taylor Robinson SD. Hepatic phosphorus-31 magnetic resonance spectroscopy in primary biliary cirrhosis and its relation to prognostic models. Gut 1996; 39(1):141-6.

100. Taylor-Robinson SD, Sargentoni J, Bell JD, Saeed N, Changani KK, Davidson BR, Rolles K, et al. In vivo and in vitro hepatic 31P magnetic resonance spectroscopy and electron microscopy of the cirrhotic liver. Liver 1997; 17(4):198-209.

101. Ruiz-Cabello J, Cohen JS. Phospholipid metabolites as indicators of cancer cell function. NMR Biomed 1992; 5(5):226-33.

102. Taylor-Robinson SD, Thomas EL, Sargentoni J, Marcus CD, Davidson BR, Bell JD. Cirrhosis of the human liver: an in vitro 31P nuclear magnetic resonance study. Biochim Biophys Acta 1995; 1272(2):113-8.

103. Menon DK, Harris M, Sargentoni J, Taylor-Robinson SD, Cox IJ, Morgan MY. In vivo hepatic 31P magnetic resonance spectroscopy in chronic alcohol abusers. Gastroenterology 1995; 108(3):776-88.

104. Kiyono K, Shibata A, Sone S, Watanabe T, Oguchi M, Shikama N, Ichijo T, et al. Relationship of 31P MR spectroscopy to the histopathological grading of chronic hepatitis and response to therapy. Acta Radiol 1998; 39(3):309-14.

105. Meyerhoff DJ, Boska MD, Thomas AM, Weiner MW. Alcoholic liver disease: quantitative image-guided P-31 MR spectroscopy. Radiology 1989; 173(2):393-400.

106. Lu W, Locke SJ, Brauer M. In vivo and in vitro 31P magnetic resonance spectroscopic studies of the hepatic response of healthy rats and rats with acute hepatic damage to fructose loading. Magn Reson Med 1994; 31(5):469-81.

107. Oberhaensli RD, Rajagopalan B, Taylor DJ, Radda GK, Collins JE, Leonard JV, Schwarz H, et al. Study of hereditary fructose intolerance by use of 31P magnetic resonance spectroscopy. Lancet 1987; 2(8565):931-4.

108. Segebarth C, Grivegnee AR, Longo R, Luyten PR, den Hollander JA. In vivo monitoring of fructose metabolism in the human liver by means of 31P magnetic resonance spectroscopy. Biochimie 1991; 73(1):105-8.

109. Otsuka H, Harada M, Koga K, Nishitani H. Effects of hepatic impairment on the metabolism of fructose and 5- fluorouracil, as studied in fatty liver models using in vivo 31P-MRS and 19F-MRS. Magn Reson Imaging 1999; 17(2):283-90.

110. Dufour JF, Stoupis C, Lazeyras F, Vock P, Terrier F, Reichen J. Alterations in hepatic fructose metabolism in cirrhotic patients demonstrated by dynamic 31phosphorus spectroscopy. Hepatology 1992; 15(5):835-42.

111. Mathews CK, Van Holde KE. Biochemistry. Redwood City, CA: The Benjamin/Cummings Publishing Company, 1990.

112. Atkinson DE. Cellular energy metabolism and its regulation. New York: Academic Press, 1977.

113. Rosser BG, Gores GJ. Liver cell necrosis: cellular mechanisms and clinical implications. Gastroenterology 1995; 108(1):252-75.

114. Madhu B, Lagerwall K, Soussi B. Phosphorus metabolites in different muscles of the rat leg by 31P image- selected in vivo spectroscopy. NMR Biomed 1996; 9(8):327-32.

115. Buchli R, Meier D, Martin E, Boesiger P. Assessment of absolute metabolite concentrations in human tissue by 31P MRS in vivo. Part II: Muscle, liver, kidney. Magn Reson Med 1994; 32(4):453-8.

116. Meyerhoff DJ, Karczmar GS, Matson GB, Boska MD, Weiner MW. Non-invasive quantitation of human liver metabolites using image-guided 31P magnetic resonance spectroscopy. NMR Biomed 1990; 3(1):17-22.

117. Roth K, Hubesch B, Meyerhoff D, Naruse S, Gober L, Lawry T, Boska M, et al. Non-invasive quantitation of phosphorus metabolites in human tissue by NMR spectroscopy. J Magn Reson 1989; 81:299-310.

118. Evelhoch JL, Ewy CS, Siegfried BA, Ackerman JJ, Rice DW, Briggs RW. 31P spin-lattice relaxation times and resonance linewidths of rat tissue in vivo:

dependence upon the static magnetic field strength. Magn Reson Med 1985; 2(4):410-7.

119. Scheele J, Stangl R, Altendorf-Hofmann A. Hepatic metastases from colorectal carcinoma: impact of surgical resection on the natural history. Br J Surg 1990; 77(11):1241-6.

120. Paquet KJ, Koussouris P, Mercado MA, Kalk JF, Muting D, Rambach W. Limited hepatic resection for selected cirrhotic patients with hepatocellular or cholangiocellular carcinoma: a prospective study. Br J Surg 1991; 78(4):459-62.

121. Wu CC, Yang MD, Liu TJ. Improvements in hepatocellular carcinoma resection by intraoperative ultrasonography and intermittent hepatic inflow blood occlusion. Jpn J Clin Oncol 1992; 22(2):107-12.

122. Miyazaki S, Takasaki K, Yamamoto M, Tsugita M, Otsubo T. Liver regeneration and restoration of liver function after partial hepatectomy: the relation of fibrosis of the liver parenchyma. Hepatogastroenterology 1999; 46(29):2919-24.

123. Nagasue N, Yukaya H, Ogawa Y, Kohno H, Nakamura T. Human liver regeneration after major hepatic resection. A study of normal liver and livers with chronic hepatitis and cirrhosis. Ann Surg 1987; 206(1):30-9.

124. Ezaki T, Koyanagi N, Toyomasu T, Ikeda Y, Sugimachi K. Natural history of hepatectomy regarding liver function: a study of both normal livers and livers with chronic hepatitis and cirrhosis. Hepatogastroenterology 1998; 45(23):1795-801.

125. Capussotti L, Borgonovo G, Bouzari H, Smadja C, Grange D, Franco D. Results of major hepatectomy for large primary liver cancer in patients with cirrhosis. Br J Surg 1994; 81(3):427-31.

126. Detroz B, Sugarbaker PH, Knol JA, Petrelli N, Hughes KS. Causes of death in patients undergoing liver surgery. Cancer Treat Res 1994; 69:241-57.

127. Didolkar MS, Fitzpatrick JL, Elias EG, Whitley N, Keramati B, Suter CM, Brown S. Risk factors before hepatectomy, hepatic function after hepatectomy and computed tomographic changes as indicators of mortality from hepatic failure. Surg Gynecol Obstet 1989; 169(1):17-26.

128. Hashimoto M, Sanjo K. Functional capacity of the liver after two-thirds partial hepatectomy in the rat. Surgery 1997; 121(6):690-7.

129. Poulsen HE, Pilsgaard H. Antipyrine metabolism during hepatic regeneration in the rat. Liver 1985; 5(4):196-9.

130. Assy N, Gong Y, Zhang M, Pettigrew NM, Pashniak D, Minuk GY. Use of proliferating cell nuclear antigen as a marker of liver regeneration after partial hepatectomy in rats. J Lab Clin Med 1998; 131(3):251-6.

131. Henriksen O. MR spectroscopy in clinical research. Acta Radiol 1994; 35(2):96-116.

132. Mann DV, Lam WW, Hjelm NM, So NM, Yeung DK, Metreweli C, Lau WY. Human liver regeneration: hepatic energy economy is less efficient when the organ is diseased. Hepatology 2001; 34(3):557-65.

133. Farghali H, Rilo H, Zhang W, Simplaceanu V, Gavaler JS, Ho C, van Thiel DH. Liver regeneration after partial hepatectomy in the rat. Sequential events monitored by 31P-nuclear magnetic resonance spectroscopy and biochemical studies. Lab Invest 1994; 70(3):418-25.

134. Nishida Y, Tanaka K, Munakata T, Kasai S. Evaluation of functional recovery of regenerating rat liver after partial hepatectomy using 31P-NMR spectroscopy. J Surg Res 1996; 61(2):385-90.

135. Kooby DA, Zakian KL, Challa SN, Matei C, Petrowsky H, Yoo HH, Koutcher JA, et al. Use of phosphorous-31 nuclear magnetic resonance spectroscopy to determine safe timing of chemotherapy after hepatic resection. Cancer Res 2000; 60(14):3800-6.

136. Campbell KA, Wu YP, Chacko VP, Sitzmann JV. In vivo 31P NMR spectroscopic changes during liver regeneration. J Surg Res 1990; 49(3):244-7.

137. Higgins G, Anderson R. Experimental pathology of the liver. I. Restoration of the liver of the white rat following partial surgical removal. Archives of Pathology 1931; 12:186-202.

138. Zieve L, Anderson WR, Lindblad S. Course of hepatic regeneration after 80% to 90% resection of normal rat liver. Comparison with two-lobe and one-lobe hepatectomy. J Lab Clin Med 1985; 105(3):331-6.

139. Antovic J, Djordjevic V, Kocic G, Koracevic D, Bjelakovic G, Bakic M. Blood coagulation factors changes during liver regeneration in rats. Arch Int Physiol Biochim Biophys 1993; 101(6):357-9.

140. Luk GD. Essential role of polyamine metabolism in hepatic regeneration. Inhibition of deoxyribonucleic acid and protein synthesis and tissue regeneration by difluoromethylornithine in the rat. Gastroenterology 1986; 90(5 Pt 1):1261-7.

141. Volkin E, Cohn W. Estimation of nucleic acids. Methods of Biochemical Analysis 1956; 1:287-305.

142. Francavilla A, Ove P, Polimeno L, Coetzee M, Makowka L, Barone M, Van Thiel DH, et al. Regulation of liver size and regeneration: importance in liver transplantation. Transplant Proc 1988; 20(1 Suppl 1):494-7.

143. Starzl TE, Fung J, Tzakis A, Todo S, Demetris AJ, Marino IR, Doyle H, et al. Baboon-to-human liver transplantation. Lancet 1993; 341(8837):65-71.

144. Lamprecht W, Trautschold I. Adenosine-5'-triphosphate: determination with hexokinase and glucose-6-phosphate dehydrogenase. In: Methods of Enzymatic Analysis. New York: Acedemic Press, 1974.

145. Sellevold OF, Jynge P, Aarstad K. High performance liquid chromatography: a rapid isocratic method for determination of creatine compounds and adenine nucleotides in myocardial tissue. J Mol Cell Cardiol 1986; 18(5):517-27.

146. Fujimoto T, Takeda H, Aoyama H, Kamiyama Y, Ozawa K, Tobe T. Relationship between initial hepatic uptake of indocyanine green and hepatic energy status in hepatectomized rabbits. Res Exp Med 1983; 183(3):193-202.

147. Ozawa K. Hepatic function and liver resection. J Gastroenterol Hepatol 1990; 5(3):296-309.

148. Yamaguchi T, Takada Y, Shimahara Y, Kiuchi T, Higashiyama H, Mori K, Kobayashi N, et al. A mixture of nucleosides and a nucleotide alters hepatic energy metabolism 24 hours after hepatectomy in rabbits. J Nutr 1992; 122(2):340-4.

149. Ho HS, Ueda T, Liu H. The impacts of experimental necrotizing pancreatitis on hepatocellular ion homeostasis and energetics: an in vivo nuclear magnetic resonance study. Surgery 1998; 124(2):372-9.

150. Ngala Kenda JF, de Hemptinne B, Lambotte L. Role of metabolic overload in the initiation of DNA synthesis following partial hepatectomy in the rat. Eur Surg Res 1984; 16(5):294-302.

151. Ozawa K, Yamada T, Ukikusa M, Ngala K, Ida T, Nakase A, Tobe T. Mitochondrial phosphorylative activity and DNA synthesis in regenerating liver of diabetic rats. J Surg Res 1981; 31(1):38-45.

152. Sekas G, Cook RT. The evaluation of liver function after partial hepatectomy in the rat: serum changes. Br J Exp Pathol 1979; 60(5):447-52.

153. George R, Shiu MH. Hypophosphatemia after major hepatic resection. Surgery 1992; 111(3):281-6.

154. Murphy EJ, Brindle KM, Rorison CJ, Dixon RM, Rajagopalan B, Radda GK. Changes in phosphatidylethanolamine metabolism in regenerating rat liver as measured by 31P-NMR. Biochim Biophys Acta 1992; 1135(1):27-34.

155. Gaub J, Iversen J. Rat liver regeneration after 90% partial hepatectomy. Hepatology 1984; 4(5):902-4.

156. Eguchi S, Kamlot A, Ljubimova J, Hewitt WR, Lebow LT, Demetriou AA, Rozga J. Fulminant hepatic failure in rats: survival and effect on blood chemistry and liver regeneration. Hepatology 1996; 24(6):1452-9.

157. Gaub J, Iversen J. 90% partial hepatectomy in rats: kinetics of regeneration, patterns of hormonal and metabolic responses. Gastroenterology 1980; 79:1107.

158. O'Grady JG, Williams R. Classification of acute liver failure. Lancet 1993; 342(8873):743.

159. Bernstein D, Tripodi J. Fulminant hepatic failure. Crit Care Clin 1998; 14(2):181-97.

160. Lee WM. Acute liver failure. N Engl J Med 1993; 329(25):1862-72.

161. Bismuth H, Samuel D, Gugenheim J, Castaing D, Bernuau J, Rueff B, Benhamou JP. Emergency liver transplantation for fulminant hepatitis. Ann Intern Med 1987; 107(3):337-41.

162. Peleman RR, Gavaler JS, Van Thiel DH, Esquivel C, Gordon R, Iwatsuki S, Starzl TE. Orthotopic liver transplantation for acute and subacute hepatic failure in adults. Hepatology 1987; 7(3):484-9.

163. Brems JJ, Hiatt JR, Ramming KP, Quinones-Baldrich WJ, Busuttil RW. Fulminant hepatic failure: the role of liver transplantation as primary therapy. Am J Surg 1987; 154(1):137-41.

164. Levinsky NG. Organ donation by unrelated donors. N Engl J Med 2000; 343(6):430-2.

165. Keeffe EB. Patient selection and listing policies for liver transplantation. J Gastroenterol Hepatol 1999; 14 Suppl:S42-7.

166. Carraro P, Burighel D, De Silvestro G, Gaiotto M, Plebani M. Early prognostic biochemical indicators of fulminant hepatic failure. Int J Clin Lab Res 1998; 28(3):196-9.

167. O'Grady JG, Alexander GJ, Hayllar KM, Williams R. Early indicators of prognosis in fulminant hepatic failure. Gastroenterology 1989; 97(2):439-45.

168. Donaldson BW, Gopinath R, Wanless IR, Phillips MJ, Cameron R, Roberts EA, Greig PD, et al. The role of transjugular liver biopsy in fulminant liver failure: relation to other prognostic indicators. Hepatology 1993; 18(6):1370-6.

169. Scotto J, Opolon P, Eteve J, Vergoz D, Thomas M, Caroli J. Liver biopsy and prognosis in acute liver failure. Gut 1973; 14(12):927-33.

170. Tygstrup N, Ranek L. Assessment of prognosis in fulminant hepatic failure. Semin Liver Dis 1986; 6(2):129-37.

171. Sekiyama K, Yoshiba M, Inoue K, Sugata F. Prognostic value of hepatic volumetry in fulminant hepatic failure. Dig Dis Sci 1994; 39(2):240-4.

172. Deasy NP, Wendon J, Meire HB, Sidhu PS. The value of serial Doppler ultrasound as a predictor of clinical outcome and the need for transplantation in fulminant and severe acute liver failure. Br J Radiol 1999; 72(854):134-43.

173. Schneeweiss B, Pammer J, Ratheiser K, Schneider B, Madl C, Kramer L, Kranz A, et al. Energy metabolism in acute hepatic failure. Gastroenterology 1993; 105(5):1515-21.

174. Terblanche J, Hickman R. Animal models of fulminant hepatic failure. Dig Dis Sci 1991; 36(6):770-4.

175. Keppler D, Lesch R, Reutter W, Decker K. Experimental hepatitis induced by D-galactosamine. Exp Mol Pathol 1968; 9(2):279-90.

176. Brennan RJ, Mankes RF, Lefevre R, Raccio-Robak N, Baevsky RH, DelVecchio JA, Zink BJ. 4-Methylpyrazole blocks acetaminophen hepatotoxicity in the rat. Ann Emerg Med 1994; 23(3):487-94.

177. Koff RS, Connelly LJ. Modification of the hepatotoxicity of D-galactosamine in the rat by cycloheximide. Proc Soc Exp Biol Med 1976; 151(3):519-22.

178. Bates TE, Williams SR, Busza AL, Gadian DG, Proctor E. A 31P nuclear magnetic resonance study in vivo of metabolic abnormalities in rats with acute liver failure. NMR Biomed 1988; 1(2):67-73.

179. Chen B, Burt CT, Goering PL, Fowler BA, London RE. In vivo 31P nuclear magnetic resonance studies of arsenite induced changes in hepatic phosphate levels. Biochem Biophys Res Commun 1986; 139(1):228-34.

180. Locke SJ, Brauer M. The response of the rat liver in situ to bromobenzene--in vivo proton magnetic resonance imaging and 31P magnetic resonance spectroscopy studies. Toxicol Appl Pharmacol 1991; 110(3):416-28.

181. Munakata T, Tanaka K, Mito M. [31P nuclear magnetic resonance study of intrahepatic energy metabolism in acute liver failure]. Nippon Geka Gakkai Zasshi 1990; 91(1):77-85.

182. Ramsoe K, Andreasen PB, Ranek L. Functioning liver mass in uncomplicated and fulminant acute hepatitis. Scand J Gastroenterol 1980; 15(1):65-72.

183. Milandri M, Gaub J, Ranek L. Evidence for liver cell proliferation during fatal acute liver failure. Gut 1980; 21(5):423-7.

184. Koukoulis G, Rayner A, Tan KC, Williams R, Portmann B. Immunolocalization of regenerating cells after submassive liver necrosis using PCNA staining. J Pathol 1992; 166(4):359-68.

185. Keppler D, Decker K. Studies on the mechanism of galactosamine-1-phosphate and its inhibition of UDP-glucose pyrophosphorylase. Eur J Biochem 1969; 10(2):219-25.

186. Keppler DO, Rudigier JF, Bischoff E, Decker KF. The trapping of uridine phosphates by D-galactosamine. D-glucosamine, and 2-deoxy-D-galactose. A study on the mechanism of galactosamine hepatitis. Eur J Biochem 1970; 17(2):246-53.

187. Mourelle M, Meza MA. Colchicine prevents D-galactosamine-induced hepatitis. J Hepatol 1989; 8(2):165-72.

188. Schuz-Henninger R, Prinz C, Decker K. Ganglioside biosynthesis in rat liver: effect of UDP-amino sugars on individual transfer reactions. Arch Biochem Biophys 1988; 262(1):49-58.

189. Decker K, Keppler D, Pausch J. The regulation of pyrimidine nucleotide level and its role in experimental hepatitis. Adv Enzyme Regul 1973; 11:205-30.

190. Sabesin SM, Koff RS. D-galactosamine hepatotoxicity. IV. Further studies of the pathogenesis of fatty liver. Exp Mol Pathol 1976; 24(3):424-34.

191. Perlman ME, Davis DG, Gabel SA, London RE. Uridine diphospho sugars and related hexose phosphates in the liver of hexosamine-treated rats: identification using 31P-[1H] two-dimensional NMR with HOHAHA relay. Biochemistry 1990; 29(18):4318-25.

192. Weisdorf S, Hendrich K, Buchthal S, Wike J, Bratt G, Merkle H, Garwood M, et al. Hepatic D-galactosamine toxicity studied with localized in vivo 31P magnetic resonance spectroscopy in intact rats. Magn Reson Med 1991; 21(2):178-90.

193. Thomas CP, Dixon RM, Tian M, Butler SA, Counsell CJ, Bradley JK, Adams GE, et al. Phosphorus metabolism during growth of lymphoma in mouse liver: a comparison of 31P magnetic resonance spectroscopy in vivo and in vitro. Br J Cancer 1994; 69(4):633-40.

194. Dixon RM, Tian M. Phospholipid synthesis in the lymphomatous mouse liver studied by 31P nuclear magnetic resonance spectroscopy in vitro and by administration of 14C-radiolabelled compounds in vivo. Biochim Biophys Acta 1993; 1181(2):111-21.

195. Taylor-Robinson SD, Sargentoni J, Bell JD, Thomas EL, Marcus CD, Changani KK, Saeed N, et al. In vivo and in vitro hepatic phosphorus-31 magnetic resonance spectroscopy and electron microscopy in chronic ductopenic rejection of human liver allografts. Gut 1998; 42(5):735-43.

196. Corbin I, Buist RJ, Peeling J, Zhang M, Minuk G. Examination of regenerative activity and liver function following partial hepatectomy in the rat utilizing hepatic phosphorus-31 magnetic resonance spectroscopy. Hepatology 2002; In Press.

197. Gazzard BG, Portmann B, Murray-Lyon IM, Williams R. Causes of death in fulminant hepatic failure and relationship to quantitative histological assessment of parenchymal damage. Q J Med 1975; 44(176):615-26.

198. Van Thiel DH, Brems J, Nadir A, Idilman R, Colantoni A, Holt D, Edelstein S. Liver transplantation for fulminant hepatic failure. J Gastroenterol 2001; 36(1):1-4.

199. Popper H. Pathologic aspects of cirrhosis. A review. Am J Pathol 1977; 87(1):228-64.

200. Hoofnagle JH. Hepatitis C: the clinical spectrum of disease. Hepatology 1997; 26(3 Suppl 1):15S-20S.

201. Nord HJ. Biopsy diagnosis of cirrhosis: blind percutaneous versus guided direct vision techniques--a review. Gastrointest Endosc 1982; 28(2):102-4.

202. Jeong DH, Jang JJ, Lee SJ, Lee JH, Lim IK, Lee MJ, Lee YS. Expression patterns of cell cycle-related proteins in a rat cirrhotic model induced by CCl4 or thioacetamide. J Gastroenterol 2001; 36(1):24-32.

203. Bachmann R, Kreft B, Dombrowski F, Block W, Oksendal A, Schild H. Enhanced tumor detection in the presence of liver cirrhosis: experimental study on the diagnostic value of a superparamagnetic iron oxide MR imaging contrast agent (NSR 0430). J Magn Reson Imaging 1999; 9(2):251-6.

204. Rozga J, Foss A, Alumets J, Ahren B, Jeppsson B, Bengmark S. Liver cirrhosis in rats: regeneration and assessment of the role of phenobarbital. J Surg Res 1991; 51(4):329-35.

205. Dupin S, Delrat P, Le Quellec A, Voigt JJ, Houin G. Indocyanine green pharmacokinetics in rats with progressive carbon tetrachloride-induced hepatocellular insufficiency. Arzneimittelforschung 1994; 44(3):367-70.

206. Kountouras J, Billing BH, Scheuer PJ. Prolonged bile duct obstruction: a new experimental model for cirrhosis in the rat. Br J Exp Pathol 1984; 65(3):305-11.

207. Dashti H, Jeppsson B, Hagerstrand I, Hultberg B, Srinivas U, Abdulla M, Bengmark S. Thioacetamide- and carbon tetrachloride-induced liver cirrhosis. Eur Surg Res 1989; 21(2):83-91.

208. Zimmermann T, Muller A, Machnik G, Franke H, Schubert H, Dargel R. Biochemical and morphological studies on production and regression of experimental liver cirrhosis induced by thioacetamide in Uje: WIST rats. Z Versuchstierkd 1987; 30(5-6):165-80.

209. Kaita KD, Pettigrew N, Minuk GY. Hepatic regeneration in humans with various liver disease as assessed by Ki-67 staining of formalin-fixed paraffin-embedded liver tissue. Liver 1997; 17(1):13-6.

210. Kawakita N, Seki S, Yanai A, Sakaguchi H, Kuroki T, Mizoguchi Y, Kobayashi K, et al. Immunocytochemical identification of proliferative hepatocytes using monoclonal antibody to proliferating cell nuclear antigen (PCNA/cyclin). Comparison with immunocytochemical staining for DNA polymerase-alpha. Am J Clin Pathol 1992; 97(5 Suppl 1):S14-20.

211. Moser M, Zhang M, Gong Y, Johnson J, Kneteman N, Minuk GY. Effect of preoperative interventions on outcome following liver resection in a rat model of cirrhosis. J Hepatol 2000; 32(2):287-92.

212. Schneeweiss B, Graninger W, Ferenci P, Eichinger S, Grimm G, Schneider B, Laggner AN, et al. Energy metabolism in patients with acute and chronic liver disease. Hepatology 1990; 11(3):387-93.

213. Muller A, Machnik F, Zimmermann T, Schubert H. Thioacetamide-induced cirrhosis-like liver lesions in rats--usefulness and reliability of this animal model. Exp Pathol 1988; 34(4):229-36.

214. Harvey PJ, Gready JE, Hickey HM, Le Couteur DG, McLean AJ. 31P and 1H NMR spectroscopic studies of liver extracts of carbon tetrachloride-treated rats. NMR Biomed 1999; 12(6):395-401.

215. McLean AJ, Morgan DJ. Clinical pharmacokinetics in patients with liver disease. Clin Pharmacokinet 1991; 21(1):42-69.

216. Harvey PJ, Gready JE, Yin Z, Le Couteur DG, McLean AJ. Acute oxygen supplementation restores markers of hepatocyte energy status and hypoxia in cirrhotic rats. J Pharmacol Exp Ther 2000; 293(2):641-5.

217. Seifter S, Englard S. Energy Metabolism. Third ed. New York: Raven Press, Ltd., 1994.

218. Murray CJ, Lopez AD. Mortality by cause for eight regions of the world: Global Burden of Disease Study. Lancet 1997; 349(9061):1269-76.

219. Herold C, Heinz R, Radespiel-Troger M, Schneider HT, Schuppan D, Hahn EG. Quantitative testing of liver function in patients with cirrhosis due to chronic hepatitis C to assess disease severity. Liver 2001; 21(1):26-30.

220. Glue P. The clinical pharmacology of ribavirin. Semin Liver Dis 1999; 19(Suppl 1):17-24.

221. Meyer B, Luo HS, Bargetzi M, Renner EL, Stalder GA. Quantitation of intrinsic drug-metabolizing capacity in human liver biopsy specimens: support for the intact-hepatocyte theory. Hepatology 1991; 13(3):475-81.

222. Kawasaki S, Imamura H, Bandai Y, Sanjo K, Idezuki Y. Direct evidence for the intact hepatocyte theory in patients with liver cirrhosis. Gastroenterology 1992; 102(4 Pt 1):1351-5.

223. Imamura H, Kawasaki S, Shiga J, Bandai Y, Sanjo K, Idezuki Y. Quantitative evaluation of parenchymal liver cell volume and total hepatocyte number in cirrhotic patients. Hepatology 1991; 14(3):448-53.

224. Ozawa K, Honjo I. Control of phosphorylative activity in human liver mitochondria through changes in respiratory enzyme contents. Clin Sci Mol Med 1975; 48(2):75-82.

225. Ozawa K, Kitamura O, Yamaoka Y, Mizukami T, Kamano T. Relation of phosphorylative capacity of liver mitochondria to cytochrome a(+a3) content. Am J Surg 1974; 127(3):306-9.

226. Jikko A, Taki Y, Nakamura N, Tanaka J, Kamiyama Y, Ozawa K, Tobe T. Adenylate energy charge and cytochrome a (+a3) in the cirrhotic rat liver. J Surg Res 1984; 37(5):361-8.

227. Rajanayagam V, Lee RR, Ackerman Z, Bradley WG, Ross BD. Quantitative P-31 MR spectroscopy of the liver in alcoholic cirrhosis. J Magn Reson Imaging 1992; 2(2):183-90.

228. Bell JD, Bhakoo KK. Metabolic changes underlying 31P MR spectral alterations in human hepatic tumours. NMR Biomed 1998; 11(7):354-9.

229. D'Amico G, Morabito A, Pagliaro L, Marubini E. Survival and prognostic indicators in compensated and decompensated cirrhosis. Dig Dis Sci 1986; 31(5):468-75.

230. Tosner Z, Dezortova M, Tintera J, Hajek M. Application of two-dimensional CSI for absolute quantification of phosphorus metabolites in the human liver. Magma 2001; 13(1):40-6.

231. Brauer M, Ling MF. The effects of chronic ethanol consumption on the intact rat liver studied by in vivo 31P NMR spectroscopy. Magn Reson Med 1991; 20(1):100-12.

232. Bodoky G, Yang ZJ, Meguid MM, Laviano A, Szeverenyi N. Effects of fasting, intermittent feeding, or continuous parenteral nutrition on rat liver and brain energy metabolism as assessed by 31P- NMR. Physiol Behav 1995; 58(3):521-7.

233. Glazer GM, Smith SR, Chenevert TL, Martin PA, Stevens AN, Edwards RH. Image localized 31P magnetic resonance spectroscopy of the human liver. NMR Biomed 1989; 1(4):184-9.

234. Cunningham CC, Bailey SM. Ethanol consumption and liver mitochondria function. Biol Signals Recept 2001; 10(3-4):271-82.

235. Morgan DJ, McLean AJ. Therapeutic implications of impaired hepatic oxygen diffusion in chronic liver disease. Hepatology 1991; 14(6):1280-2.

236. Kristensen SR. A critical appraisal of the association between energy charge and cell damage. Biochim Biophys Acta 1989; 1012(3):272-8.

237. Martin DS, Spriggs D, Koutcher JA. A concomitant ATP-depleting strategy markedly enhances anticancer agent activity. Apoptosis 2001; 6(1-2):125-31.

238. Reimer KA, Jennings RB, Hill ML. Total ischemia in dog hearts, in vitro 2. High energy phosphate depletion and associated defects in energy metabolism, cell volume regulation, and sarcolemmal integrity. Circ Res 1981; 49(4):901-11.

239. Reimer KA, Jennings RB. Energy metabolism in the reversible and irreversible phases of severe myocardial ischemia. Acta Med Scand Suppl 1981; 651:19-27.

240. Boustany RN, Aprille JR, Halperin J, Levy H, DeLong GR. Mitochondrial cytochrome deficiency presenting as a myopathy with hypotonia, external ophthalmoplegia, and lactic acidosis in an infant and as fatal hepatopathy in a second cousin. Ann Neurol 1983; 14(4):462-70.

241. Krahenbuhl S, Krahenbuhl-Glauser S, Stucki J, Gehr P, Reichen J. Stereological and functional analysis of liver mitochondria from rats with secondary biliary cirrhosis: impaired mitochondrial metabolism and increased mitochondrial content per hepatocyte. Hepatology 1992; 15(6):1167-72.

242. Vilaseca MA, Briones P, Ribes A, Carreras E, Llacer A, Querol J. Fatal hepatic failure with lactic acidaemia, Fanconi syndrome and defective activity of succinate:cytochrome c reductase. J Inherit Metab Dis 1991; 14(3):285-8.

243. Yamauchi H, Koyama K, Otowa T, Ouchi K, Anezaki T, Sato T. Morphometric studies on the rat liver in biliary obstruction. Tohoku J Exp Med 1976; 119(1):9-25.

244. Morelli A, Narducci F, Pelli MA, Farroni F, Vedovelli A. The relationship between aminopyrine breath test and severity of liver disease in cirrhosis. Am J Gastroenterol 1981; 76(2):110-3.

245. Abei M, Tanaka E, Tanaka N, Matsuzaki Y, Ikegami T, Ishikawa A, Osuga T. Clinical significance of the trimethadione tolerance test in chronic hepatitis: a useful indicator of hepatic drug metabolizing capacity. J Gastroenterol 1995; 30(4):478-84.

246. Lee RG, Clouse ME, Lanir A. Liver adenosine triphosphate and pH in fasted and well-fed mice after infusion of adenine nucleotide precursors. Liver 1988; 8(6):337-43.

247. Leij-Halfwerk S, Agteresch HJ, Sijens PE, Dagnelie PC. Adenosine triphosphate infusion increases liver energy status in advanced lung cancer patients: an in vivo 31P magnetic resonance spectroscopy study. Hepatology 2002; 35(2):421-4.

248. Rapaport E, Fontaine J. Generation of extracellular ATP in blood and its mediated inhibition of host weight loss in tumor-bearing mice. Biochem Pharmacol 1989; 38(23):4261-6.

249. Dagnelie PC, Sijens PE, Kraus DJ, Planting AS, van Dijk P. Abnormal liver metabolism in cancer patients detected by (31)P MR spectroscopy. NMR Biomed 1999; 12(8):535-44.

250. Leij-Halfwerk S, Dagneli PC, Kappert P, Oudkerk M, Sijens PE. Decreased energy and phosphorylation status in the liver of lung cancer patients with weight loss. J Hepatol 2000; 32(6):887-92.

251. Haskell CM, Mendoza E, Pisters KM, Fossella FV, Figlin RA. Phase II study of intravenous adenosine 5'-triphosphate in patients with previously untreated stage IIIB and stage IV non-small cell lung cancer. Invest New Drugs 1998; 16(1):81-5.

252. Agteresch HJ, Dagnelie PC, van der Gaast A, Stijnen T, Wilson JH. Randomized clinical trial of adenosine 5'-triphosphate in patients with advanced non-small-cell lung cancer. J Natl Cancer Inst 2000; 92(4):321-8.

253. Torres MI, Fernandez MI, Gil A, Rios A. Effect of dietary nucleotides on degree of fibrosis and steatosis induced by oral intake of thioacetamide. Dig Dis Sci 1997; 42(6):1322-8.

254. Torres-Lopez MI, Fernandez I, Fontana L, Gil A, Rios A. Influence of dietary nucleotides on liver structural recovery and hepatocyte binuclearity in cirrhosis induced by thioacetamide. Gut 1996; 38(2):260-4.

255. Agteresch HJ, Dagnelie PC, van den Berg JW, Wilson JH. Adenosine triphosphate: established and potential clinical applications. Drugs 1999; 58(2):211-32.

256. Froomes PR, Morgan DJ, Smallwood RA, Angus PW. Comparative effects of oxygen supplementation on theophylline and acetaminophen clearance in human cirrhosis. Gastroenterology 1999; 116(4):915-20.

257. Hickey PL, Angus PW, McLean AJ, Morgan DJ. Oxygen supplementation restores theophylline clearance to normal in cirrhotic rats. Gastroenterology 1995; 108(5):1504-9.

258. Harvey PJ, LeCouteur D, McLean AJ. Hepatic oxygen supplementation as therapy in cirrhotic liver disease. Gastroenterology 1999; 117(4):1025-6.

259. Heinzow BG, Somogyi A, McLean AJ. Influence of hydralazine on the pharmacokinetics of orally administered d-propranolol and lidocaine in conscious dogs. Arch Int Pharmacodyn Ther 1987; 286(1):5-14.

260. Le Couteur DG, Hickey H, Harvey PJ, Gready J, McLean AJ. Hepatic artery flow and propranolol metabolism in perfused cirrhotic rat liver. J Pharmacol Exp Ther 1999; 289(3):1553-8.

261. Satoh S, Tanaka A, Hatano E, Inomoto T, Iwata S, Kitai T, Shinohara H, et al. Energy metabolism and regeneration in transgenic mouse liver expressing creatine kinase after major hepatectomy. Gastroenterology 1996; 110(4):1166-74.

262. Miller K, Halow J, Koretsky AP. Phosphocreatine protects transgenic mouse liver expressing creatine kinase from hypoxia and ischemia. Am J Physiol 1993; 265(6 Pt 1):C1544-51.

263. Ishibashi S, Brown MS, Goldstein JL, Gerard RD, Hammer RE, Herz J. Hypercholesterolemia in low density lipoprotein receptor knockout mice and its reversal by adenovirus-mediated gene delivery. J Clin Invest 1993; 92(2):883-93.

264. Ledley FD. Hepatic gene therapy: present and future. Hepatology 1993; 18(5):1263-73.

265. Huber BE, Richards CA, Krenitsky TA. Retroviral-mediated gene therapy for the treatment of hepatocellular carcinoma: an innovative approach for cancer therapy. Proc Natl Acad Sci U S A 1991; 88(18):8039-43.